CHIRAL METAL COMPLEXES ANCHORED ONTO MESOPOROUS SILICA AS HETEROGENEOUS CATALYSTS FOR ASYMMETRIC ORGANIC TRANSFORMATIONS

THESIS

SUBMITTED FOR THE DEGREE OF

DOCTOR OF PHILOSOPHY

IN CHEMISTRY

TO THE

UNIVERSITY OF PUNE

BY

Suman Sahoo

Research guide

Dr. S. B. Halligudi

INORGANIC CHEMISTRY AND CATALYSIS DIVISION

NATIONAL CHEMICAL LABORATORY

PUNE - 411 008, INDIA

June-2008

राष्ट्रीय रासायनिक प्रयोगशाला
(वैज्ञानिक तथा औद्योगिक अनुसंधान परिषद)
डॉ. होमी भाभा मार्ग पुणे - 411 008. भारत
NATIONAL CHEMICAL LABORATORY
(Council of Scientific & Industrial Research)
Dr. Homi Bhabha Road, Pune - 411 008. India.

CERTIFICATE

Certified that the work incorporated in the thesis entitled **"CHIRAL METAL COMPLEXES ANCHORED ONTO MESOPOROUS SILICA AS HETEROGENEOUS CATALYSTS FOR ASYMMETRIC ORGANIC TRANSFORMATIONS"** submitted by **Miss Suman Sahoo**, for the Degree of **Doctor of Philosophy**, in **Chemistry** was carried out by the candidate under my supervision in the Inorganic Chemistry and Catalysis Division, National Chemical Laboratory, Pune - 411008, India. Materials obtained from other sources have been duly acknowledged in the thesis.

Dr. S. B. Halligudi

(Research Supervisor)

Communication Channels
NCL Level DID : 2590
NCL Board No. : +91-20-25902000
EPABX : +91-20-25893300
+91-20-25893400
FAX
Director's Office : +91-20-25893355
COA's Office : +91-20-25893619
COS&P's Office : +91-20-25893008
WEBSITE
www.ncl-india.org

Candidate's Declaration

I hereby declare that the thesis entitled **"*Chiral metal complexes anchored onto mesoporous silica as heterogeneous catalysts for asymmetric organic transformations*"** submitted by me for the degree of ***Doctor of Philosophy*** in ***Chemistry*** to the ***University of Pune*** is the record of work carried out by me during the period of September, 2005 to June, 2008 and has not been submitted by me for a degree to any other University or Institution. This work was carried out at Inorganic Chemistry and Catalysis Division, National Chemical Laboratory, Pune, India. Any inadvertent omissions that might have occurred due to oversight or error in judgment are regretted.

Suman Sahoo

June 2008
Inorganic chemistry and Catalysis Division
National Chemical Laboratory
Pune 411008, Maharashtra
India

In the hands of….

My beloved Parents
& Teachers

ACKNOWLEDGEMENT

It is my great pleasure to express my heartfelt gratitude to my research supervisor, Dr. S. B. Halligudi, for his unending support and invaluable guidance throughout the period of this investigation. I sincerely thank for the care and affection that I received from him and his family in the entire period. I take this opportunity to express my deepest sense of gratitude and reverence towards my co-guide Dr. Pradip Kumar, for his constant inspiration and for guiding me in the right direction throughout the course of this work. My deep personal regards are due for him forever.

I would like to express my profound gratitude to former Head of catalysis division, Dr. Rajiv Kumar, for providing the facilities required for my work. I would like to take the opportunity to thank Prof. F. Lefebvre for his help in NMR spectroscopy.

It gives me a great pleasure to express my deep sense of gratitude and indebtedness to Dr. Anil Kumar, Dr. Rane, Dr. Pardhy, Dr. Deshpande, Dr. Shubhangi, Dr. Singh, Dr. Dongare, Dr. Jacob, Dr. Kalaraj, Mr. Jha, Mr. Purushothaman, Mr. Dipak, Mr. Madhu, Mr. Kashinathan, Mr. Milind, Mr. Punekar and all the other scientific and non-scientific staff of NCL for their help and inspiring guidance and suggestions in carrying out the research work.

I sincerely thank my labmates Dr. Biju, Dr. Tresa, Dr. Dhanashri, Dr Ganapati, Ankur, Nevin, Suresh, Josena, Nishita, Nilesh, Amol and Palraj for their friendly help and kind cooperation during the period of my work. I also thank all my friends in the division and in NCL especially Shraeddha, Manu, Roopa, Dibya, Dibyadarshani, Bibhas, Rohit, Ramakant, Atul, Lakshi, Devu, Ganesh, Sachin, Ankush, Maitri, Pallaivi, Selva, Surendran, Nagarajan, Shivram, Prashant, Shankar, Nitasha, Rahul, Debasish, Sabita, Sitaram, Gokarneswar, Rosy, Pitambar, Subas and many others for their encouragement, invaluable help and moral support in one way or other, which made my work much easier.

I would like to thank my friends Jyoti, Suchitra, Lina, Sarada, Saroj, and roja for their encouragements, love and never failing supports during my many years of studies.

I take this occasion to thank all my teachers, well-wishers classmates & friends in various stages for their love, encouragement and kind cooperation that I received from them whose names are not mentioned here.

The words are not enough to express all my love and thankfulness towards my parents and all my beloved family members for their blessings that I could reach here.

Finally, my thanks are due to Dr. S. Sivaram, Director, NCL for allowing me to carryout the research work at NCL and CSIR, New Delhi, India, for the financial support in the form of research fellowship.

(Suman Sahoo)

"THE ESSENTIAL PRODUCTS OF LIFE ARE ASYMMETRIC AND POSSESS SUCH ASYMMETRY THAT THEY ARE NOT SUPERIMPOSABLE ON THEIR IMAGES? THIS ESTABLISHES PERHAPS THE ONLY WELLMARKED LINE OF DEMARCATION THAT CAN AT PRESENT BE DRAWN BETWEEN THE CHEMISTRY OF DEAD MATTER AND THE CHEMISTRY OF LIVING MATTER"

Louis Pasteur, 1822-1895

Contents

ABBREVIATIONS

BET	**Brunauer-Emmett-Teller**
BJH	**Barret−Joyner−Halenda**
[BMIM]PF_6	**Butylmethylimidazolium hexaflurophosphate**
BINOL	**1,1'-bi-2-naphthol**
COD	**Cyclooctadiene**
CP	**Cross polarization**
CTAB	**Cetyltrimethylammonim bromide**
ee	**Enantiomeric excess**
F123	**Poly-(ethylene oxide)-poly(propylene oxide)-poly(ethylene oxide) EO20PO70EO20**
FID	**Flame ionized detector**
FT-IR	**Fourier-transform Infrared**
GC	**Gas Chromatography**
GCMS	**Gas Chromatography-Mass Spectroscopy**
HPLC	**High performance liquid chromatography**
HRTEM	**High resolution transmission electron microscopy**
ICP-AES	**Induced coupled plasma – Atomic emission spectroscopy**
IL	**Ionic liquid**
IBX	**2-Iodoxybenzoic acid**
KBr	**Potassium bromide**
LCT	**Liquid crystal template**
LDH	**Layer double hydroxide**
MAS	**Magic angle spinning**
MCM	**Mobil composition of mater**
MIMBr	**1,3-Dimethylimidazlium bromide**
NMR	**Nuclear magnetic resonance**
$PhI(OAc)_2$	**Diacetoxy iodobenzene**

RTIL	**Room temperature ionic liquid**
SBA	**Santa Barbara Amorphous**
SEM	**Scanning electron microscopy**
SILP	**Supported ionic liquid phase**
TBHP	***tert*- Butyl hydrogen peroxide**
TCD	**Thermal conductivity detector**
TEM	**Transmission electron microscopy**
TEOS	**Tetraethyl orthosilicate**
TG-DTA	**Thermogravimetry-Differential thermal analysis**
TLC	**Thin layer chromatography**
$Ti(OiPr)_4$	**Titanium tetraisopropoxide**
TOF	**Turn over frequency**
TON	**Turn over number**
UV-Vis	**Ultra violet-visible**
XRD	**X-ray diffraction**

Research Student	Suman Sahoo
Research Guide	Dr. S. B. Halligudi
Title of the thesis	*Chiral metal complexes anchored onto mesoporous silica as heterogeneous catalysts for asymmetric organic transformations*
Registration No.	El/191/Ph.D/2006
Date of Registration	23/09/2005
Place of work	Inorganic Chemistry and Catalysis Division, National Chemical Laboratory, Pune 411 008

Abstract

Although homogeneous asymmetric catalysis has the advantages of high enantioselectivity and catalytic activity in various asymmetric transformations under mild reaction conditions, the difficulties associated with the recovery and reuse of expensive chiral catalysts severely hamper its practical applications. Furthermore, the potential contamination of the products caused by metal leaching from the homogeneous catalysts is particularly unacceptable for pharmaceutical production. One of the most promising ways to circumvent these difficulties is the immobilization of the homogeneous chiral catalysts using various strategies.

The thesis will focus on the immobilization of chiral metal complexes onto mesoporous silica, its characterization by different physico-chemical techniques and assessment of its catalytic activity in some asymmetric organic transformations.

Objectives of the present investigation

The primary objective of the research proposal was to design and develop chiral transition metal complex catalysts using new ligands, covalent anchoring of them to mesoporous silica support and assessment of these immobilized catalysts in different asymmetric organic transformation, such as hydrogenation, kinetic resolution.

The following objectives were taken into consideration:

1. Preparation and characterization of chiral ligands and transition metal complexes.
2. Preparation and characterization of functionalized mesoporous silica materials of MCM-41, MCM-48, and SBA-15 (inorganic-organic hybrid materials) using chloropropyl triethoxy silane and ionic liquid.
3. Anchoring metal complexes or ligands and its complexes covalently to the functionalized mesoporous supports and their characterization by different physicochemical techniques like, IR, NMR, UV-Vis, SEM, TEM, powder XRD, N_2 sorption analysis.
4. Screening of catalysts for their catalytic activities and product enantioselectivities in asymmetric hydrogenation of prochiral ketones, α, β- unsaturated ketones, imines, olefins, oxidative kinetic resolution of secondary alcohol and asymmetric oxidation tandem kinetic resolution of sulfides.
5. Comparison of activities of the covalently anchored and neat homogeneous catalysts with respect to their performance.

Outline of the thesis

The thesis has been divided into six chapters

CHAPTER I

Chapter I give a brief introduction of asymmetric catalysis and their importance. It also gives an introduction to both industrially and synthetically important various organic transformations. Immobilization of different metal complexes by different strategy has been discussed. A review of the literature to date in these areas is included. Finally, the aim of the thesis is outlined briefly.

CHAPTER II

This chapter deals with all materials used for synthesis and catalyst screening. Immobilized metal complexes were characterized by different techniques such as N_2

sorption, AAS, EDAX, XRD, TEM, SEM, FT-IR, MAS NMR and UV-Vis. For each technique, its theory and experimental procedures are described briefly.

CHAPTER III

Chiral cyclohexyldiamine based Ru triphenylphosphine complex has been immobilized over mesoporous silica SBA-15 and used in the chemo- and enantioselective hydrogenation of prochiral and α, β- unsaturated ketones and imines to corresponding products. ^{31}P NMR, SEM, TEM, XRD, N_2 sorption measurements and FTIR analysis supported the retention of the complex over mesoporous silica. This catalyst was found to catalyze preferentially the hydrogenation of C=O over coexisting conjugated C=C linkages in the hydrogenation of α, β- unsaturated ketones with high turnover frequencies (TOF = mole of substrates converted per mole of Ru complex per hour) and gave excellent enantioselectivities in the hydrogenation of prochiral ketones compared to its homogeneous analogue. It also showed good activity in the hydrogenation of less reactive imines to secondary amines.

CHAPTER IV

Chiral monodentate phosphorous-based ligands are proved to be effective for the enantioselective hydrogenation of olefins. Binol derived monodentate phosphorothioite (PS) ligand was synthesized from binol and thiopropyltriethoxysilane and its iridium complex was covalently anchored to mesoporous silica supports like SBA-15, MCM-41 and MCM-48. These catalysts were characterized by different physicochemical techniques and assessed for their catalytic performances in the heterogeneous asymmetric hydrogenation of itaconic acid and its derivatives. It was found that the catalytic activities and enantioselectivities of the heterogenised iridium complex (IrPSSBA-15) in the hydrogenation reactions were comparable to its homogeneous analogue. Binol derived monodentate phosphorothioite ligand in heterogeneously anchored form (iridium complex) is a more effective catalyst than the reported monodentate phosphorous ligand systems in the hydrogenation reactions which could be due to the change in electronic properties around the iridium metal centre. Effects of substrate to catalyst molar ratio, solvents and temperature on substrate conversions and enantioselectivities of the products were investigated in hydrogenation reactions.

CHAPTER V

The supported ionic liquid strategy has been applied for the immobilization of chiral Mn(III)salen complex onto ionic liquid modified mesoporous silica SBA-15. The catalyst was characterized by different physicochemical methods. The immobilized catalyst demonstrates good enantioselectivity and activity in the oxidative kinetic resolution of secondary alcohol, which could be recycled for five times without obvious loss of its functionalities. The effect of additives, organic solvent, and oxidant on the enantioselectivity of the reactions is reported. Hexane water solvent system was found to be the best solvent of choice due to absence of leaching.

CHAPTER VI

This chapter deals with the immobilization of chiral Ti-binol complex onto mesoporous silica SBA-15. This catalyst system has been applied for enantioselective oxidation of sulfur compounds giving excellent yields at room temperature with good recyclability.

CHAPTER VII

This chapter summarizes the conclusions reached in this thesis.

CHAPTER I

Introduction

1. Introduction

1.1. Asymmetric Synthesis

In nature, symmetry is imperfect, although mathematicians may treat it as an ideal. In art, too, it seems that the approximation of symmetry, rather than its precision, teases the mind as it pleases the eye. Where there is a matter, there is asymmetry. We come across with various facts of asymmetry in day to day life [1]. We eat optically active bread and meat, live in houses, wear clothes, and read books made of optically active cellulose. The proteins that make up our muscles, the glycogen in our liver and blood, the enzymes and hormones … are all optically active. Naturally occurring substances are optically active because the enzymes which bring about their formation … are optically active.

In 1904 Macwald defined asymmetric synthesis as "reactions which produce optically active substances from symmetrically constituted compounds with the intermediate use of optically active material but with the exclusion of all analytical processes" [2]. The asymmetric synthesis of both natural and unnatural compounds in *chiral nonracemic* form is a fundamental challenge and objective in chemistry. As such, the development of new chiral auxiliaries, reagents, ligands, and catalysts for use in asymmetric synthesis is at the forefront of chemical research.

Chirality is an intrinsic feature of all matter, which can't be superimposed on its mirror image [3]. The word 'chiral' is derived from the greek word *cheir*, which means hand. Our left hand and right hand are mirror images of each other and not superimposable (Fig. 1.1.), which is the minimum criterion for chirality.

The first evidence of molecular chirality came in 1884, when Louis Pasteur noted the spontaneous crystallization of the sodium ammonium salt of tartaric acid, which was found in wine caskets into enantiomorphic crystals [4]. After careful physical separation of the two types of crystals by tweezers, Pasteur made the discovery that solutions of the crystals rotated the plane polarized light but in opposite directions. The only explanation

for this observation is that the molecules in each of the crystals were non superimposable mirror images of one another.

Enantiomers have identical physical properties (solubility, boiling/melting point). They also have the same chemical properties (reactivity). However, when they act in a chiral environment (e.g. human body) they exhibit a different physiological activity (odour, receptor binding, pharmacological effect). As for example, (R)-thalidomide is a sedative but its (S) isomer cause birth defects [5], dextromethorphan is a cough suppressant but levomethorphan (its enantiomer) is a narcotic. The public demands for single enantiomer have been transferred first to the pharmaceutical and related companies [6], mainly through the questions of regulatory agencies, and second to the scientific community, which in turn has to provide highly efficient and reliable methods of asymmetric synthesis. In fact, these demands have already had an important response, since the worldwide sales of single enantiomer drugs are continuously growing. In 2001, 70% of the new drugs approved were single enantiomers [7].

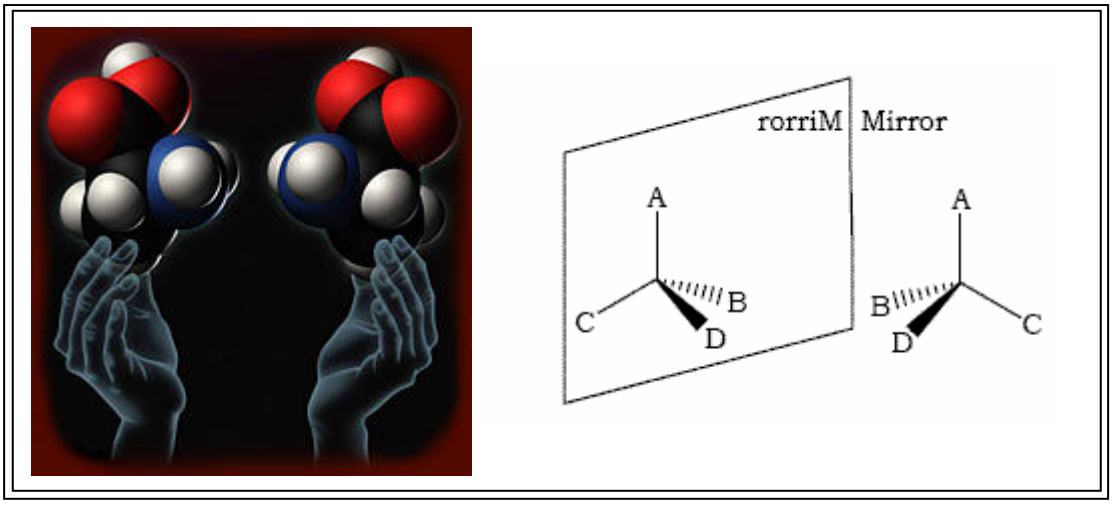

Fig. 1.1. A pair of enantiomers: mirror images of a chiral molecule

The advantages associated with enantioselective synthesis are well-recognized, and can include: (a) access to either enantiomer of product based on which enantiomer of reagent/ auxiliary/catalyst is employed; (b) use of a readily-available achiral substrate; and (c) minimization of waste typically associated with resolution processes [8].

1.2. Routes to enantiomerically pure compounds

Enantiomerically pure compounds can be obtained in three different ways (Figure 1.2). The first route makes use of chiral compounds which are obtained from agriculture or via fermentation, the so called 'chiral pool'. These compounds can be used as obtained or modified without loss of the chiral information. The second route makes use of racemates *i.e.*, a 1:1 mixture of enantiomers. Separation of these racemates by resolution can be done in two ways [9]. One is crystallization, which is still the most used method in industry to obtain enantiomerically pure compounds [10]. In the other one, a racemate is derivatized with another chiral compound (auxiliary), so that diastereomers are formed, which can be separated by crystallization. Removal of the auxiliary gives the enantiomerically pure compound.

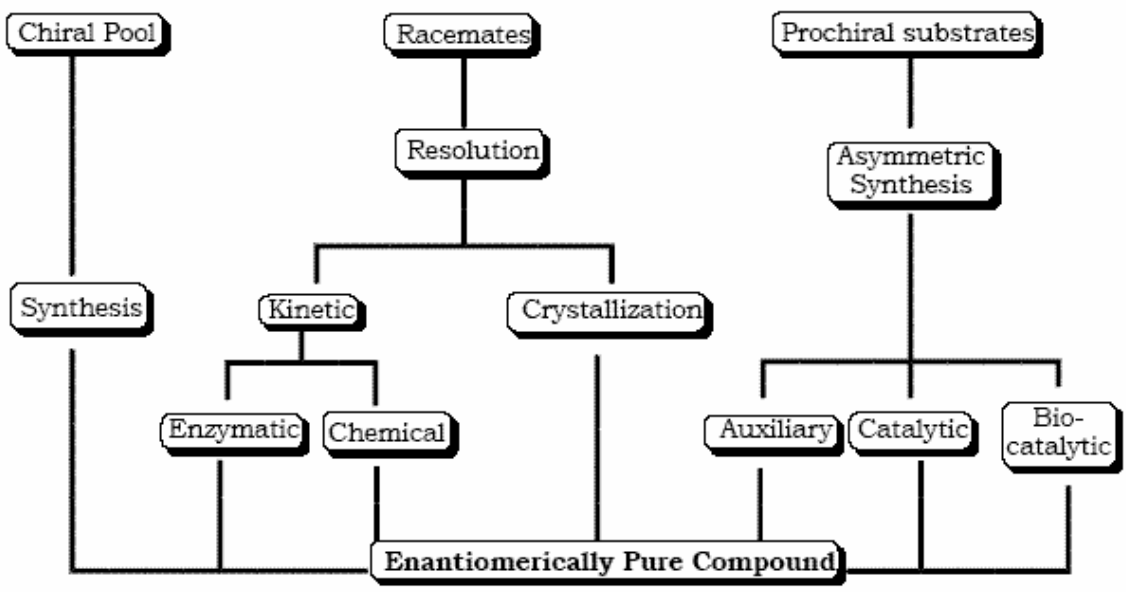

Fig. 1.2. Routes to enantiomerically pure compounds

In kinetic resolution, a racemate is modified by chemical or enzymatical conversion and one of the enantiomers of the racemic mixture will be transformed into a product faster than the other (scheme 1.1. (a)). In an ideal case the reaction stops after 50% of conversion and only one of the enantiomers is completely converted and the other one did not react at all [11]. In dynamic kinetic resolution, one of the enantiomers is transformed into the product, whereas the remaining enantiomer racemizes [12]. This racemic mixture undergoes a resolution again until all the starting material has been

consumed (scheme 1.1 (b)). This can lead in an optimal case to a yield of 100% and an enantioselectivity of 100%. In parallel kinetic resolution, both enantiomers undergo reaction at comparable rates to give different products [13]. In this case, as with standard kinetic resolutions described above, the maximum yield is 50% for each product. However, the ee of the products is much less dependent on the degree of conversion. In fact, in the extreme case wherein the two product-forming pathways occur at the same rate, the ee is constant throughout the reaction.

The third route makes use of prochiral substrates which can be transformed into enantiomerically pure compounds by an asymmetric synthetic modification. The asymmetric synthesis can be performed in different ways *i.e.,* using a chiral auxiliary [14] or applying catalysts [15]. In the case of a chiral auxiliary, a chiral group is attached to the substrate. Introduction of an additional chiral centre will make the resulting product a diastereomer. In an ideal case the introduction of the additive stereogenic centre will be completely controlled by the chirality of the auxiliary and thus the reaction will be diastereoselective. Drawback of this method is that stoichiometric amounts of a chiral auxiliary have to be used, which have to be introduced and removed with two additional synthetic steps.

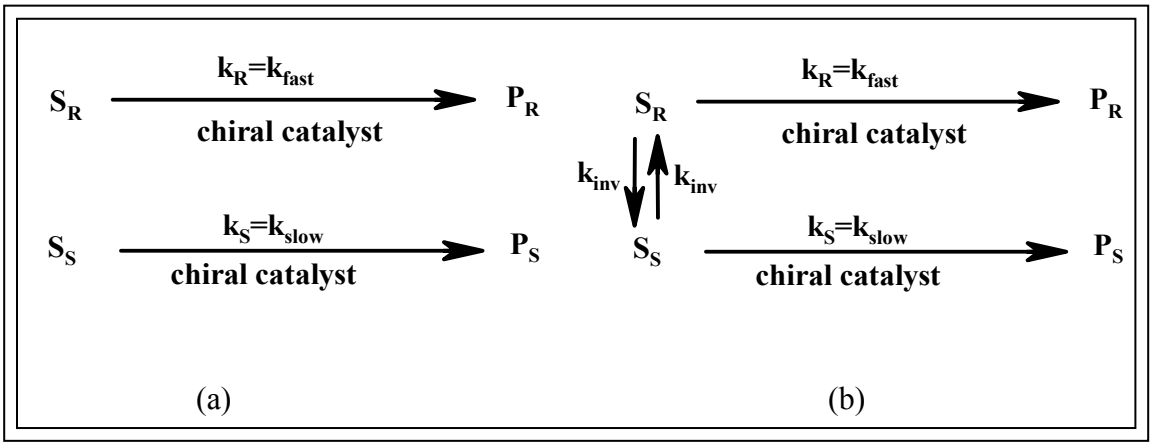

Scheme 1.1. (a) Kinetic resolution (b) Dynamic kinetic resolution

A more elegant method is the application of catalysis, which is the main objective of this thesis. This method employs small amounts of a biological, *e.g.* antibodies or enzymes, or chemical catalysts to transform a prochiral substrate into large quantities of enantiomerically pure compounds. Biocatalysts are frequently highly specific for one

substrate. In general, it is not possible to obtain both enantiomers of a product since usually only one of the enantiomers of a biocatalyst is available although recently directed enzyme evolution techniques have provided a solution to this problem [16]. On the other hand, chemical catalysts are commonly based on transition metals modified with enantiomerically pure organic ligands, which makes it possible to obtain both enantiomers of the product by changing the configuration of the ligand.

1.3. Asymmetric catalysis

Although a broad range of organocatalysts have been developed in recent years [17, 18], metal (transition) catalysts are still the most abundantly used. The importance and elegance of homogeneous asymmetric catalysis was also recognized by the Nobel Prize Committee, who awarded the 2001 Noble Prize in chemistry to Knowles, Noyori and Sharpless for their pioneering work on asymmetric hydrogenation and oxidation reactions. The field of transition metal-catalyzed asymmetric synthesis has developed tremendously and a wide variety of reactions have been developed employing a range of transition metals, *e.g.* Pd, Rh, Ru, Ir, Cu *etc*.

The substances used as the starting point for these syntheses are in general *not* chiral. The trick is to make the product chiral. This is done using a chiral catalyst molecule. Suppose we compare this molecule with a left hand. A left hand will make a better match in a handshake with another left hand (one of the two emerging product forms) than with a right hand (the other form of the product) (fig. 1.3). Thus a chiral catalyst can control production of the desired chiral product.

Currently, efficient asymmetric catalysis primarily uses a molecular catalyst that consists of a metallic element and chiral organic ligand (s) [19]. Fig. 1.4. illustrates a typical (but not general) catalytic scheme. Under reaction conditions, the initially used precatalyst 1 is converted to the true catalyst 2 (induction process) that activates achiral molecules A and B and transforms them to chiral product A-B (catalytic cycle). Although the ligand must create a distinct enantio-differentiating environment in transition metal based complexes, such an architectural design does not suffice to achieve asymmetric catalysis. Some of the steps in the multistep transformation are reversible, whereas the

first irreversible step, for example 3⟶4, kinetically determines the absolute stereochemistry of A-B.

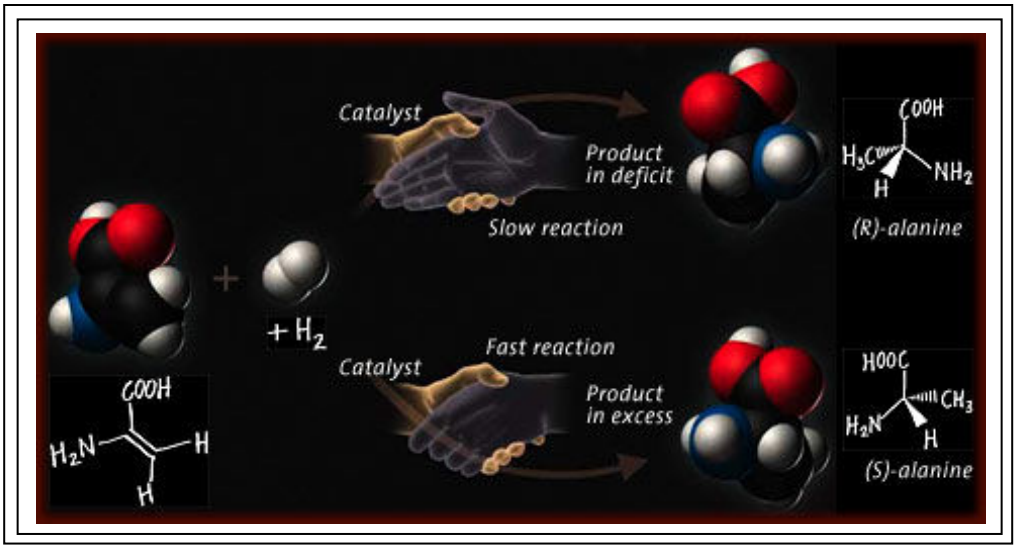

Fig. 1.3. Working of a chiral catalyst

Efficient asymmetric catalysis requires a high turnover number and high turn over frequency, but the best way to generate high catalytic activity is not immediately apparent. First the induction process of converting 1 to 2 is often not straightforward. Furthermore, to obtain a high turn over frequency, all of the transition metal based entities 2-4 in this cycle must be neither very unstable nor very stable, avoiding substrate and/or product inhibition. Instead, 2-4 are required to interconvert one another smoothly by means of a low kinetic barrier, and without any destructive side reactions. The reaction conditions strongly influence the stability and reactivity of 1-4 in general, both suitable architectural and functional engineering are crucial for obtaining sufficient catalytic efficiency. "Molecular Catalysis" can cope with such requirements, because any molecules, by definition, can be designed and synthesized at will.

Asymmetric catalysts have the greatest potential for general asymmetric synthesis since virtually no constraints exist in terms of molecular design, except those imposed by the human designing them, or in terms of what reactions are potentially capable of being performed asymmetrically. Perhaps the earliest example is the utilization of cinchona alkaloids as catalysts for cyanohydrins formation in 1912, a type of catalysis recently dubbed ''organocatalysis.'' The use of metal complexes for asymmetric catalysis dates

from efforts in the 1950s to effect asymmetric hydrogenation [20–26]. Several developments accelerated the growth of defined transition metal complexes for asymmetric catalysis. First, the ability to synthesize and characterize well defined transition metal complexes improved dramatically. Second, access to defined complexes set the stage for understanding the implication of structure for function, which begot the development of defined transition metal complexes, typically hybrids of organic entities and transition metals, for chemical catalysis. Third, the ability for individuals to wed the understanding that arises by integrating theoretical and physical, organic, and inorganic chemistry with solving complex problems becomes enabling [27].

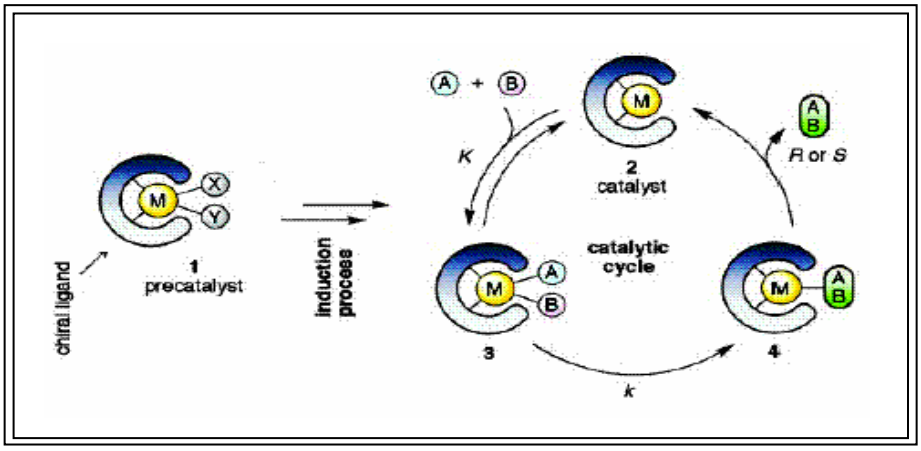

Fig. 1.4. The principle of asymmetric catalysis with chiral organometallic molecular catalysts. M, metal; A and B, reactant and substrate; X or Y, neutral or anionic ligand.

1.4. Homogeneous asymmetric catalyzed reactions

1.4.1. Asymmetric Hydrogenation

Probably, the most important strategy to introduce chirality involves the ability of a catalyst to differentiate the enantiotopic faces of a prochiral functional group, notably a π-unsaturation like a carbon–carbon or carbon–oxygen double bond. The discovery of tris(triphenylphosphine) rhodium chloride as a catalyst for hydrogenation by Wilkinson and colleagues in 1966 [28] set the stage for the development of asymmetric catalysts. Replacing triphenylphosphine with chiral phosphines is a straightforward extrapolation. In 1972, Knowles *et al.* [29] reported excellent results with a monodentate phosphine CAMP. Most notably, the development of DIOP by Kagan, first reported in 1971, proved

the validity of the approach [30, 31]. In 1975, Knowles [32] reported the bis-phosphine analog DIPAMP of his CAMP series of monodentate ligands. This ligand became the key to an asymmetric synthesis of β-arylalanines such as the anti-Parkinson drug (*S*)-DOPA and (*S*)-phenylalanine, one of the two amino acids that constitutes the artificial sweetener aspartame. Indeed, this reaction is practiced commercially for these applications [33, 34]. Despite the commercial success of DIPAMP, the real broad potential of asymmetric hydrogenation was not realized until the introduction of 2,2-bis-(diphenylphosphino)-1,1-binaphthyl (BINAP) by Noyori and colleagues in 1980 [35, 36]. For example, hydrogenation of the benzamide with a Rh complex of BINAP produced the corresponding phenylalanine derivative with near perfect enantioselectivity. The production of the chiral piperazine unit that is one of the components of the clinically important HIV protease inhibitor is also accessed with this catalyst in high yield and ee [37]. Replacing Rh by Ru increased the scope of such reductions dramatically, notably by embracing carbonyl compounds as substrates [38–40]. The success of iridium for imine reductions ultimately led to a commercially successful synthesis of the herbicide (*S*)-metolachor, which is produced on the scale of >10,000 tons per year [41].

1.4.2. Asymmetric Oxidation

The discovery of metal-catalyzed epoxidation methods set the stage for the development of an asymmetric version. The first successful asymmetric epoxidation is the combination of a simple tartarate ligand with titanium (Sharpless asymmetric epoxidation) [42] and it led to early commercialization for the synthesis of both enantiomers of glycidol, an important chiral building block [43, 44]. The requirement of this method for a hydroxyl group proximal to the double bond, preferably allylic, was relieved to some extent by the development of epoxidations based on manganese embraced by salen ligands 10 pioneered by Jacobsen and colleagues [45, 46] and Katsuki and colleagues [47-48]. This example highlights the significance of these new methodologies by facilitating the development of novel and selective Iks-channel blockers for control of cardiac arrhythmias, such as HMR 1556 [49]. The sharpless reagent ($Ti(O\text{-}i\text{-}Pr)_4$/ diethyl tartarate) for asymmetric epoxidation was modified by Kagan and his group [50] by the addition of 1 mol equiv. of H_2O and used in the

asymmetric oxidation of sulfides to give 90% ee of the corresponding sulfoxide. This method was modified further by using binol as the ligand instead of diethyl tartarate, which provided upto 99% ee of the sulfoxide after a tandem oxidation and oxidative kinetic resolution [51].

1.4.3. Asymmetric C-C Bond Formation

Complexes of BINAP, BINOL, salen, and bisoxazolines, which all shares the same feature of being C2 symmetric ligands, have been effective for numerous [4 + 2] cycloadditions [52]. Shibasaki revealed the first such catalysts based on a novel class of BINOL complexes (Scheme 14, structure 20) formed by self-assembly of BINOL in the presence of a lanthanide and base [53, 54]. Asymmetric hydroformylation [55] and hydrocyanation have been early areas of endeavor with only modest success [56]. An asymmetric Heck reaction has been reported by Mikami laboratories utilizing an axially chiral non-C2 symmetric ligand [57]. Titanium and zirconium complexes such as sandwich complexes also promote asymmetric carbametallation of alkenes but with simple alkyl moieties, as illustrated by syntheses of vitamins E and K [58] and hydrosilylations of carbonyl and imine groups [59, 60], among others. Related sandwich complexes have been important in asymmetric polymerizations of propylene involving a similar asymmetric carbametallation as the chain propagation step [61–62].

1.5. Heterogeneous Asymmetric Catalysis

Inspite of the large growth, the obstacles in the catalyst separation and recycle in homogeneous catalysis often make the practical application difficult. Heterogeneous catalysis supplies the opportunity for easy separation and recycle of the catalyst, easy purification of product, and continuous or multiple processing of chiral compounds. Furthermore, the solid chiral catalysts, particularly the chiral catalysts accommodated in the pores or cavities of the porous materials, possess quite different effects of the surface and the pore on the catalytic performance. It is a desired objective to immobilize the homogeneous catalysts without losing its merits, and even enhancing the enantioselectivity. Although the heterogeneous asymmetric catalysis has potential advantages in comparison to the homogeneous one, research in this area has not been

paid enough attention until recently. One reason is that the enantioselectivity is often deteriorated after the homogeneous catalyst is heterogenized, because the complex structure of the homogeneous catalyst might be distorted after the immobilization. Another reason might be the decrease of the activity while the homogeneous catalyst is immobilized on surface and in pores, due to the slow diffusion and the difficulty in accessing the active sites for reactants. Leaching of the catalysts from the solid surfaces is also a problem for the immobilized chiral catalyst.

However, recent progress made in the heterogeneous asymmetric field has demonstrated that the heterogeneous asymmetric catalysis is gaining interest in industrial applications [63]. The newly developed immobilization methods make it possible for preparing the robust heterogeneous chiral catalysts while still maintaining the high enantioselectivity. Some heterogeneous catalysts even show the catalytic performance as good as homogeneous catalysts, and the stability of the catalyst is also significantly improved.

Over the past three decades, a number of methodologies and new concepts have been developed for immobilizing chiral catalysts. The choice of a suitable support plays an important, although not fully understood, role and remains challenging. Numerous problems can occur during the immobilization of a homogeneous catalyst and diminish its performance:

- undesired interactions between the support and the metal–ligand complex,
- the optimal geometry of the catalyst, crucial for high enantio induction, is disturbed by the support,
- unsatisfactory stability of the linkage between the catalyst and support or the catalyst itself which results in leaching,
- limited accessibility of the active site,
- undesired isolation of catalyst centers that need to cooperate during the reaction [64].

In general, there are two types of immobilized catalysts: (1) chiral catalysts with “mobile carriers” such as aqueous phase, supercritical carbon dioxide (Sc CO_2) or ionic liquid, (2) insoluble chiral catalysts bearing stationary supports such as organic cross-linked polymers or inorganic materials.

1.5.1. Immobilization using biphasic methodology

Liquid–liquid biphasic catalysis (‘‘biphasic catalysis’’) has emerged as an important alternative for the separation of the products and the recovery of the catalysts from the reaction mixture. The concept of this system implies that the molecular catalyst is soluble in only one phase whereas the substrates/products remain in the other phase. The reaction can take in one (or both) of the phases or at the interface. Accordingly, the catalyst phase can be reused and the products/substrates are simply removed from the reaction mixture by separation of the two phases. Biphasic catalysis can be typically divided into following four areas.

1.5.1.1. Aqueous biphasic system [65]

Aqueous biphasic system using water-soluble complexes have attracted a great deal of interest. Substantial efforts have been made to prepare water-soluble chiral catalysts for biphasic applications. Most of the reported water-soluble chiral ligands were prepared by incorporation of anionic groups such as sulfonate or carbonate, cationic groups such as quaternary ammonium ions, or neutral hydrophilic groups such as polyethers. However, in most cases, chiral catalysts in aqueous two-phase systems led to much lower activity and/or stereoselectivity than in a homogeneous organic phase which is attributed mainly to the poor mass transport between the two phases.

1.5.1.2. Fluorous biphasic methodology [66–68]

Fluorous biphasic methodology is based upon separation and immobilisation technique using catalysts having a number of long perfluoroalkyl side chains, called ‘‘fluorous pony tails’’. Such catalysts are dissolved in fluorous solvents, but immiscible with typical organic solvents and water at ambient temperature, facilitating catalyst recovery from the reaction mixture. Unfortunately, in most reactions in FBS system, a significant drop in activity and enantioselectivity were generally observed.

1.5.1.3. Asymmetric catalysis in supercritical fluids [69]

The use of supercritical fluids, such as supercritical carbon dioxide, as a reaction media offers the opportunity to replace organic solvents with an environmentally less hazardous reaction medium, and exert interesting solvent effects on the selectivity of the

reaction. A unique and potentially advantageous characteristic of supercritical fluid solvents is that their density, polarity, viscosity, diffusivity, and overall solvent strength could be dramatically altered by changing a relatively small range of pressure and/or temperature.

1.5.1.4. Enantioselective catalysis in ionic liquids

All of the biphasic approaches mentioned above are of interest but require additional catalyst modifications. Moreover, the activity and/or enantioselectivity of the immobilised catalysts are usually reduced because of unsuitable chemical modifications, and mass transfer limitations, etc.

A new approach has recently been developed for catalyst separation and recycling, which involves the use of ionic liquids, i.e., a salt mixture with a melting point below ambient [70–75]. Ionic liquids are regarded as eco-friendly alternatives to volatile organic solvents in chemical processes, due to their negligible vapour pressure and non-flammable nature. Moreover, their hydrophobicities/hydrophilicities and solvent miscibility can be tuned by selecting the appropriate cation and anion. Thus, depending on their structures, they can be designed to be immiscible with water or some organic solvent (e.g., alkanes, ether, i-PrOH, etc.), which renders them more useful for facilitating catalyst recovery from the reaction mixture. Moreover, switching from an organic solvent to an ionic liquid often results in marked improvements in catalytic performance [76–81]. A broad range of enantioselective catalytic reactions have already been described, and most examples studied to date show that the use of ionic liquids can confer many advantages upon enantioselective catalytic reactions over reactions in organic solvents in terms of activity, enantioselectivity, stability and the reusability of the solvent–catalyst systems [82–84]. It has been reported that ionic liquids can accelerate asymmetric epoxidation of olefins catalysed by the chiral Mn(III) salen complex [85]. For example, the epoxidation of 2,2-dimethylchromene using 4 mol% of Mn(III) salen catalyst in the presence of [Bmim][PF_6] was completed in 2 h, whereas the same reaction without the ionic liquid, required 6 h to achieve complete conversion. Moreover, the use of an ionic liquid as a solvent allows easier catalyst recycling, without the need for catalyst modification. By washing the organic phase with water, concentrating the organic phase,

and then extracting the product with hexane, the ionic catalyst solution can be recovered. However, the enantioselectivity and activity of the recovered catalyst decreased upon reuse. After five cycles, the yield and enantioselectivity dropped from 83 to 53% and from 96 to 88% ee, respectively. This deterioration may be due to degradation of the salen catalyst under oxidation conditions. Jessop et al. have shown that ionic liquids can enhance the enantioselectivity in asymmetric reduction of tiglic acid using Ru-tolBINAP catalyst [86]. Using the viscous ionic liquids such as [Bmim][PF_6] and [Emim][NTf_2], the ees reported were found to increase from 88% in MeOH to 93 and 95%, respectively.

1.5.2. Immobilization on polymeric resins

The success of the solid phase peptide synthesis developed by Merrifield in the 1960s has resulted in the covalent attachment of chiral ligands onto a functionalized polymer becoming a popular approach. In addition to only slightly cross-linked Merrifield resins (poly(styrenedivinylbenzene)-polymers) [87], other resins such as JandalJEL (polystyrene polymers containing a tetrahydrofuran-derived cross linker) [88], TentaGel (polystyrene-poly(ethyleneglycol-OC_2H_4-$NHCOC_2H_5$)) [89], and other PS-PEG (polystyrene-polyethyleneglycol) resins [90] have been employed successfully for anchoring metal-ligand complexes.

1.5.3. Immobilization onto inorganic supports

Inorganic materials have been used as alternative supports for the immobilization of homogeneous chiral catalysts since mid-1980s. Unlike polymers, inorganic solids prevent the intermolecular aggregations of the active species because of their rigid structure. They do not swell, and are insoluble in organic solvents. The last two properties are interesting in regard to their application as stationary chiral phases in a continuous process. In addition, inorganic supports possess better thermal and mechanical stability under catalysis conditions.

The inorganic supports to immobilize enantioselective catalysts are generally inert porous structures with highly specific surface area. Amorphous oxides, in particular silica and, to a lesser extent, alumina, zirconia or ZnO, are most routinely used. A broad range of such materials with a variation in pore size, pore size distribution and particle size are commercially available or can be synthesized easily [91].

Other commonly applied supports with a more defined structure are clay minerals, pillared clays and LDHs. Pillared clays contain stable metal oxide clusters which separate the layers that build the clay. A two dimensional gallery is thus created with an opening that can be larger than 1 nm. LDHs, often denoted as hydrotalcite-like compounds, belong to the class of synthetic anionic clays. They show a positively charged layered structure with compensating anions between the sheets [92].

Other popular supports include zeolites. These crystalline materials mostly aluminosilicates, have well-defined pores and channels in the micropore range. Zeolite β is a large pore high-silica zeolite with intersecting channels of 0.55 nmx 0.55 nm and 0.76 nm x 0.64 nm [93]. The hypercages (1.3 x 1.3 x 1.4 nm) of EMT are accessible through three elliptical windows with free dimensions of 0.69 x 0.74 nm and two 0.74 nm circular apertures, while the hypocages miss these circular apertures. The pore structure of zeolite Y consists of almost spherical 1.3 nm cavities interconnected through smaller apertures of 0.74 nm [94]. Through steaming, zeolite Y can turn into a mesoporous structure, the so called USY [95]. This channel porosity can be beneficial to prevent hindered mass transport and to enable reactivity towards more bulky molecules.

In contrast to the undefined mesoporosity of a USY zeolite, a rather recent type of regular mesoporous structures is the so called M41S-materials: MCM-41 and MCM-48 possess a uni- and tri-dimensional pore system respectively with pore diameters varying between 1.5 nm to 100 nm [96].

As the thesis mainly deals with mesoporous silica material as the support, brief introduction of mesoporous silica has been given below.

1.6. Mesoporous materials

Even though, zeolites, having pore dimensions of 5 to 7 Å, served the purpose of most of the industrial reactions by providing high surface area, the pore dimensions are not sufficient enough to accommodate broad spectrum of larger molecules. The performance of zeolite systems is limited by diffusion constraints associated with smaller pores.

With the first successful report on the mesoporous materials (M41S) by Mobil researchers [97-100], with well-defined pore sizes of 20-500 Å, the pore-size constraint (15 Å) of microporous zeolites was broken. The high surface area (>1000 m^2/g) and precise tuning of the pores are among the desirable properties of these materials. Mainly these materials used in a new synthetic approach where, instead of a single molecule as templating agent as in the case of zeolites, self-assembly of molecules aggregates or supramolecular assemblies are employed as templating agent. The pores of this novel material are nearly as regular, yet considerably larger than those present in crystalline materials such as zeolites, thus offering new opportunities for applications in catalysis [101] and advanced composite materials [102].

The important members of the M41S mesoporous family are MCM-41, MCM-48 and MCM-50 [103-105]. MCM-41 possess honeycomb arrays of nonintersecting uniformly sized channels with diameters ranging from 15 to 100 Å depending on the template used, the addition of auxiliary organics and the synthesis parameters like synthesis time, synthesis temperature or post synthesis treatments. MCM-48 is a cubic phase with *Ia3d* symmetry consisting of an enantiomeric pair of nonintersecting three-dimensional channel systems that are mutually intertwined. Among the M41S materials, the hexagonally channel oriented MCM-41(Fig. 1.5.) receives much attention than the cubic three dimensionally channel oriented MCM-48, due to the simple synthesis protocols. Moreover, the classical surfactants used in the synthesis of M41S related materials, like the alkyl trimethyl ammonium halides, preferentially form hexagonal or lamellar phases, which imply that the synthesis of high quality MCM-48 is subjected to a very narrow margin. However, the synthesis of MCM-48 with *Ia3d* symmetry is alluring as it has a more appealing structure and offers potential advantages than the MCM-41 material. MCM-50 posses lamellar phases and after surfactant removal the structure usually gets collapsed.

The number of research papers dealing not only with mesoporous silica, but also with other oxides, such as alumina, titania, and zirconia, has grown tremendously during the last decade [107-109]. Obviously when new types of materials such as these are discovered, an explosion of scientific and commercial development swiftly follows, and new investigations on every conceivable aspect of their nature, the synthesis procedures

and synthesis mechanisms, heteroatom insertion, characterization, adsorption, and catalytic properties, rapidly occurs [110].

SBA-15 has recently been synthesized by Stucky and co workers [111], in an acidic medium with poly(alkylene oxide) triblock copolymers, such as poly(ethylene oxide)–poly(propylene oxide)–poly(ethylene oxide) (PEO–PPO–PEO) and found to have uniform and large tubular channels up to 30 nm in diameter [112].

Since SBA-15 also possesses thick pore walls, the hydrothermal stability is much higher than MCM-41. Such features may provide high potential as supports for catalytic applications.

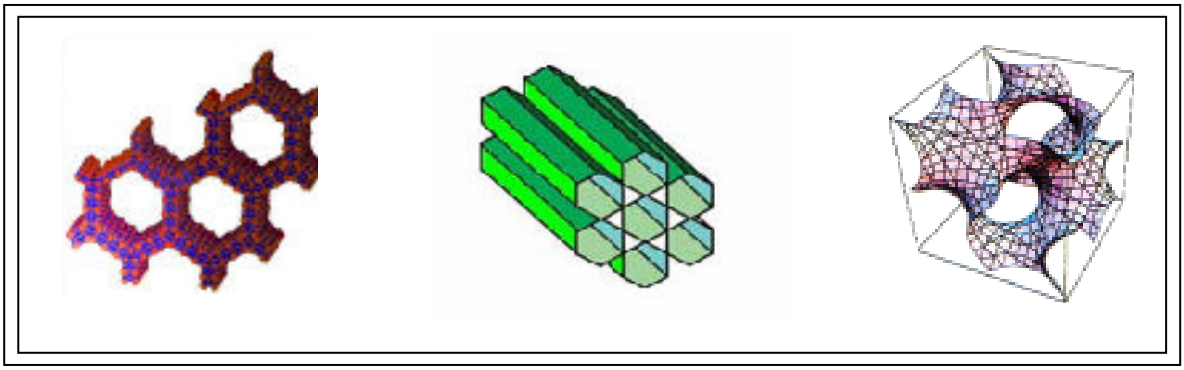

Fig 1.5. Mesoporous siliceous materials

The purpose and advantages of synthesizing mesoporous materials is as follows.

1. To overcome the diffusional constraints with zeolites.
2. Very high surface are (>1000 m^2/g) and pore size distribution (20-100 Å).
3. Good host material for guest species (i.e. heterogenization of homogeneous species or metal complexes on the walls).
4. Easier to monitor the changes made with active species via surface area measurement and pore size distribution experiment.

1.6.1. Synthesis and mechanism of formation

Mesoporous materials such as MCM-41 are invariably synthesized by using organic structure directing agents called templates. *e.g*., cationic surfactants containing long alkyl chain quaternary ammonium compounds containing 10-20 carbons often followed with addition of co-surfactants. Even though synthesis parameters such as temperature and time have a role in the formation of the materials, the surfactant or polymer template certainly plays a dominating factor for obtaining a specific structure. The surfactants have a hydrophilic head group and a long chain hydrophobic tail group, within the same molecule, and in solution they will aggregate and self-organize in such a way so as to minimize the contact between the incompatible ends. Therefore, the mechanism responsible for the formation of M41S materials from its precursors had attracted much scientific attention.

Different synthesis mechanisms have been postulated in the literature to explain the formation mechanism of mesoporous materials.

1.6.1.1. Liquid Crystal Templating (LCT) Mechanism

Mobil researchers proposed two Synthesis mechanisms [97,98]. In the first route, the cationic surfactant species organize into lyotropic liquid crystal phase, which can serve as template for the formation of hexagonal structure. Surfactant micelles aggregate into hexagonal array of rods, followed by the interaction of silicate anions present in the reaction mixture with the cationic head groups of the surfactant species. The condensation of the silicate species further leads to the formation of an inorganic polymeric species. The template is removed by calcination to get hexagonally arranged inorganic hollow cylinders.

In the second route, the hexagonal ordering is assumed to be initiated by the presence of silicate species in the reaction mixture. Chen *et al.* proposed that randomly distributed surfactant micelles interact with silicate oligomers by columbic interactions which results in randomly oriented surfactant micelles surrounded by two or three silica monolayers. These species spontaneously pack into a highly ordered mesoporous phase with an energetically favorable hexagonal arrangement, accompanied by silicate condensation. Further condensation between silicate species on adjacent rods occurs on

heating and the inorganic wall continues to condense to form the stable hexagonal network.

1.6.1.2. Generalized Liquid Crystal Templating Mechanism

Many researchers have tired to explain the possible ways by which a surfactant species interacts with the silica species under various synthesis conditions for the development of mesoporous materials having interesting textual and structural properties: (i) Ionic Route Electrostatic Interaction by Huo et al, (ii) Neutral Templating Route (Hydrogen bonding Interaction) by Tanev and Pinnavaia and (iii) Ligand-Assisted Templating Route (Covalent Interaction) by Antonelli and Ying.

1.6.1.3. Mechanism of formation of SBA-15 molecular sieves

Monnier et al. and Tanev showed that the assembly of mesoporous materials can also be driven by hydrogen bonds in the case of neutral templates such as nonionic poly (ethylene oxide) (PEO) surfactants and inorganic precursors. The assembly of the mesoporous silica organized by non-ionic alkyl-ethylene oxide (alkene oxide) triblock copolymer species in acid media occurs through an (S^0H^+) (X^-I^+) path way. First, alkoxysilane species are hydrolysed at a pH less than 2.

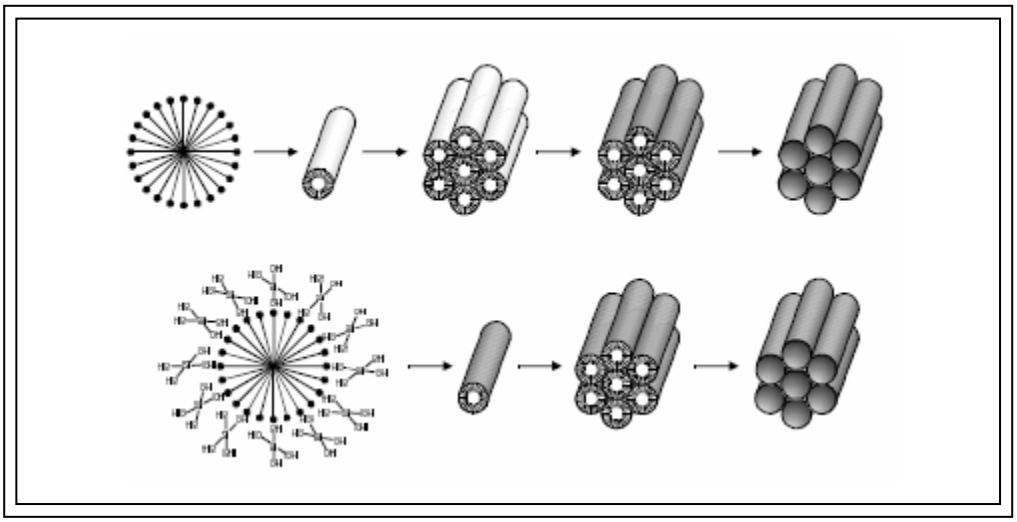

Fig 1.6. Mechanism of formation of mesoporous material

$$Si(OEt)_4 + n\,H_3\overset{+}{O} \xrightarrow[pH < 2]{\text{Hydrolysis}} Si(OEt)_{4-n}(\overset{+}{O}H_2)n + nEtOH$$

This is followed by partial oligomerisation of the silica. The EO moieties of the surfactant in strong acid media associating with hydronium ions

$$REO_m + yHX \xrightarrow{H_2O} REO_{m-y}[(EO)H_3\overset{+}{O}]_y + y\overset{-}{X}$$

Where R = alkyl, poly (propylene oxide) and X- = Cl^-, Br^-, I^-, NO_3^-, $H_ySO_4^{-2+y}$, $H_yPO_4^{-3+y}$

Zhao et al. proposed that the formation of SBA-15 occurs through a scheme where the silica source is first hydrolyzed at low pH to form $Si(OMe)_{4-n}(OH_2^+)n$ species and the PEO moieties of the block copolymer associate with hydronium ions. Then, the charged PEO units and the cationic silica species are assembled together, via Cl^-, by a combination of electrostatic, hydrogen bonding and van der Waals interactions to form $REO^{m-y}[(EOH_3O^+]y\ldots yX^-\ldots.I^+$, which can be designated as $(S^0H^+)(X^-I^+)$. Coordination sphere expansion around the silicon atom by anion (e.g. Cl^-) coordination of the form $X^-{\cdot}Si^-OH_2^+$ may play an important role [113]. Further condensation of the silica species and the organization of the surfactant and inorganic species result in the formation of the lowest energy silica-surfactant mesophase structure allowed by the solidifying inorganic network [114]. Furthermore, the time required for silica mesopore precipitation depends on the acid anion and is found to be the shortest in the presence of Cl^- anion when used in the form of hydrochloric acid. It was shown that the EO-length determines which mesostructure is formed [115]. The length of the hydrophilic EO-block determines the silica mesostructure and influences the wall thickness of SBA-15. The hydrophobic PO-block affects the pore diameter and further, the PO-block length influences the templating ability as a longer PO-block results in more highly ordered domains and better defined particles.

1.7. Immobilization methods

There are different methods of immobilization of metal complexes onto the support depending on the mode of immobilization such as covalent or noncovalent

attachment of the chiral ligand, the metal, or the preassembled complex to the support (Fig. 1.7.)

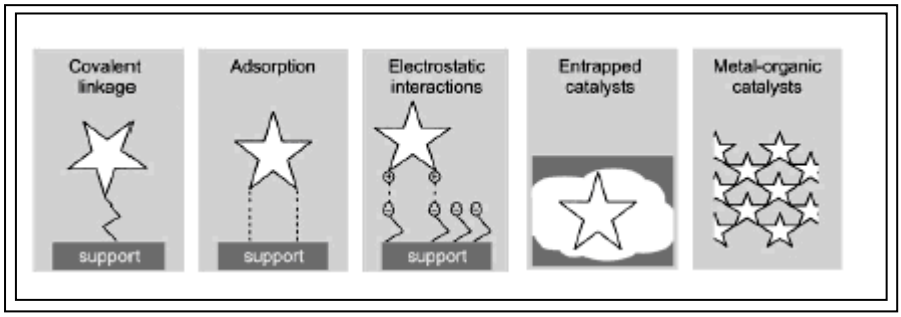

Fig. 1.7. Strategies for the immobilization of chiral homogeneous catalysts (symbolized by stars)

1.7.1. Chemical Grafting

Covalent grafting is one of the most effective methods for the immobilization of metal complexes onto supports. Grafting means attaching the homogeneous complex to the support by a linkage group. The grafting method can also avoid forming dimer or polymer of complex catalyst, and thus achieve isolation of active site, which is often required for asymmetric catalytic reaction. Heckel and Seebach reported that grafted Cr(salen) catalysts can be reused for ten times with constant activity and enantioselectivity for asymmetric hetero-Diels-Alder reactions [116].

The grafting method can also keep optimized configuration of the complexes under heterogeneous reaction condition. Bigi et al. [117] reported that immobilization of Mn(III) salen onto silica through triazine-based linker allows the conformational mobility of the complex, and obtains a high level of asymmetric induction. The presence of the pore, and the surface of the support, may result in unexpected activity and enantioselectivity in the heterogeneous asymmetric catalysis. Zhou et al. [118] grafted chromium binaphthyl Schiff complex onto amine modified MCM-41, and these heterogeneous catalysts were employed for asymmetric epoxidation of cis-β-methylstyrene. The heterogeneous catalyst exhibited higher ee values (73%) than the homogeneous one (54%).

Catalyst grafting is usually carried out via the reaction of silicate precursors with siliceous hydroxyl groups in anhydrous toluene (or $CHCl_3$) under reflux. The supports should be dehydrated in high vacuum or by azeotropic dehydration with toluene as described in Scheme 1.2, where the X in silicate precursor represents organic groups.

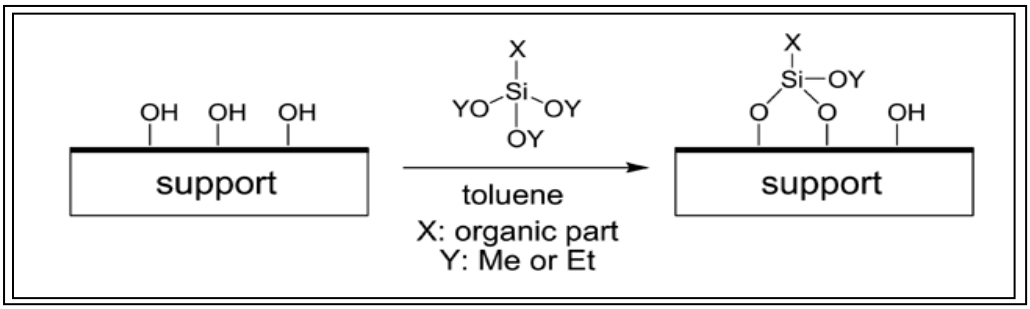

Scheme 1.2. Grafting organic compound onto inorganic oxide surface via the reaction with surface OH groups [119]

Anchoring binap through the 4,4'-position to the inner surface of a mesoporous SBA-15 has also been shown to be especially rewarding (Fig. 1.8)). Methyl acetoacetate was hydrogenated to β-hydroxy ester with 98.6% ee and the chiral catalyst could be recycled three times with full conversion and a slightly reduced ee value (96.2–98.6%) [120].

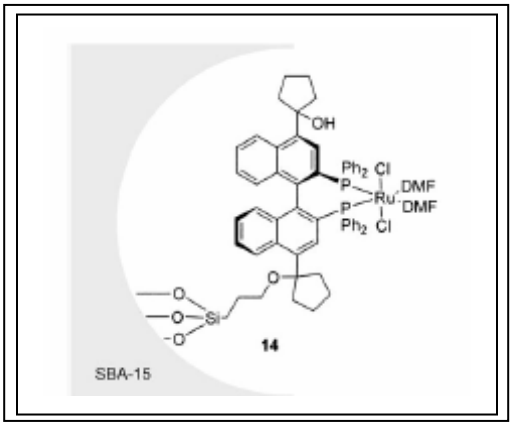

Fig. 1.8. Ru complex immobilized in a pore of SBA-15

1.7.2. Adsorption or Ion-pair Formation

The easy preparation of these types of immobilizations is a clear advantage, but their sensitivity to solvent effects is an important drawback.

Charges were created on silica via reaction with a SO_3^--terminated silylating agent. The positively charged Rh(I)-complexes were then ion-exchanged and used in hydrogenations, where leaching could be avoided in toluene and water but not in methanol [121].

In addition to the ways mentioned already above to heterogenize chiral salen complexes via a covalent link, Piaggio et al. [122] described an immobilization method for these complexes based on ion exchange. Salen ligands were contacted with a Mn-exchanged Al-MCM-41, in such a way that 10% of Mn was ligated. The turnover frequency of the heterogeneous catalyst was reported to be higher than one of the homogeneous reaction, even though slightly less chemo- and enantioselective.

Alternatively, the *tert*-butyl-salen complexes were immobilized by simple impregnation on Al-MCM like structures [123]. Guest/host interactions, mainly between the aromatic rings of the complex and the internal surface silanol groups of the walls of the mesopores were found to be strong enough to prevent leaching of the complex. The epoxidation of 1,2-dihydronaphthalene proceeded with exactly the same activity and enantioselectivity (but lower yields) as the homogeneous reference reaction. No complex leaching was observed, but the regeneration experiments were not reported.

In a third approach, the the *tert*-butyl substituted salen complex was ion-exchanged with a Na-laponite clay and used in the same epoxidation [124]. Showing similar activity as the homogeneous complex, the ee was slightly reduced when using the clay supported complex. Since addition of pyridine as axial ligand did not change the ee of the heterogeneous reaction, it was speculated that the clay, itself acted as an axial ligand. In contrast to the absence of leaching, the regeneration experiment showed decreased activities and ee. A gradual decomposition of the salen ligand- probably by oxidation- was postulated as the main reason, in addition to the coke formation when applying certain reactants.

Layered double hydroxides (LDHs) were used to retain a sulfonated BINAP-complex- bearing 4 negative charges – via coulombic interactions [125]. Hydrogenation of dimethylitaconate proceeded with same rate and ee as the homogeneous reaction. Similar ion exchange on organic resins resulted in inactive catalysts, alternative exchange methods failed and the use of a Zn, Al-NO_3 LDH strongly decreased ee in the

hydrogenation of dimethylitaconate. The importance of the surface properties of the support was confirmed when the unmodified Ru-BINAP complex was impregnated on zeolites [126, 127]. Only one type of zeolite β, with small particle size so that monolayer coverage of the particles was created resulted in a catalyst with good activity for hydrogenation of MAA.

Surprising results were reported by Augustine et al. [128-130]. These authors used heteropoly acid as a tethering agent for a whole set of support/ catalyst combinations. The concept is claimed to be generally applicable as proved by the variety of systems prepared: montmorillonite, carbon, aluminum and lanthana were used as supports, while P/W, Si/W and Si/Mo heteropolyacids were applied as tether and DIPAMP, BPPM, dppb, Wilkinson's catalyst, ProPHOS, Me-DUPHOS and BINAP were used as catalysts in chiral allylation and hydrogenations. The preparation of heterogeneous catalysts simply involves mixing of supports with the heteropolyacid prior to adding a solution of the transition metal complex. None of the systems reported showed any leaching even after 15 cycles, despite the fact that the ligands are not modified.

1.7.3. Encapsulation in Porous Supports

Molecular sieves with three-dimensional channel systems may provide site isolation as well as shape selectivity. Complexes encapsulated in zeolite pores, but not necessarily bound to the surface, are often referred to as "ship-in-bottle" complexes. Encapsulation is one of the most often used methods for homogeneous catalyst immobilization, and is an effective way to mimic the homogeneous asymmetric catalysis. This method brings no changes to the chemical properties of the immobilized catalyst except for the steric confinement of porous supports [131]. Encapsulation of transition metal complexes in the nanopores of molecular sieves mainly depends on the sizes of both the complex and the pore. The site match of the two is very important to prevent the immobilized catalysts from leaching during reactions. Regular pores or cages are essential requirements for the support. Zeolites are a class of excellent candidates for encapsulation of the homogeneous catalysts [63].

The incorporation of transition metal complexes in porous supports, such as faujasite zeolites, has been known for a long time. This method is typically used to immobilize metal Salen complexes within the supercages of faujasite type zeolites [132, 133]. To avoid the leaching of catalyst during the reaction, a larger transition metal complex than the pore size of the zeolite is encapsulated into the supercage of the zeolite through following three methods [134, 135].

1.7.3.1. Coordination of the Ligands with Transition Metal Atoms Previously Introduced into the Pores of Zeolites (Flexible Ligand Method)

This approach is based on the principle that the free ligands are flexible enough to pass through the restricting windows and get into the larger cages of the host support. The ligand coordinates to the transition metal atoms previously exchanged onto the host support, zeolite, producing the homogeneous complex catalyst in the zeolite cage. The encapsulation of chiral metal-salen complexes in zeolite is shown in scheme 1.3. [135].

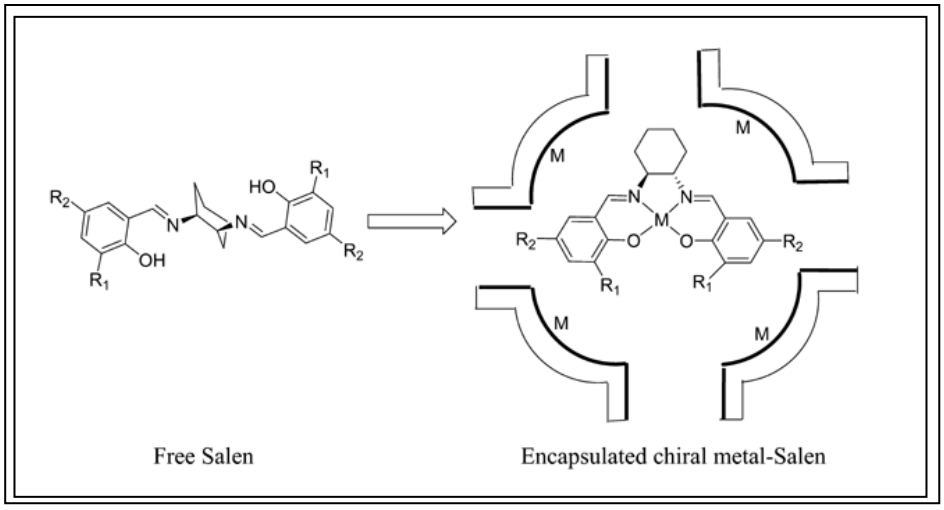

Scheme 1.3. Zeolite-encapsulation of chiral metal-salen complex via flexible ligand method

It is reported that $[Rh(COD)L]^+$ complexes (L = L-prolinamide or N-tert-butyl-Lprolinamide) were successfully encapsulated in NaY zeolite [136]. Yang et al have reported asymmetric reactions on chiral catalysts entrapped within a mesoporous cage of SBA-16 [137].

1.7.3.2. Assembling Ligands from Smaller Species Inside the Nanopores (Ship-in-Bottle Method)

If the transition metal complex is formed in limited reaction steps, assembly of the ligand from small species within the pores is preferred. Generally, the metal is introduced into pores of supports by ion exchange, or by pre adsorption of a labile metal complex, and followed by reaction of the smaller molecular fragments with metal ions to form metal complex within the pores. The manganese-*trans*-(R,R)-1,2-bis(salicyideneamino)-cyclohexane complex was encapsulated within the pores of zeolite Y or EMT by this ship-in-bottle method [138, 139]. Initially, the zeolite was partially ion exchanged with Mn^{2+} followed by addition of the building units of the chiral ligand (salicylaldehyde and *trans*-(R, R)-1, 2- diaminocyclohexane) as shown in scheme 1.4. The Mn-salen complex was formed in the zeolite supercage and no leaching of active site from the interior of the zeolite occurred during the epoxidation process.

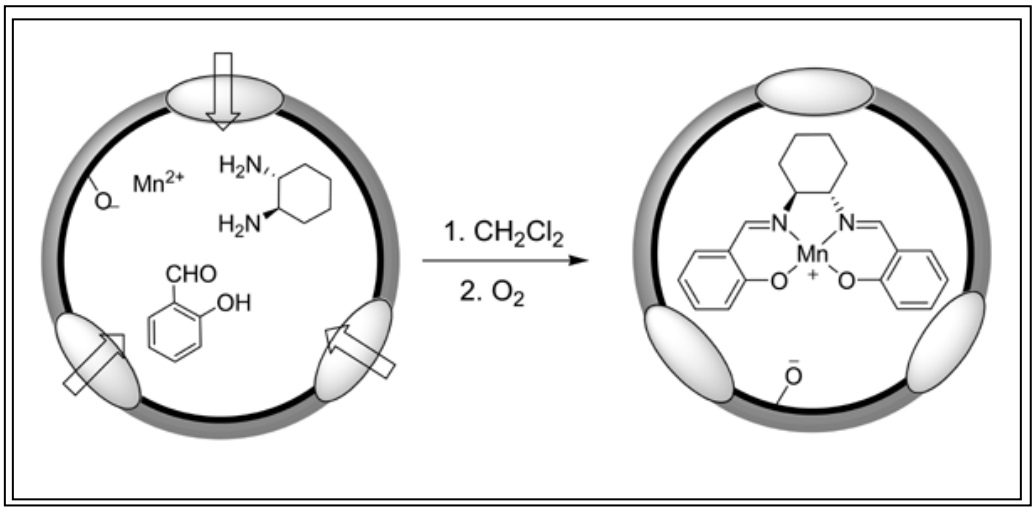

Scheme 1.4. Immobilization of Mn(III)(salen) complex in zeolite Y by encapsulation [138]

1.7.4. Organic-Inorganic Hybrid

In the attempt to design a chiral heterogeneous catalyst, many approaches have been explored, including attaching the catalysts to organic polymers, dendrimers, membranes, and porous inorganic solids by covalent bonding, electrostatic interaction or

confinement in the compartments of the supports. However, the catalysts obtained by the aforementioned methods are still phase-separated, nonuniformly distributed, and leaching of the active sites is often observed. In contrast, organic-inorganic hybrid materials with both organic and inorganic molecules as building blocks of an infinite framework are very promising in the heterogeneous catalysis. Alternation of the kind and concentration of the organic/inorganic parts can result in materials with different hydrophobic/hydrophilic and mechanical properties. By synthesizing a porous hybrid with chiral group as the building block, chiral catalyst with more uniformly distributed active sites may be obtained. In the past few years, two kinds of hybrid porous materials have been applied in the chiral catalysis (i.e., porous hybrid oxides and coordination polymers).

1.7.4.1. Hybrid Chiral Catalyst Synthesized Through Sol-Gel Method

Sol-gel chemistry [139,140] has been well developed and widely used for the preparation of materials with specific properties. Owing to the mild reaction conditions involved in this process, it becomes one of the most promising routes to obtain hybrid organic-inorganic materials. Polysilsesquioxanes [141-143] resulting from sol-gel hydrolysis of silylated organic molecules are potential candidates for heterogeneous catalysis, since they provide the possibility of covalent inclusion of many kinds of organic groups into rigid amorphous silica networks (scheme 1.5).

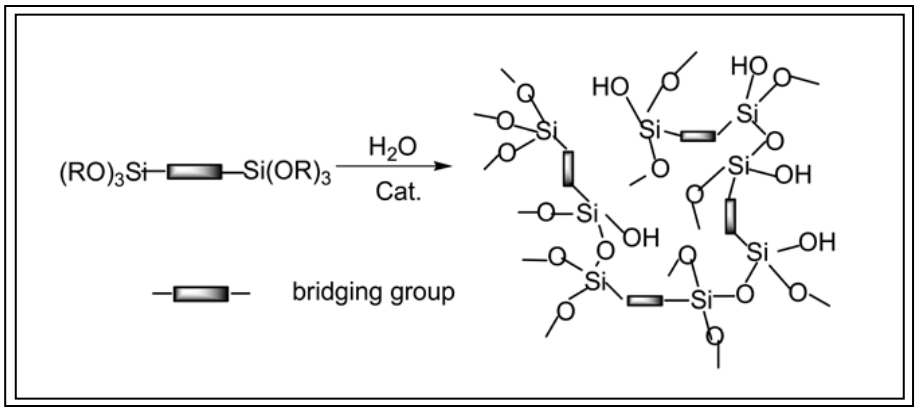

Scheme 1.5.

Such hybrid solids can be well defined at both the molecular scale and the nanoscale. Moreover, the texture properties (porosity, specific surface area, pore arrangement) of the resulting solid catalysts could be adjusted by careful tuning of the kinetic parameters of the sol-gel process (temperature, pH, additive, etc.). With chiral molecule incorporation, the 3-D network of the solid materials may posses some special characters and, thus, unique catalytic activity and enantioselectivity. In the past few years, however, only a few examples of hybrid chiral solids with catalytic properties were reported.

Adima et al. [144, 145] reported the synthesis of chiral hybrid catalysts by sol-gel hydrolysis of mono- and bis-silylated diaminocyclohexanes in scheme 1.6. In the asymmetric hydride transfer reduction of acetophenone, the solid catalysts showed enhanced ee value compared to the homogeneous catalyst.

1.7.4.2. Hybrid Chiral Catalysts Prepared from Coordination Polymers

Coordination polymers are another big family of porous hybrids prepared from the coordination of metal ions to organic "linker" moieties. Such solids have shown their potential to control the host-guest chemistry of the framework by tailoring the various chemical building blocks [146-152]. By varying the bridging organic groups, porous hybrids with a high degree of functionalization and tunable pore size can be obtained. The main problem of this kind of hybrids is their low stability. However, because of the relative ease to incorporate accessible chiral groups compared to porous oxides, coordination polymers with chiral building blocks are promising candidates for enantiomeric separation [153] and catalysis [154, 155], under moderate conditions. However, until now, very few studies have demonstrated their properties in catalysis, especially in chiral catalysis.

Evans and coworkers reported a more active porous chiral porous Zr phosphonate containing bisphosphine (BINAP) derivatives (scheme 1.7) [155]. By refluxing Ru complexes of two different BINAP derivatives 2,2-bis(diphenylphosphino)-1,1-binaphthyl-6,6-bis (phosphonic acid) and 2,2-bis(diphenylphosphino)-1,1-binaphthyl-4,4-

bis(phosphonic acid) with $Zr(O^tBu)_4$ in MeOH, two kinds of porous chiral solids were obtained. In the asymmetric hydrogenation of aromatic ketones, high ee values in the range of 90.6-99.2% were obtained for the substrates tested.

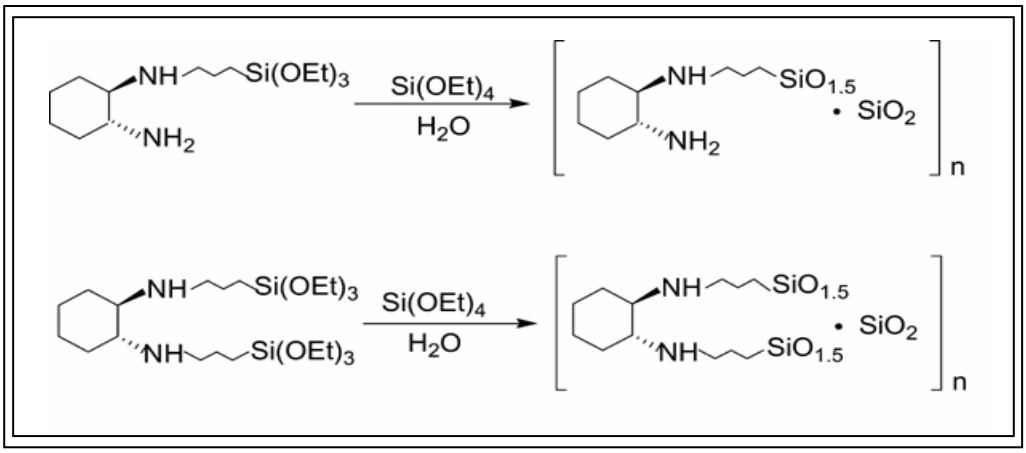

Scheme 1.6.

1.7.5. Supported Liquid Phase

A genuine hybrid of homogeneous and heterogeneous catalyst type is formed by an SLP where a solution of the catalyst is attached to the surface of a porous support and contacted with a solvent phase that contains the reagent. The triphasic system imposes serious solvent restrictions on reagents and catalysts, and mass transfer between the two liquid phases might be problematic due to the generally small contact area.

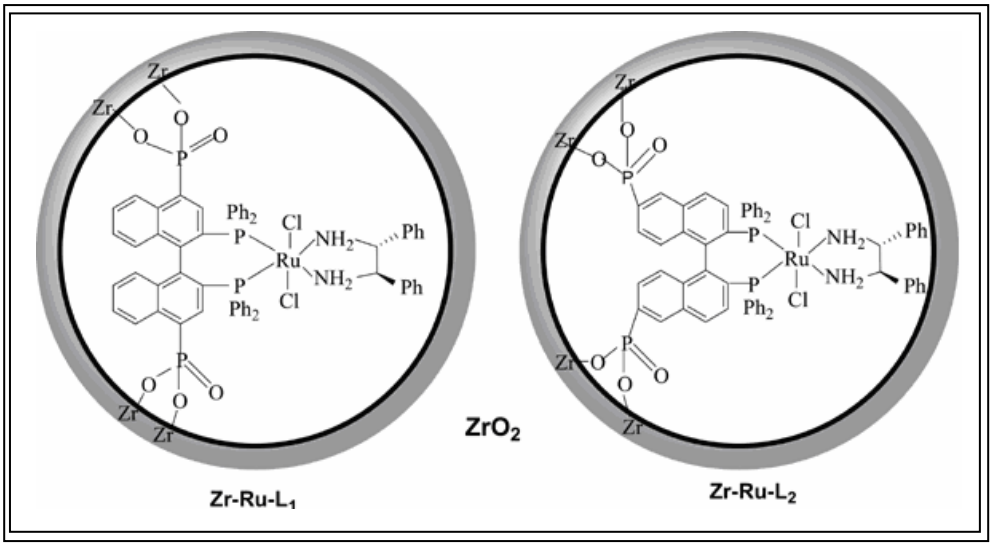

Scheme 1.7.

One of the best known heterogeneous enantioselective catalysts of this kind is the SAP (supported aqueous phase)-Ru-BINAP-4(SO_3Na) system developed by Wan and Davis [156-158]. Starting from a sulfonated Ru-BINAP with activities in methanol compared to the nonsulfonated analog (TOF = 131 h^{-1}; 96 % ee), biphasic hydrogenation of the naproxen precursor in water/ ethylacetate resulted in a very slow reaction due to low solubility of the substrate in the water phase. The activity increased 50 times upon using a SAP catalyst (TOF= 18.2 h^{-1}; 70% ee), which is due to the increase in interfacial surface area. The ee was limited by the presence of water which caused the loss of the Cl-ligand of the complex through aquation of the Ru-Cl bond. On the other hand, a certain amount of water was needed in the SAP system in order to give the complex some rotational mobility, crucial to reach the activity. Ru-analysis and the absence of reactivity in the filtrate proved that the system was really heterogeneous. The SAP-catalyst was later improved by changing the water film on the glass beads for an ethylene glycol film (SLP); the TOF tripled compared to the earlier reported SAP and remained only 2-2.5 times below the TOF of the homogeneous analogue [159]. An ee of 87.7%, equaling the one obtained under homogeneous conditions, was reached. The Ru-leaching, due to significant solubility of ethylene glycol in organic phase, was eliminated by using a cyclohexane/chloroform mixture as organic phase. Enantioselectivities remained comparable to those of the homogeneous systems, and the activity decreased only slightly compared to the earlier SAP. Now a days supported ionic liquid phase strategy is being used for the immobilization of metal complexes onto ionic liquid modified supports (Fig. 1.9) because of the high solubility of metal complexes in ionic liquids [160-162].

1.7.6. Modification of an Achiral Heterogeneous Catalyst with a Chiral Auxiliary

The most known and successful application in this area are the Ni-tartarate and the Pt-cinchonidine systems.

An interesting concept has been developed by Hutchings et al. [163] and applied in the first example of a heterogeneous enantioselective gas phase reaction. A chiral acidic zeolite was created by loading one molecule of R-1,3-dithiane-1-oxide per supercage of Zeolite Y, either during, or after zeolite synthesis. In competing experiments, the dehydration of S-butan-2-ol was found to be up to 39 times faster than

that of the R-enantiomer, much higher than what could be expected from the conversions of the separate enantiomers. Using computational simulation methods this was attributed to higher binding energy of the S-enantiomer on the catalytic site [164]. Later a specific interaction was suggested between the dithiane oxide and both the extra-framework aluminum and the Bronsted acid site associated with the framework aluminum [165]. A similar effect was observed with S-2-phenyl-1, 3-dithiane 1-oxide as modifier.

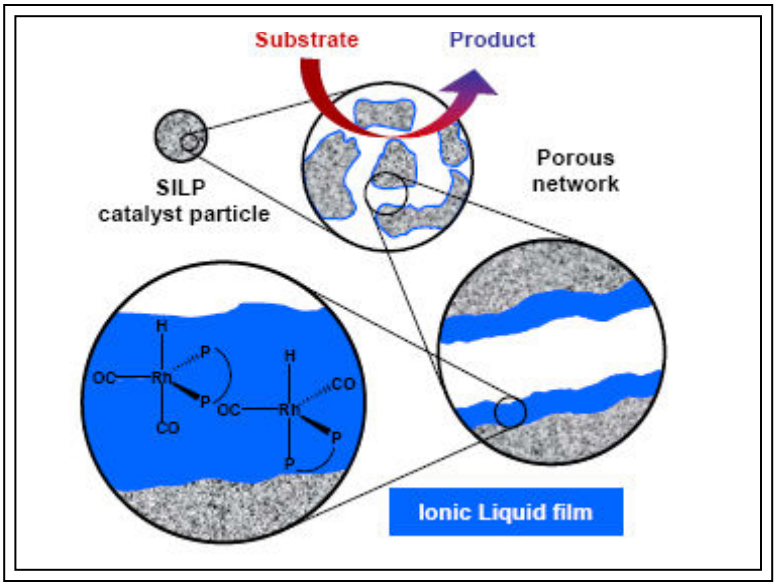

Fig 1.9. Pictorial representation of a supported ionic liquid phase catalyst system

A variety of Ti-catalysts, combined with various chiral auxillaries and supported on alumina, silica, zirconia, clays and pillared clays, was used in the oxidation of sulfides [166]. The best results, approaching the ones obtained under homogeneous conditions, were realized with the pillared clays (based on montmorillonite). This was ascribed to the ease of complexation-similar to the homogeneous analogue of the titanium hydroxyl oligomer with the reactant, oxidant and chiral auxiliary in the available interlayer space (~ 13 Å), and to the presence of Lewis acidity in the pillared clay. This hypothesis was confirmed by the inactivity observed when using larger auxiliaries.

1.7.7. Achiral Metal Catalysts on Chiral Supports

In 1932, Pt and Pd were deposited on the enantiomers of quartz single crystals, and ees of 10 % were reached in hydrogenation. Later this was also done with natural fibers such as silk [167].

Some degree of success in catalysis was also accomplished by using the chiral polymorph of zeolite β [168]. This polymorph contains helical pores which are either left- or right-handed. By applying a chiral template in zeolite synthesis, a sample could be prepared that was enriched in this chiral polymorph. Very low but still significant ee's of 5% were reported for the hydrolysis of trans-stilbene oxide.

1.8. Confinement Effect on Enantioselectivity

The heterogenization (or immobilization) of chiral homogeneous catalysts, mostly transition metal complexes immobilized on/in porous supports (mesoporous silica and zeolites) are very different from their homogeneous analogues. For some catalysts immobilized via chemical bonding, their activity and enantioselectivity are often decreased because the strong bonding and rigid tether may slightly change the structure of the catalysts. So it is desired to use longer and more flexible tether to immobilize the catalyst. On the other hand, the stability and enantioselectivity can be improved for the chemically immobilized catalyst because the active sites can be isolated, while the active site polymerization is one of the main causes for the deactivation of homogeneous catalysts.

A more interesting phenomenon is that the enantioselectivity can be enhanced when the homogeneous catalysts are assembled in the pores or on the surfaces of solid supports (e.g., microporous and mesoporous materials). This phenomenon has been ascribed to the confinement effect, which could be simply interpreted as the reactant within the pores leads to a larger influence on the chiral directing groups on the orientation of the reactant relative to the catalyst center compared with homogeneous solution [169, 170]. Generally, the confinement effect is a result of the various interactions involved in the chiral reactions in the pores or on the surfaces. Essentially the confinement effect is a reflection of the interaction on the transition states of the chiral products. The confinement effect may increase the enantioselectivity (positive effect) or

decrease the enantioselectivity (negative effect) depending on how the interaction changes the transition states of the chiral products.

1.8.1. Positive Effect

There have been a quite few examples which show that the enantioselectivity is increased when the homogeneous catalyst is immobilized in the pores of the porous supports. Corma et al. found that the steric constraints of the support (especially using zeolite as support) have positive effect on the catalytic performance (enantioselectivity and activity) compared to the homogeneous catalyst [171]. The reaction catalyzed by the immobilized catalysts takes place in the confined space of the pores. The interaction of the catalyst with the electrostatic fields in the pores may assist the formation of the catalytic active species, which may be the main reason for the improved catalytic performance of the immobilized chiral transition metal complexes in the porous material.

Raja et al. [172] designed a homogeneous, metal-containing ferrocenyl precursor, which possesses functionality capable of reacting directly with a silica surface. The catalysts were tested in the one-step hydrogenation of ethyl nicotinate and E-α-phenyl cinnamic acid. Both the heterogeneous catalyst and the homogeneous catalyst gave the desired products under mild conditions. However, the homogeneous catalyst resulted in a racemic product, while the catalyst anchored to MCM-41 exhibits 96.5% ee. This remarkable change in enantioselectivity demonstrates the profound importance of confinement effect in the chiral catalysis. These results imply that the porous support has the potential for creating an efficient solid chiral catalyst by carefully designing the active sites.

1.8.2. Negative Effect

It has been reported that many homogeneous catalysts show considerable drop of the enantioselectivity after they are immobilized on the surfaces and in the pores of solid supports. The following examples represent the phenomena of the negative effect on enantioselectivity.

The heterogeneous Cr(salen) catalysts ion-exchanged into zeolite EMT [173] gave the greatly reduced ee value of 16%, compared to their homogeneous result of 68% for ring-opening reaction. Similarly, chiral Mn(III) salen complex immobilized onto silica gel [174] were used for asymmetric catalytic epoxidation of 1-phenylcyclohexene with m-CPBA/NMO. The heterogeneous catalyst only showed 58% ee value, however, the ee values reached up to 90% under homogeneous conditions. The decrease in ee value is mainly due to the unfavorable confinement effect caused by the support. Grafted Mn(III) salen on silica only produced 0-15% ee for asymmetric epoxidation of unfunctionalised olefins [166], while the homogeneous analogue usually gives much higher enantioselectivity. Obviously, the support shows unfavorable effect on the chiral selectivity.

1.8.3. Kinetic Insight of the Confinement Effect

Why do the pore and surface have so great confinement effect on the enantioselectivity for the heterogeneous asymmetric catalytic reactions? This issue can be discussed based on kinetics of the chiral reactions. Fig. 1.10. schematically shows how the difference between the transition states is correlated to the enantioselectivity. For most chiral reactions the energy difference between the *R*-product and the *S*-product transition states is very small, less than 15 kJ/mol [175, 176]. It is this small energy difference that results great changes in enantioselectivity.

From the viewpoint of kinetics, it could be possible to explain the dramatic change (either increase or decrease) of the enantioselectivity for a homogeneous catalyst immobilized in a pore or on the surface of a solid catalyst. As schematically described in Fig. 1.11., assuming a homogeneous chiral catalyst with moderate enantioselectivity is immobilized into pores of a mesoporous materials, such as MCM-41, its enantioselectivity may have three possible cases: increase, decrease, and unchanged. For the unchanged case, the pore/surface interaction involved in the chiral reaction is negligible. When the interaction is beneficial to enhancing the energy difference between the S-product and the R-product, the enantioselectivity is increased, namely the pore exerts the positive effect or the R-effect on the chiral reaction.

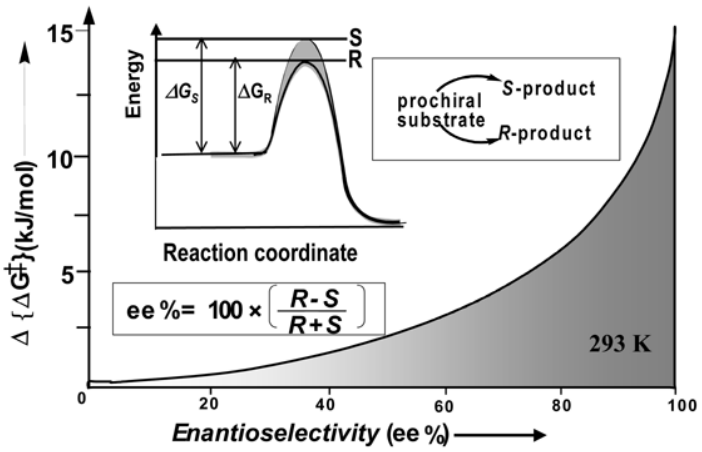

Fig. 1.10. Difference in the Gibbs free energy change for the *R* and *S* transition states (at 293 K) as a function of product enantioselectivity for the reaction of a prochiral substrate for the *R* and *S* enantiomers. A subtle difference (less than 15 kJ/mol) in the energy for the *R* and *S* transition states makes a big difference in the enantioselectivity [176]

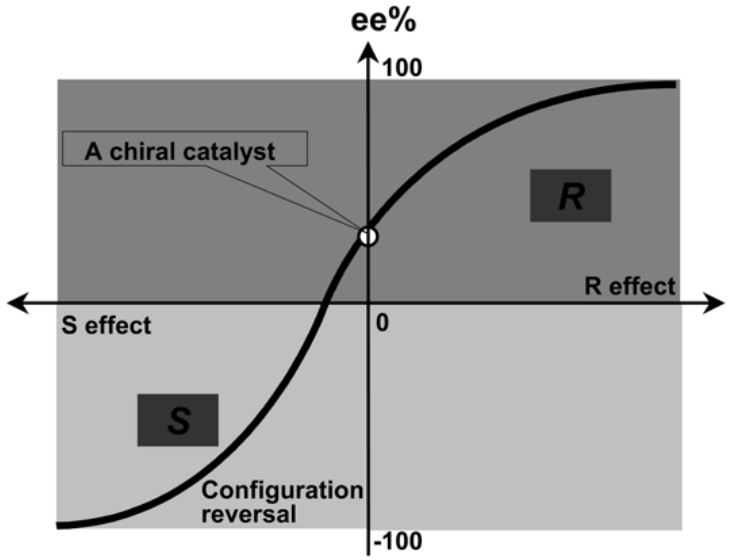

Fig. 1.11. A schematic description of the pore/surface effect on enantioselectivity for a chiral catalyst immobilized into the porous materials

On the other hand, when the interaction tends to decrease the energy difference between the two states, the enantioselectivity is decreasing, even to zero (racemic products), when the energy difference is approaching to zero. Furthermore, if the energy

difference between the two transition states is reversed, the S-product becomes the major product and the configuration reversal occurs (S-region in Fig 1.11). This can be referred to as negative effect or the S-effect.

This overview suggests that the heterogeneous chiral catalysis is promising to make a significant impact in the industrial synthesis of chiral compounds. A number of excellent examples have demonstrated that the surface and the pores of the solid supports exert evident effect, called confinement effect, on both the activity and enantioselectivity. Interestingly, the confinement effect can significantly increase the enantioselectivity for some chiral reactions in the pores. The enantioselectivity could be improved by tuning the confinement effect based on the molecular designing of the pore/surface and the catalysts according to the requirements of chiral reactions. The enantioselectivity, activity, and stability are needed to be significantly improved for most heterogeneous chiral catalysts before these catalysts are widely applied in industrial production of the chiral compounds.

1.9. References

1. M.M. Cohen, Am. J. Med. Genet. 101 (2001) 292.
2. W. Mackwald, Asymmetric Syntheis, Ber. Dtsh. Chem. Ges., 37 (1904) 1368.
3. See, for example: a) M. Gardner, Ed.; The New Ambidextrous Universe, 3rd Ed. W. H. Freeman & Co. New York, 1990; b) E. Heilbronner, J.D. Dunitz, ed.; Reflections on Symmetry, VHCA, Bassel, 1993; c) R. Hoffmann, Ed.; The Same and Not The Same, Columbia University Press, New York, 1995.
4. L. Pasteur, Ann. Chim. Phys. 24 (1848) 442.
5. (a) T. Eriksson, S. Björkman, P. Höglund, Eur. J. Clin. Pharmacol. 57 (2001) 365; (b) S. Sleijfer, W.H.J. Kruit, G. Stoter, Eur. J. Cancer 40 (2004) 2377.
6. (a) A.N. Collins, G.N. Sheldrake, J. Crosby, Eds. Chirality in Industry, John Wiley & Sons: Chichester, 1992; (b) K.G. Gadamasetti, Ed.; Process Chemistry in the Pharmaceutical Industry; Marcel Dekker: New York, 1999; (c) H.U. Blaser, F. Spindler, M. Studer, Appl. Catal. A: 221 (2001) 119; (d) H.U. Blaser, E. Schmidt, Eds.; Asymmetric Catalysis on Industrial Scale-Challenges, Approaches and Solutions, Wiley-VCH: Weinheim, 2004.
7. I. Agranat, H. Caner, J. Caldwell, Putting Chirality to Work: The Strategy Of Chiral Switches. Nat. Rev. Drug Discovery, 2002, 1, 753.
8. J.M. Keith, J.F. Larrow, E.N. Jacobsen, Adv. Synth. Catal. 343 (2001) 5.
9. J. Jaques, A. Collet, S.H. Wilen, Enantiomers, racemates, and resolutions, Wiley, New York, 1981.
10. T. Vries. H. Wynberg, E. Van Echten, J. Koek,; W. Ten Hoeve, R.M. Kellogg, Q.B. Broxterman, A.J. Minnaard, B. Kaptein, S. Van der Sluis, L. Hulshof, J. Kooistra, Angew. Chem. Int. Ed. 37 (1998) 2349.
11. Reviews: (a) H.B. Kagan, J.C. Fiaud, (Eds.: E.L. Eliel, J.C. Fiaud), Topics in Stereochemistry, Willey, New York, 1988; Vol. 18, pp 249; (b) A.H. Hoveyda, M.T. Didiuk, Curr. Org. Chem. 2 (1998) 537.
12. (a) R. Noyori, M. Tokunaga, M. Kitamura, Bull. Chem. Soc. Jpn. 68 (1995) 36; (b) U.T. Strauss, U. Felfer, Tetrahedron Asymmetry, 10 (1999) 107.
13. (a) E. Vedejs, X. Chen, J. Am. Chem. Soc. 119 (1997) 2584; (b) J. Eames,

Angew. Chem. Int. Ed. 39 (2000) 885.

14. J. Seyden-Penne, Chiral auxiliaries and ligands in asymmetric catalysis, Wiley, New York, 1995
15. (a) A.M. Kibanov, Nature 409 (2001) 241; (b) J. Wagner, R.A. Lerner, C.F. Barbas, Science 270 (1995) 1797.
16. M.T. Reetz, Methods in enzymology 388 (2004) 238.
17. A. Berkessel, H. Gröger, Asymmetric Organocatalysis: From Biomimetic Concepts to Applications in Asymmetric Synthesis, New York, Wiely, 2005.
18. P.I. Dalko, L. Moisan, Angew. Chem., Int. Ed. 40 (2001) 3726.
19. R. Noyori, Angew. Chem. Int. Ed. 41 (2002) 2008.
20. I. Ojima, Catalytic Asymmetric Synthesis, 2nd ed., Wiley-VCH, Inc, New York, 2000.
21. E.N. Jacobsen, A. Pfaltz, H. Yamamoto, Comprehensive Asymmetric Catalysis I-III, Springer-Verlag, Berlin Heidelberg, 1999.
22. B. Cornils, W.A. Herrman, Applied Homogeneous Catalysis with Organometallic Compounds, VCH, Weinheim 1996.
23. R. Noyori, Asymmetric Catalysis In Organic Synthesis, John Wiley & Sons, Inc, New York, 1994.
24. F. Fache, E. Schulz, L. Tommasino, M. Lemaire, Chem. Rev. 100 (2000) 2159.
25. J.K. Whitesell, Chem. Rev. 89 (1989) 1581.
26. H. Brunner, W. Zettlmeier, Eds. Handbook of Enantioselective Catalysis; VCH: New York, 1993.
27. B.M. Trost, PNAS 101 (2004) 5349.
28. J.A. Osborn, F.S. Jardine, J.F. Young, G. Wilkinson, J. Chem. Soc. (1966) 1711.
29. W.S. Knowles, M.J. Sabacky, B.D. Vineyard, J. Chem. Soc. Chem. Commun. (1972) 10.
30. T.P. Dang, H.B. Kagan, J. Chem. Soc. Chem. Commun. (1971) 481.
31. H.B. Kagan, T.P. Dang, J. Am. Chem. Soc. 94 (1972) 6429.
32. W.S. Knowles, M.J. Sabacky, B.D. Vineyard, D.J. Weinkauff, J. Am. Chem. Soc. 97 (1975) 2567.

33. W.S. Knowles, Adv. Synth. Catal. 345 (2003) 3.
34. W.A. Nugent, T.V. Rajan Babu, M.J. Burk, Science 259 (1993) 479.
35. A. Miyashita, A.Yasuda, H. Takaya, K. Toriumi, T. Ito, T. Souchi, R. Noyori, J. Am. Chem. Soc. 102 (1980) 7932.
36. R. Noyori, Adv. Synth. Catal. 345 (2003) 15.
37. D. Askin, Curr. Opin. Drug Discovery Dev. 1 (1998) 338.
38. R. Noyori, in Asymmetric Catalysis in Organic Synthesis (Wiley-Interscience, New York), (1994) p 16.
39. R. Noyori, Science 248 (1990) 1194.
40. R. Noyori, Acc. Chem. Res. 23 (1990) 345.
41. H.U. Blaser, H.P. Buser, K. Loers, R. Hanreich, , H.P. Jalett, E. Jelsch, B. Pugin, H.D. Schneider, F. Spindler, A. Wagmann, Chimica 53 (1999) 275.
42. T. Katsuki, K.B. Sharpless, J. Am. Chem. Soc. 102 (1980) 5974.
43. J.M. Klunder, T. Onami, K.B. Sharpless, J. Org. Chem. (1989) 54 1295.
44. W.P. Shum, M.J. Cannarsa, Chirality Ind. 2 (1997) 363.
45. W. Zhang, J.L. Loebach, S.R. Wilson, E.N. Jacobsen, J. Am. Chem. Soc. 112 (1990) 2801.
46. E.N. Jacobsen, W. Zhang, L.C. Muci, J.R. Ecker, L. Deng, J. Am. Chem. Soc. 113 (1991) 7063.
47. R. Irie, K. Noda, Y. Ito, N. Matsumoto, T. Katsuki, Tetrahedron Lett. 31 (1990) 7345.
48. H. Sasaki, R. Irie, T. Hamada, K. Suzuki, T. Katsuki, Tetrahedron 50 (1994) 11827.
49. U. Gerlach, J. Brendel, H.-J. Lang, E.F. Paulus, K. Weidmann, A. Bru¨ggemann, A. Busch, H. Suessbrich, M. Bleich, R. Greger, J. Med. Chem. 44 (2001) 3831.
50. P. Pichen, E. Dunach, M.N. Deshmukh, H. B. Kagan, J. Am. Chem. Soc. 106 (1984) 8188.
51. X. Zia, X. Li, L. Xu, Y. Li, Q. Shi, T.L. Terry, A. Yeung, C.W. Yip, X. Yao, A.S.C. Chan, Adv. Synth. Catal. 346 (2004) 723 and the references cited therein.
52. K. Maruoka, in Catalytic Asymmetric Synthesis, ed. I. Ojima, (Wiley-VCH, New York), (2000) pp. 467.

53. N. Yoshikawa, Y.M.A. Yamada, J. Das, H. Sasai, M. Shibasaki, J. Am. Chem. Soc. 121 (1999) 4168.

54. N. Kumagai, S. Matsunaga, T. Kinoshita, S. Harada, S. Okada, S. Sakamoto, K. Yamaguchi, M. Shibasaki, J. Am. Chem. Soc. 125 (2003) 2169.

55. F. Agbossou, J.-F. Carpentier, A. Mortreux, Chem. Rev. 95 (1995) 2485.

56. A.L. Casalnuovo, T.V. Rajan Babu, Chirality Chem. 2 (1997) 309.

57. M. Hatano, M. Yamazaka, K. Mikami, Eur. J. Org. Chem. (2003) 2552.

58. S. Huo, J.-C. Shi, E. Negishi, Angew. Chem., Int. Ed. Engl. 41 (2002) 2141.

59. M.B. Carter, B. Schiott, A. Gutie´rrez, S.L. Buchwald, J. Am. Chem. Soc. 116 (1994) 11667.

60. X. Verdauger, U.E.W. Lange, S.L. Buchwald, Angew. Chem., Int. Ed. Engl. 37 (1998), 1103.

61. G.W. Coates, R.M. Waymouth, J. Am. Chem. Soc. 115 (1993) 91.

62. G. Natta, Science 147 (1965) 261.

63. **For reviews on the immobilization of asymmetric homogeneous catalysts,** see: a) H.-U. Blaser, B. Pugin, (Ed.s: V. Dubois, G. Jannes), Chiral Reactions in Heterogeneous Catalysis, Plennum, New York, 1995, p. 33; b) Chiral catalyst Immobilization and Recycling (Ed.s: D.E. De Vos, I.F.J. Vankelecom, P.A. Jacobs), Wiley-VCH Weinheim, 2000; c) A. Baiker, Chimia, 55 (2001) 796; d) Recoverable Catalysts and Reagents (Ed.s: J.A. Gladysz), Chem. Rev. 102 (2002) 3215-3892; e) Q.-H. Fan, Y.-M. Li, A.S.C. Chan, Chem. Rev. 102 (2002) 3385; f) M. Jacoby, Chem. Eng. News 82 (2004) 37; g) J. Horn, F. Michalek, C.C. Tzschucke, W. Bannwarth, Top. Curr. Chem. 242 (2004) 43; h) P. McMorn, G. Hutchings, Chem. Soc. Rev. 33 (2004) 108; i) M. Heitbaum, F. Glorius, I. Escher, Angew. Chem. Int. Ed. 45 (2006) 4732.

64. B. Pugin, J. Mol. Catal. A 107 (1996) 273.

65. B. Cornils, W.A. Herrmann, Aqueous-Phase Organometallic Catalysis, VCH, New York, 1998.

66. I.T. Horvath, Acc. Chem. Res. 31 (1998) 641.

67. D.P. Curran, Angew. Chem., Int. Ed. 37 (1998) 1174.

68. D.P. Curran, Synlett. (2001) 1488.
69. P.G. Jessop, T. Ikariya, R. Noyori, Chem. Rev. 99 (1999) 475.
70. Ionic Liquids in Synthesis, ed. P. Wasserscheid, T. Welton, Wiley-VCH, Weinheim, 2003.
71. Ionic Liquids: Industrial Applications for Green Chemistry, ed. R. D. Rogers and K.R. Seddon, ACS Symp. Ser. 818, Washington, DC, 2002.
72. J. Dupont, R.F. de Souza, P.A.Z. Suarez, Chem. Rev. 102 (2002) 3667.
73. R. Sheldon, Chem. Commun. (2001) 2399.
74. P. Wasserscheid, W. Keim, Angew. Chem., Int. Ed. 39 (2000) 3772.
75. T. Welton, Chem. Rev. 99 (1999) 2071.
76. C.E. Song, W.H. Shim, E.J. Roh, J.H. Choi, Chem. Commun. (2000) 1695.
77. C.E. Song, W.H. Shim, E.J. Roh, S.-G. Lee, J.H. Choi, Chem. Commun. (2001) 1122.
78. D.W. Kim, C.E. Song, D.Y. Chi, J. Am. Chem. Soc. 124 (2002) 10278.
79. D.W. Kim, C.E. Song, D.Y. Chi, J. Org. Chem. 68 (2003) 4281.
80. D.W. Kim, D.J. Hong, J.W. Seo, H.S. Kim, H.K. Kim, C.E. Song, D.Y. Chi, J. Org. Chem. 69 (2004) 3186.
81. C.E. Song, D.-U. Jung, S.Y. Choung, E.J. Roh, S.-G. Lee, Angew. Chem., Int. Ed. 43 (2004) 6183.
82. C.E. Song, Chem. Commun. (2004) 1033.
83. C.E. Song, in Methodologies in Asymmetric Catalysis, ed. S.V. Malhotra, ACS Symp. Ser. 880, Washington, DC, 2004, pp. 145.
84. C. Baudequin, J. Baudoux, J. Levillain, D. Cahard, A.-C. Gaumont J.-C. Plaquevent, Tetrahedron: Asymmetry 14 (2003) 3081.
85. C.E. Song, E.J. Roh, Chem. Commun. (2000) 837.
86. P.G. Jessop, R.R. Stanley, R.A. Brown, C.A. Eckert, C.L. Liotta, T.T. Ngo, P. Pollet, Green Chem. 5 (2003) 123.
87. R.B. Merrifield, J. Am. Chem. Soc. 85 (1963) 2149.
88. a) R. Manzotti, T.S. Reger, K.D. Janda, Tetrahedron Lett. 41 (2000) 8417; b) P.H. Toy, K.D. Janda, Tetrahedron Lett. 40 (1999) 6329.
89. a) S. Lundgren, S. Lutsenko, C. Jonsson, C. Moberg, Org. Lett. 5 (2003) 3663;

b) H. Nakano, K. Takahashi, Y. Suzuki, R. Fujita, Tetrahedron: Asymmetry 16 (2005) 609.

90. H. Hocke, Y. Uozumi, Tetrahedron 60 (2004) 9297.
91. C.J. Brinker, G.W. scherer, Sol-gel Science, The physics and Chemistry of Sol-Gel Processing, Academic press, 1990.
92. F. Cavani, F. Trifiro, A. Vaccari, Catal. Today, 11 (1991) 173.
93. http://www.iza-sc.ethz.ch/IZA-SC/Atlas/data/BEA.html.
94. J.M. Thomas, S. Ramdas, G.R. Millward, J. Kilnowski, M. Audier, J. Conzalec-Calbet, C.A. Fyfe, J. Solid State Chem. 45 (1982) 368.
95. A. Corma, Chem. ReV., 97 (1997) 2373.
96. X.S. Zhao, G.Q. Lu, G.J. Millar, Ind. Eng. Chem. Res. 35 (1996) 2075.
97. C.T. Kresge, M.E. Leonowicz, W.J. Roth, J.C. Vartulli, J.S. Beck, Nature 359 (1992) 710.
98. J.S. Beck, J.C. Vartulli, W.J. Roth, M.E. Leonowicz, C.T. Kresge, K.D. Schmitt, C.T.W. Chu, D.H. Olson, E.W. Sheppard, S.B. McCullen, J.B. Higgins, J.L. Schlenker, J. Am. Chem. Soc. 114 (1992) 10834.
99. M. Dubois, Th. Gulik-krzywicki, B. Cabane, Langmuir 9 (1993) 673.
100. J.C. Vartulli, K.D. Schmitt, C.T. Kresge, W.J. Roth, M.E. Leonowicz, S.B. McCullen, S.D. Hellring, J.S. Beck, J.L.Schlenker, D.H. Olson, E.W. Sheppard, Chem. Mater. 6 (1994) 2317.
101. A. Corma, A. Martinez, Adv. Mater. (1995) 137.
102. C. Huber, K. Moller, T. Bein, J. Chem. Soc. Chem. Commun. (1994) 2619.
103. C.T. Kresge, M.E. Leonowicz, W.J. Roth, J.C. Vartulli, J.S. Beck, Nature 359 (1992) 710.
104. J.S. Beck, J.C. Vartulli, W.J. Roth, M.E. Leonowicz, C.T. Kresge, K.D. Schmitt, C.T.W. Chu, D.H. Olson, E.W. Sheppard, S.B. McCullen, J.B. Higgins, J.L. Schlenker, J. Am. Chem. Soc. 114 (1992) 10834.
105. T. Yanagisawa, T. Shimizu, K. Kuroda, Bull. Chem. Soc. Jpn. 63 (1990) 988.
106. S. Inagaki, Y. Fukushima, K. Kuroda, J. Chem. Soc., Chem. Commun. (1993) 680.
107. J.M. Thomas, Angew. Chem. Int. Ed. 38 (1999) 3588.

108. A. Taguchi, F. Schuth, Micropor. Mesopor.Mat. 77 (2005) 1.

109. J.A. Melero, R.V. Grieken, G. Morales, Chem. Rev. 106 (2006) 3790.

110. P.J. Langley, J. Hulliger, Chem. Soc. Rev. 28 (1999) 279.

111. D. Zhao, J. Feng, Q. Huo, N. Melosh, G.H. Fredrickson, B.F. Chmelka, G.D. Stucky, Science 279 (1998) 548.

112. D. Zhao, Q. Huo, J. Feng, B.F. Chmelka, G.D. Stucky, J. Am. Chem. Soc. 120 (1998) 6024.

113. D.H. Olson, G.D. Stucky, J. C. Vartuli, U.S. Patent, 5, 364, 79 (1994).

114. A. Firouzi, F. Atef, A.G. Oertli, G.D. Stucky, B.F. Chmelka, J. Am. Chem. Soc. 119 (1997) 3596.

115. P. Kipkemboi, A. Fogden, V. Alfredsson, K. Flodstrom, Langmuir 17 (2001) 5398.

116. A. Heckel, D. Seebach, Helv. Chim. Acta. 85 (2002) 913.

117. F. Bigi, B. Franca, L. Moroni, R. Maggi, G. Sartori, J. Chem. Soc. Chem. Commun. (2002) 716.

118. X. Zhou, X. Yu, J. Huang, S. Li, , L. Li, C. Che, Chem. Commun. (1999) 1789.

119. C. Bianchini, P. Barbaro, Top. Catal. 19 (2002) 17.

120. A. Hu, H.L. Ngo, W. Lin, Angew. Chem. Int. Ed. 43 (2004) 2501.

121. R. Selke, M. Capka, J. Mol. Catal. 63 (1990) 319.

122. P. Piaggio, P. McMorn, C. Langham, D. Bethell, P.C. Bullman Page, F.E. Hancock, G.J. Hutchings, New J. Chem. (1998) 1167.

123. L. Frunza, H. Kosslick, H. Landmesser, E. Hoft, R. Fricke, J. Mol. Catal. A: Chem., 123 (1997) 179.

124. J.M. Fraille, J.I. Garcia, J. Massam, J.A. Mayoral, J. Mol. Catal. A. Chem. 136 (1998) 47.

125. D. Tas, D. Jeanmart, R.F. Parton, P.A. Jacobs, in Stud. Surf. Sci. Cat. Part 108: Heterogeneous Catalysis and Fine chemicals IV, Ed. H.U. Blaser, A. Baiker, R. Prins, Elsevier (1997) 493.

126. D. Tas, Ph. D. Thesis, K.U. Leuven, Belgium (1997).

127. W. Van Brussel, M. Renard, D. Tas, R. Parton, P.A. Jacobs, V.H. Rane, US Patent 5997840 (1999).

128. S.K. Tanielyan, R.L. Augustine, in Chemical Industries, Chem. Ind., Dekker, 75 (1998) 101.
129. R. Augustine, S. Tanielyan, S. Anderson, H. Yang, Chem. Commun. (1999) 1257.
130. R.L. Augustine, S.K. Tanielyan, S. Anderson, H. Li, Proc. Chiratech' 98, November 9-11, Barcelona, Spain (1998).
131. P. McMorn, G. Hutchings, J. Chem. Soc. Rev. 33 (2004) 108.
132. S.B. Ogunwumi, T. Bein, Chem. Commun. (1997) 901.
133. M.J. Sabatier, A. Corma, A. Domenech, V. Fornes, H. Garcia, Chem. Commun. (1997) 1285.
134. G. Schulz-Ekloff, S. Ernst, (Ertl, G. and Knozinger, H. eds.) Preparation of Solid Catalysts p. 405. Wiley-VCH.
135. I.T. Horvath, Encyclopedia of Catalysis 4, p. 178. Wiley-Interscience.
136. Á. Zsigmond, K. Bogár, F. Notheisz, J. Catal. 213 (2003) 103.
137. Y. Hengquan, J. Li, J. Yang, Z. Liu, Q. Yang, C. Li, Chem. Commun. (2007) 1086–1088
138. F. Bigi, B. Franca, L. Moroni, R. Maggi, G. Sartori, J. Chem. Soc. Chem. Commun. (2002) 716.
139. S. Sakka, K.J. Kamiya, Non-Cryst. Solids 42 (1980) 403.
140. C.J. Brinker, G.W. Scherer, Sol-Gel Science: the Physics and Chemistry of Sol-Gel Processing, Academic Press, San Diego, (1990).
141. D.A. Loy, K.J. Shea, Chem. Rev. 95 (1995) 1431.
142. R.H. Baney, M. Itoh, A. Sakakibara, T. Suzuki, Chem. Rev. 95 (1995) 1409.
143. R.J.P. Corriu, Angew. Chem. Int. Ed. 39 (2000) 1376.
144. A. Adima, J.J.E. Moreau, M.J. Man, C. Wong, Mater. Chem. 7 (1997) 2331.
145. A. Adima, J.J.E. Moreau, M. Man, C. Wong, Chirality 12 (2000) 411.
146. J. Chin, S.S. Lee, K.J. Lee, S. Park, D.H. Kim, Nature 401 (1999) 254.
147. J.M. Rivera, T. Martin, J. Rebek, Science 279 (1998) 1021.
148. T.E. Mallouk, J.A. Gavin, Acc. Chem. Res. 31 (1998) 209.
149. M.M. Treacy, J.M. Newsam, Nature 332 (1988) 249.
150. G.B. Gardner, D. Venkataraman, J.S. Moore, S. Lee, Nature 374 (1995) 792.

151. B.F. Abrahams, B.F. Hoskins, D.M. Michail, R. Robson, Nature 369 (1994) 727.
152. S.S.-Y. Chui, S.M.-F. Lo, I.P.H. Charmant, A.G. Orpen, I.D.A. Williams, Science 283 (1999) 1148.
153. R. Xiong, X. You, B.F. Abrahams, Z. Xue, C. Che, Angew. Chem. Int. Ed. 40 (2001) 4422.
154. J.S. Seo, D. Whang, H. Lee, S.I. Jun, J. Oh, Y.J. Jeon, K. Kim, Nature 404 (2000) 982.
155. A. Hu, H.L. Ngo, W. Lin, J. Am. Chem. Soc. 125 (2003) 11490.
156. K.T. Wan, M.E. Davis, US Patent 5827794 (1998).
157. K.T. Wan, M.E. Davis, J. Catal. 152 (1995) 25.
158. S. Feast, D. Bethell, P.C. Bulman Page, F. King, C.H. Rochester, M.R.H. Siddiqui, D.J. Willock, G.J. Hutchings, J. Chem. Soc., Chem. Commun. (1995) 2409.
159. S. Feast, M.R.H. Siddiqui, R.P.K. Wells, D.J. Willock, F. King, C.H. Rochester, G.J. Hutchings, J. Catal. 167 (1997) 533.
160. J.M. Thomas, T. Maschmeyer, B.F.G. Johnson, D.S. Shephard, J. Mol. Catal. A: Chem. 141 (1999) 139.
161. C. P. Mehnert Chem. Eur. J. 11 (2005) 50.
162. A. Riisagera, R. Fehrmann. M. Haumann, P.Wasserscheid, Top. in Catal.. 40 (2006) 91.
163. S. Feast, M. rafiq, D. Bethell, P.C. Bulman Page, F. King, C.H. Rochester, M.R. H. Siddiqui, D.J. Willock, G.J. Hutchings, J. Mol. Catal. A: Chem. 107 (1996) 291.
164. G.J. Hutchings, Chem. Commun. (1999) 301.
165. G. Sunderbabu, M. Leibovitch, D.R. Corbin, J.R. Scheffer, V. Ramamurthy, Chem. Commun. (1997) 2159.
166. B.M. Choudhury, S. Shobha Rani, N. Narender, Cata. Lett. 19 (1993) 299.
167. Ref.s in G.J. Hutchings, D.J. Willock, Topics in Catal. 5 (1998) 177.
168. M.E. Davis, R.F. Lobo, Chem. Mater. 4 (1992) 756.
169. J.M. Thomas, T. Maschmeyer, B.F.G. Johnson, D.S. Shephard, J. Mol. Catal. A: Chem. 141 (1999) 139.

170. S.A. Raynor, J.M. Thomas, R. Raja, B.F.G. Johnson, R.G. Bell, M.D. Mantle, Chem. Commun. (2000) 1925.

171. A. Corma, M. Iglesias, C. del Pino, F. Sanchez, J. Organomet. Chem. 431 (1992) 233.

172. R. Raja, J.M. Thomas, J. Mol. Catal. A: Chem. 181 (2002) 3.

173. B. Gigante, A. Corma, H. Garcia, M.J. Sabater, Catal. Lett. 68 (2000) 113.

174. D. Pini, A. Mandoli, S. Orlanddi, P. Salvadori, Tetrahedron: Asymmetry 10 (1999) 3883.

175. D.G. Blackmond, Cattech 3 (1998) 17.

176. K. Ishihara, H. Yamamoto, Cattech 1 (1997) 51.

CHAPTER II

Preparation and characterization of catalysts

2. Preparation and characterization of catalysts

2.1. Introduction

The successful heterogeneous chiral catalyst should possess high catalytic activity for the desired reaction, high enantioselectivity of the desired product and acceptable commercial viability. Immobilization of Transition Metal Complexes (TMCs) generates heterogeneous catalysts that are generally more complicated than the homogeneous catalysts. It is therefore not surprising that, the effect of immobilization is very often unpredictable. Unfortunately, most heterogeneous analogs of homogeneous catalysts are less active or lose part of their activity in every recycle. However, in some cases, the activities, chemo- or enantioselectivities of the heterogenised systems are superior to the homogeneous analogues. The reason of positive or negative effect of the immobilized catalyst could be best understood by different catalyst characterization techniques.

Preparation and characterization of catalyst material is the most important step in the process of catalyst development, which gives insight into the relation between physical and chemical properties of the catalyst and the reasons for their its activity. If the structure and composition of the catalyst can be correlated with its catalytic activities and product selectivities, the work of the catalyst can be understood clearly.

The thesis mainly deals with the synthesis of immobilized catalysts by covalent anchoring of metal complexes onto the mesoporous silica support, characterization by various techniques such as surface area, X-ray diffraction, N_2-sorption, FTIR spectra, DRUV-vis spectroscopy, NMR, SEM and TEM, etc. for structural integrities and retention of the support and the presence of metal complexes in the resulting materials and their catalytic activity in different asymmetric organic transformations. The synthesis of mesoporous silica supports and the theory and experimental procedure of various characterization techniques used are briefly described in the following sections.

2.2. Catalyst preparation

2.2.1. Synthesis of MCM-41

The pure siliceous MCM-41 material was prepared as described in the literature [1]. The gel composition used for preparing Si-MCM-41 material was 10 SiO_2: 5.4

$C_nH_{2n+1}(CH_3)_3NBr$: 4.25 Na_2O: 1.3 H_2SO_4: 480 H_2O. C16-MCM-41 is prepared using CTABr (32.0 g) and 115 g of water and this mixture was stirred for 30 min at room temperature. Sodium silicate solution (37.4 g) was added drop wise to the surfactant solution under vigorous stirring for another 30 min. Then 2.4 g of H_2SO_4 in 10 g of water was added to the above mixture and the stirring was continued for another 30 min. The resulting gel was transferred into a polypropylene bottle and kept in an oven at 373 K for 24 h. After cooling to room temperature, the resultant solid was recovered by filtration, washed with distilled water and dried in an oven at 373 K for 6 h. Finally the material was calcined in a muffle furnace at 813 K for 10 h to give MCM-41.

2.2.2. Synthesis of MCM-48

MCM-48, was synthesized by the conventional hydrothermal pathway by following the procedure described in literature [2, 3]. The molar composition of the gel was 1 TEOS: 0.25 Na_2O: 0.65 $C_{16}H_{33}(CH_3)_3NBr$: 0.62 H_2O. CTABr (31.2 g) was dissolved in (93.6 g) deionized water at 318 K and stirred for 40 min. Then TEOS (30 g) followed by sodium hydroxide (69 g, 1 M) solution were added to the above mixture and the stirring was continued for another 1 h at room temperature. The resulting gel was transferred into a polypropylene bottle and kept in an oven at 373 K for 72 h under static condition. After cooling to room temperature, the solid was recovered by filtration, washed with ethanol followed by distilled water and dried in an air oven at 373 K for 6 h. Finally, the material was calcined in a muffle furnace at 813 K for 10 h to give MCM-48.

2.2.3. Synthesis of SBA-15

SBA-15 was synthesized with a gel composition of 4 g Polymer: 0.041 TEOS: 0.24 HCl: 6.67 H_2O as per literature procedure [4, 5]. In a typical synthesis, 4 g of amphiphilic triblock copolymer, poly(ethylene glycol)-block-poly(propylene glycol)-block-poly(ethylene glycol), (average molecular weight = 5800) was dispersed in 30 g of water and 120 g of 2 M HCl solution was added while stirring. It was followed by the addition of 8g of tetraethyl orthosilicate to the homogeneous solution with stirring. This gel mixture was continuously stirred at 40 °C for 24 h, and finally crystallized in a Teflon-lined autoclave at 100 °C for 2 days. After crystallization the solid product was

filtered, washed with distilled water, and dried in air at room temperature. The material was calcined in static air at 550 °C for 24 h to decompose the triblock copolymer and obtain a white powder (SBA-15).

2.2.4. Preparation of 1-butyl 3-methylimidazolium hexafluorophosphate ([BMIM]$^+PF_6^-$)

The ionic liquid BMIM]$^+PF_6^-$ was prepared as reported in the literature [6]. In a typical procedure 1-Butyl 3-methylimidazolium chloride (1.74 g, 0.01 mol) was dissolved in 50 ml of acetone in a 100 ml round bottom flask provided with a stirrer. Then KPF_6 (1.84 g, 0.01 mol) was added and the solution was stirred for 24 h. at room temperature (Fig. 1). The resulting precipitate of KCl was filtered and acetone was removed on a rotavapor to obtain a yellow colored liquid.

2.3. Catalyst characterization – Theory and experimental procedure

2.3.1. Elemental analysis

Inductively coupled plasma atomic emission spectroscopy (ICP-AES), also referred to as Inductively Coupled Plasma Optical Emission Spectrometry (ICP-OES), is an analytical technique used for the detection of trace metals. It is a type of emission spectroscopy that uses the inductively coupled plasma to produce excited atoms and ions that emit electromagnetic radiation at wavelengths characteristic of a particular element [7, 8]. The intensity of this emission is indicative of the concentration of the element within the sample. This technique was adopted in the determination of metal content in the immobilized catalysts. ICP-OES analysis was done on Perkin-Elmer Optima 2000 DV with Winlab software instrument. Standard solutions were used for calibration. This instrument can analyze aqueous solutions for metals with either a Radial or an axial plasma configuration.

2.3.2. Surface area measurement by BET method

The common method of measuring the surface area of catalyst materials is based on the theory developed by Brunauer, Emmett and Teller in 1938 considering the concept

of multilayer adsorption. The isotherm points are transformed into the linear version of BET equation 2.1 [9, 10]:

$$P/V(P_0-P) = 1/V_mC + [(C-1)/V_mC] (P/P_0) \quad (2.1)$$

Where, P is the adsorption equilibrium pressure, P_0 is the saturation vapor pressure of the adsorbate at the experimental temperature, V is the volume of gas adsorbed at pressure P, V_m is the volume of adsorbate required for monolayer coverage and C, a constant that is related to the heat of adsorption and liquefaction.

The specific surface areas of the catalysts were measured by N_2 physisorption at liquid nitrogen temperature with Omnisorb 100 CX Colulter instrument. Samples were dried at 300 °C in a dynamic vacuum for 2 h before N_2 physisorption measurements were performed. The specific surface area was determined by using the standard BET method on the basis of adsorption data. The pore size distributions were calculated from both adsorption and desorption branches of the isotherms using BJH method and the corrected with Kelvin equation [11]. Pore volumes were determined by using the t-plot method of De Boer.

2.3.3. X-ray diffraction

X-ray diffraction (XRD) is used to identify bulk phases, if desired under *in situ* conditions and to estimate particle sizes. In catalyst characterization, diffraction patterns are mainly used to identify the crystallographic phases that are present in the catalyst [12]. This method involves the interaction between the incident monochromatized X-rays (like Cu Kα or Mo Kα source) with the atoms of a periodic lattice. X-rays scattered by atoms in an ordered lattice interfere constructively in directions given by Bragg's law eqn. 2.2 [13]:

$$n\lambda = 2\ d\ \sin\theta;\ n = 1, 2, 3,\ldots. \quad (2.2)$$

where, λ is the wavelength of the X-rays, d is the distance between two lattice planes, θ is the angle between the incoming X-rays and the normal to the reflecting lattice plane and n is the integer called order of the reflection.

The width of the diffraction lines can be used to estimate the crystal size by the relation given by Debye-Scherrer formula eqn. 2.3 [9],

$$D_{hkl} = 0.9\lambda/\beta\cos\theta \quad (2.3)$$

where, D_{hkl}, λ, β and θ are the volume averaged particle diameter, X-ray wavelength, full width at half maximum (FWHM), and diffraction angle respectively.

Powder X-ray diffraction patterns of the clay catalysts were recorded using a Rigaku (Model D/MAXIII VC, Japan), setup with Cu Kα radiation and graphite monochromatic with scan speed 16 °/min and scanning in the 2θ range from 5 to 50 θ. Silicon was used to calibrate the instrument.

SAXS patterns of the samples were obtained in reflection mode with a Philips X'Pert Pro 3040/60 diffractometer using Co*Kα* radiation (λ = 0.17890 nm), an iron filter, and an X'celerator as a detector. XRD pattern of the samples at wide-angle region was measured on Rigaku Model D/MAXIII VC, Japan, λ =1.5418 Å with Ni filtered Cu-K*α* radiation.

2.3.4. Scanning Electron Microscopy (SEM)

The scanning electron microscope (SEM) is a type of electron microscope that images the sample surface by scanning it with a high-energy beam of electrons in a raster scan pattern. SEM is a straightforward technique to probe the morphological features of mesoporous molecular sieve materials. SEM scans over a sample surface with a probe of electrons (5-50 eV) and detects the yield of either secondary or back-scattered electrons as a function of the position of the primary beam. Contrast is generally caused by the orientation that parts of the surface facing the detector appear brighter than parts of the surface with their surface normal pointing away from the detector. The interaction between the electron beam and the sample produces different types of signals providing detailed information about the surface structure and morphology of the sample [14, 15]. A major advantage of SEM is that bulk samples can also be directly studied by this technique. SEM was employed to characterize the surface morphology with Leica stereoscan, Cambridge 440 Microscope (UK) with a Kevex model EDAX system.

2.3.5. Transmission Electron Microscopy (TEM)

Transmission electron microscopy is typically used for high resolution imaging of thin films of a solid sample for micro structural and compositional analysis. The technique involves: (i) irradiation of a very thin sample by a high-energy electron beam, which is diffracted by the lattices of a crystalline or semi crystalline material and

propagated along different directions, (ii) imaging and angular distribution analysis of the forward scattered electrons (unlike SEM where backscattered electrons are detected) and (iii) energy analysis of the emitted X-rays [16]. In detail, a primary electron beam of high energy and high intensity passes through a condenser to produce parallel rays, which impinge on the sample. As the attenuation of the beam depends on the density and the thickness, the transmitted electrons forms a two-dimensional projection of the sample mass, which is subsequently magnified by the electron optics to produce the so-called bright field image. The dark field image is obtained from the diffracted electron beams, which are slightly off angle from the transmitted beam. Typical operating conditions for TEM instruments are 100-200 keV electrons, 10-6 mbar vacuum, 0.5 nm resolutions and a magnification of 105 to 106. The topographic information obtained by TEM in the vicinity of atomic resolution can be utilized for structural characterization and identification of various phases of mesoporous materials, *viz*., hexagonal, cubic or lamellar [17].

TEM photographs were taken from JEOL Model 1200 EX instrument operated at an accelerating voltage at 120 kV. Samples were prepared by placing droplets of a suspension of the sample in isopropanol on a polymer micro grid supported on a Cu grid for TEM measurements.

2.3.6. Fourier Transform Infrared Spectroscopy (FT-IR)

Infrared spectroscopy (IR) can be considered as the first and the most important of the modern spectroscopic techniques that has found profound applications in the field of catalysis. This is primarily due to the fact that IR provides actual information on the structure, geometry and orientation of practically all molecules that are present in the sample, irrespective of the physical state, temperature or pressure. IR is therefore a feasible tool to identify phases that are present in the catalyst or its precursor stages, the adsorbed species, adsorption sites and the way in which the adsorbed species are chemisorbed on the surface of the catalyst [18, 19].

Infrared spectroscopy is the common form of vibrational spectroscopy and it depends on the excitation of vibrations in molecules or in solid lattices by the absorption of photons. Absorption of an infrared photon occurs only if a dipole moment changes

during the vibration. However, it is not necessary that the molecule possess a permanent dipole, it is sufficient if a dipole moment changes during the vibrations. The intensity of the infrared band is proportional to the change in the dipole moment.

A variety of IR techniques have been used to attain information on the surface chemistry of different solids. A great advantage of infrared spectroscopy is that the technique can be used to study catalysts *in situ*. FTIR and diffuse reflectance IR (DRIFT) experiment has been performed using Shimadzu FTIR-8201PC equipment.

2.3.7. Diffuse reflectance UV-visible spectroscopy

Diffuse reflectance spectroscopy (DRS) is a spectroscopic technique based on the reflection of light in the ultraviolet (UV), visible (VIS) and near-infrared (NIR) regions by a powdered sample. In a DRS spectrum, the ratio of the light scattered from an "infinitely thick" closely packed catalyst layer and the scattered light from an infinitely thick layer of an ideal non-absorbing (white) reference sample is measured as a function of the wavelength λ. The scattered radiation, emanating from the sample, is collected in an integration sphere and detected. UV-Vis spectroscopy generally deals with the study of electronic transitions between orbital or bands of atoms, ions or molecules. One of the advantages of DRS is that the obtained information is directly chemical in nature since outer shell electrons of the transition metal ions are probed. This further provides information about the oxidation state and coordination environment of transition metal ions in the solid matrices [20, 21].

Diffuse reflectance spectroscopy (DRS) is a spectroscopic technique based on the reflection of light in the ultraviolet (UV), visible (VIS) and near-infrared (NIR) region by a powdered sample. In a DRS spectrum, the ratio of the light scattered from an "infinitely thick" closely packed catalyst layer and the scattered light from an infinitely thick layer of an ideal non-absorbing (white) reference sample is measured as a function of the wavelength λ. The scattered radiation, emanating from the sample, is collected in an integration sphere and detected. The most popular continuum theory describing diffuse reflectance effect is Schuster-Kubelka-Munk (SKM) theory. If the sample is infinitely thick, the diffuse reflection of the sample (R_∞) is related to an apparent absorption (K) and apparent scattering coefficient (S) by the SKM equation [20]:

$$F(R_\infty) = (1-R_\infty)^2 / 2R_\infty = K/S \quad (2.4)$$

At low concentrations of supported transition metal ions (TMI), this equation is a good representation of the absorbing spectrum and allows a quantitative determination of the TMI.

$$F(R_\infty) = (1-R_\infty)^2 / 2R_\infty = K/S = \alpha C_{TMI} / S = k\, C_{TMI} \quad (2.4)$$

At a given wavelength λ, S is constant, the above equation gives a linear relation between $F(R_\infty)$ and the TMI concentration, C_{TMI}. The coefficients α and k are proportionality constants.

Diffuse reflectance UV-vis (DRUV–vis) spectra of catalyst samples were obtained using a Shimadzu UV-2101 PC spectrometer equipped with a diffuse-reflectance attachment, with $BaSO_4$ as the reference. The reflectance spectra were converted into the Kubelka-Munk function, *F(R)*, which is proportional to the absorption coefficient for low values of *F(R)*. The spectra were measured in the range of 200-800 nm in air at room temperature.

2.3.8. Solid-state nuclear magnetic resonance spectroscopy

In solid-state NMR, the line shape is determined by dipolar and quadrupolar interactions. The lines are usually broader because of the rigid structure of the solid phase prevents the averaging of the dipolar interaction (H_D) by motions. Since, the first order quadrupolar and dipolar interactions are proportional to ($3\cos^2\theta - 1$), where, θ is the angle between an internuclear vector and the magnetic field, these interactions can be removed, to a first order approximation, by spinning the sample around the so-called magic angle β with respect to the external magnetic field, for which $3\cos^2\beta - 1 = 0$, i.e. $\beta = 54.74^o$. This technique is known as Magic Angle Spinning (MAS) [22, 23].

Magic angle spinning (MAS) NMR spectra for ^1H, ^{13}C, ^{29}Si, nuclei were recorded on BRUKER DSX300 spectrometer at 7.05 T (resonance frequencies 59.63 MHz, rotor speed 4000 Hz, number of scans 5275, external reference $Si(OCH_3)_4$ and 78.19 MHz, rotor speed 6000 Hz, number of scans 2800). The ^{31}P MAS NMR spectra were recorded using a Bruker DSX-300 spectrometer at 121.5 MHz with high power decoupling with a Bruker 4 mm probe head. The spinning rate was 10 KHz and the delay between two

pulses was varied between 1 and 30 s to ensure the complete relaxation of the ^{31}P nuclei occurred. The chemical shifts are given relative to external 85 % H_3PO_4.

2.3.9. Thermal analysis

Thermo analytical techniques involve the measurement of the response of the solid under study (energy or mass released or consumed) as a function of temperature (or time) dynamically by the application of a linear temperature program. Thermogravimetry (TG) is a technique, which measures the variation in mass of a sample when it undergoes temperature scanning in a controlled atmosphere. Differential thermal analysis (DTA) is a technique, which measures the difference in temperature between a sample and a reference (a thermally inert material) as a function of time or temperature, when they undergo temperature scanning in a controlled atmosphere. DTA method enables any transformation to be detected for all the categories of materials, providing information on exothermic and endothermic reactions taking place in the sample, which includes phase transitions, dehydration, decomposition, redox, or solid-state reactions. In catalysis, these techniques are used to study the genesis of catalytic materials via solid-state reactions [24].

Differential thermal analysis (DTA) measurements of the immobilizd transition metal complex catalysts were performed on a Pyris Diamond TG-DTA apparatus from room temperature to 1000 ^oC in flowing dry oxygen (ca. 50 ml min^{-1}), using α-Al_2O_3 as reference. In each experiment, 5-8 mg of the sample was used with a heating rate of 20 $^oC\ min^{-1}$.

Thermogravimetric and differential thermal analysis (TG-DTA) measurements of immobilized chiral catalysts were performed on a Setaram TG-DTA 92 apparatus from ambient to 1000 ^oC in flowing dry air (ca. 50 ml min^{-1}), using α-Al_2O_3 as reference. In each experiment, 25-30 mg of the sample was used with a heating rate of 10 $^oC\ min^{-1}$. TGA curves are depicted as first derivative DTG of the direct weight loss traces.

2.4. References

1. M. Hartmann, S. Racouchot, C. Bischof, Micropor. Mesopor. Mater. 27 (1999) 309.
2. K. Schumacher, M. Grün, K.K. Unger, Micropor. Mesopor. Mater. 27 (1999) 201.
3. A. Monnier, F. Schüth, Q. Huo, D. Kumar, D. Margolese, R.S. Maxwell, G.D. Stucky, P. Petroff, A. Firouzi, M. Janicke, B.F. Chmelka, Science 261 (1993) 1299.
4. D. Zhao, J. Feng, Q. Huo, N. Melosh, G.H. Fredrickson, B.F. Chmelka, G.D. Stucky, Science, 279 (1998) 548.
5. D. Zhao, J. Sun, Q. Li, G.D. Stucky, Chem. Mater. 12 (2000) 275.
6. T. Joseph, S. Sahoo, S.B. Halligudi, J. Mol. Catal. A: Chemical 234 (2005) 107–110.
7. A. Stefánsson, I. Gunnarsson, N. Giroud, Anal. Chim. Acta 582 (2007) 69-74.
8. J.M. Mermet, J. Anal. At. Spectrom. 20 (2005) 11-16.
9. J.M. Thomas, W.J. Thomas, Principles and Practice of Heterogeneous catalysis, VCH, Weinheim, 1997.
10. S. Brunauer, P.H. Emmett, E. Teller, J. Am. Chem. Soc. 1938, 60, 309.
11. E.P. Barrett, L.G. Joyner, P.P. Halenda, J. Am. Chem. Soc. 1951, 73, 373.
12. S. Biz, M. Occelli, Catal. Rev-Sci. Eng. 1998, 40, 329.
13. W.H. Bragg, W.L. Bragg, The Crystalline State, Vol. 1, McMillan, New York, 1949.
14. J.I. Goldstein, H. Yakowitz (Eds.), *Practical Scanning Electron Microscopy*, Plenum Press, New York, 1975.
15. G. Lawes, Scanning Electron Microscopy and X-Ray Microanalysis, John Wiley and Sons Ltd., Chichester, 1987.
16. J.R. Fryer, Chemical Applications of Transmission Electron Microscopy, Academic Press, San Diego, 1979.
17. J.M. Thomas, O. Terasaki, P.L. Gai, W. Zhou, J. Gonzalez-Calbet, Acc. Chem. Res. 34 (2001) 583.
18. R.P. Eischens, W.A. Pliskin, Adv. Catal. 10 (1958) 1.
19. J.W. Niemantsverdriet, Spectroscopic methods in Heterogeneous catalysis, VCH,

Weinheim, 1993.

20. (a) B.M. Weckhuysen, I.P. Vannijvel, R.A. Schoonheydt, Zeolites 15 (1995) 482; (b) X.T. Gao, I.E. Wachs, J. Phys. Chem. B104 (2000) 1261; (c) X.T. Gao, I.E. Wachs, J. Catal. 188 (1999) 325.
21. R.A. Schoonheydt, Diffuse Reflectance Spectroscopy, Chapter 4, in: Characterization of Heterogeneous Catalysts, F. Delannay (Ed.), Marcel Dekker, New York, 1984.
22. R.A. Wind, in A.I. Popov, K. Hallenga (Eds.), Modern NMR Techniques and Their Application in Chemistry, p. 156, Marcel Dekker, Inc., New York, 1991.
23. R.H.H. Smits, Ph. D. Thesis, Netherlands, 1994.
24. P. Gabbott (Ed.:), Principles and Applications of Thermal Analysis, Willey, Blackwell 2007.

CHAPTER III

Hydrogenation of ketones and imines

3. Immobilized chiral diamino Ru complex as catalyst for chemo- and enantio-selective hydrogenation

3.1. Introduction

Asymmetric hydrogenation is a core technology in fine chemicals synthesis particularly for pharmaceuticals, agrochemicals, flavours, and fragrances, which requires a high degree of stereochemical precision [1]. Asymmetric hydrogenations of C=C, C=O, and C=N functionalities have found important applications in organic synthesis and in the fine chemical business [2, 3]. Hydrogenative reduction of prochiral ketones to chiral alcohols is a powerful tool for precise stereocontrolled organic synthesis. A high turnover frequency (TOF) can be obtained by designing suitable molecular catalysts and reaction conditions. Preferential reduction of a C=O function over a coexisting C=C linkage is an important and difficult task. Its versatility is manifested by the asymmetric synthesis of some biologically significant chiral compounds [4-9]. Chiral amines are also key structural elements in a multitude of biologically active natural products and pharmaceuticals rendering their synthesis an objective of high priority from the perspective of medicinal chemistry and organic synthesis [10, 11]. Although there are many examples of highly efficient catalysts for olefin and ketone reduction, imine hydrogenation is still a challenge in terms of both the turnover frequency and the lifespan of the active catalyst. This is due to the fact that C–N double bonds have certain traits, such as their preferred mode of binding and the strong donor character of the nitrogen, that are unfavorable for homogeneous catalytic hydrogenation [12, 13]. Reductive amination of ketones, in which a mixture of a carbonyl compound and an amine is treated with a reductant in a “one-pot” fashion, is one of the most useful methods for the preparation of secondary or tertiary amines and related functional compounds; thus, a number of methods have been developed to carry out this direct process [14-17]. One of the best transition-metal complexes for ketone hydrogenation that has been discovered is the chiral RuII-diphosphine/1, 2-diamine complex, which was developed by Noyori and co-workers [18-24]. This system was found to be active in the chemoselective hydrogenation of carbonyl over olefin functional groups and in the reduction of imines [2, 25, 26].

The immobilization of metal complexes enables the long-term use of expensive or toxic catalyst and provides a clean and straightforward separation of the product [27-33]. Compared to organic polymers, inorganic material-immobilized catalysts possess some advantages, though they attract little attention [34]. For example, they prevent the intermolecular aggregations of the active species because of their rigid structures, do not swell or dissolve in organic solvents, and often exhibit superior thermal and mechanical stability under the catalytic conditions [35, 36]. A recently discovered pure silica phase, designated SBA-15, has long-range order, large monodispersed mesopores (up to 50 nm), and thicker walls (typically between 3 and 9 nm), which makes it more thermally and hydrothermally stable than the M41S-type materials [37-39]. There are many reports on the immobilization of Ru catalyst on different supports for the hydrogenation of ketones [40-43], but very few reports on the chemoselective hydrogenation of α, β-unsaturated ketones and the hydrogenation of imines.

We have synthesized the novel heterogeneous catalysts by directly grafting a chiral 1, 2-diaminocyclohexane (dach) based ruthenium triphenylphosphine complex onto the surface of mesoporous silica SBA-15 that was very successful in the heterogeneous asymmetric hydrogenation of a series of ketones. This high activity of the Ru amine immobilized catalysts (here after $[Ru(dach)(PPh_3)_2(Cl_2)]$-SBA-15) comes with high selectivity for the hydrogenation of ketones over olefin functional groups and promising activity in the imine hydrogenation.

3.2. Experimental

3.2.1. Chemicals

All the solvents procured from Merck, India were of AR grade and were distilled and dried prior to their use. All the ketones and α, β-unsaturated ketones were purchased from Aldrich chemicals and used as received. The (1S, 2S)-1,2-diaminocyclohexane was purchased from Aldrich chemicals. All the imines were freshly prepared by the condensation of requisite amine and ketone in toluene in the presence of 4Å molecular sieves according to literature [44]. $RuCl_2(PPh_3)_3$ was synthesized according to published paper [45]. Si-SBA-15 was synthesized using a similar procedure reported in the literature [37].

3.2.2. Catalyst preparation

3.2.2.1. Chloro functionalization of SBA-15

Surface functionalization of SBA-15 was carried out by post synthesis method. SBA-15 (3 g), Chloropropyltriethoxysilane (3 mL) was refluxed overnight in toluene (50 mL) (Scheme 3.1.). After that it was filtered and washed with toluene for several times. It was soxhelt extracted with toluene to remove the ungrafted chloropropyl triethoxysilane group.

3.2.2.2. Ligand functionalization of SBA-15 (dach-SBA-15)

The chloro functionalized SBA-15 (2 g) was treated with (S, S)-diaminocyclohexane (0.3 g) in the presence of catalytic amount of triethylamine in dichloromethane under nitrogen atmosphere. It was refluxed at 313 K for 24 h and then filtered, washed with dichloromethane for several times and soxhelt extracted with dichloromethane to remove the unreacted amine.

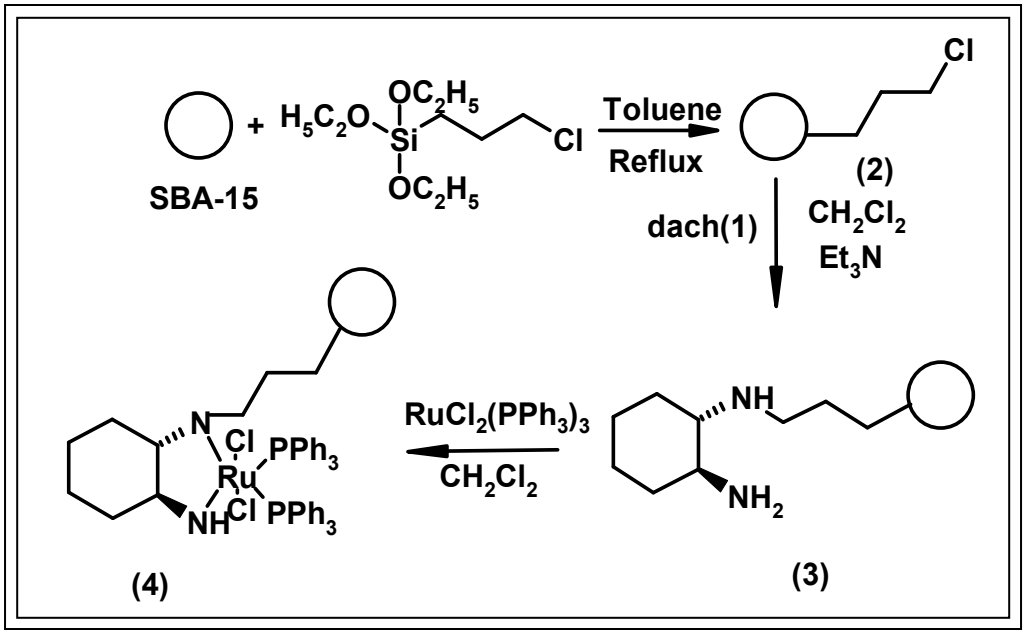

Scheme 3.1. Synthesis of immobilized chiral ligand dach-SBA15 (3) and immobilized complex [Ru(dach)(PPh_3)$_2$(Cl_2)]-SBA-15 (4)

3.2.2.3 Anchoring of the complex inside the ligand functionalized mesoporous material ([Ru(dach)(PPh$_3$)$_2$(Cl$_2$)]-SBA-15)

One gram of ligand functionalized SBA-15 was added to a solution containing 38 mg (0.04 mmol) of the $RuCl_2(PPh_3)_3$ complex dissolved in 30 mL of dry dichloromethane, and the mixture was stirred at room temperature for 12 h under inert atmosphere. After 12 h it was filtered, washed and soxhelt extracted with dry dichloromethane, and dried under vacuum to provide the complex functionalized mesoporous silica ([Ru(dach)(PPh_3)$_2$(Cl_2)]-SBA-15).

3.2.3. Catalytic experiments

3.2.3.1. General procedure for the hydrogenation of ketone

Synthesis of 1-(naphthalen-2-yl) ethanol (Table 3.2, Entry1): To a test tube, the precatalyst, Ru complex immobilized over mesoporous silica SBA-15 (0.2 g, 0.00039 mmol of Ru) and 1 M tBuOK (potassium *tert*.butoxide) in isopropyl alcohol (0.3 mL, 0.02 mmol) was added under nitrogen and stirred at room temperature for 30 min before 2-methylnaphthyl ketone (10 mmol, 1.70 g) and isopropyl alcohol (40 mL) was introduced. The contents of the test tube was transferred to 300 mL autoclave and then sealed. After purging with hydrogen for 5 times, the final H_2 pressure was adjusted to 27 atm. After stirring at 343 K for 20 h, the reaction was stopped. The conversion was determined by GC to be 90%. The reaction mixture was filtered and washed several times with isopropyl alcohol. The filtrate was removed under reduced pressure and purified by column chromatography on silica as the stationary phase (pet ether: ethyl acetate-85:15) to give 1-(naphthalene-2-yl) ethanol (85%, 76% ee), white solid, the enantiomeric excess was determined from HPLC (chiracel OD-H column, Mobile phase: Isopropyl alcohol: Pet ether - 10:90, Wave length: 254 nm, flow rate: 0.5 mL/min, minor isomer-19.74, major isomer-20.45), ^{1}H NMR ($CDCl_3$, 200MHz): δ=7.73-7.78 (m, 4H), 7.37-7.46 (3H, m), 4.95-5.05 (1H, q), 1.49-1.53 (3H, d), ^{13}C NMR ($CDCl_3$): δ=133.5 (C), 131.2 (C), 128.0 (CH), 127.6 (CH), 127.5 (CH), 127.3 (CH), 126.9 (CH), 126.1(CH), 124.9 (CH), 123 (C), 76.1 (CH), 22.6 (CH_3).

3.2.3.2. General procedure for the hydrogenation of α, β-unsaturated ketone

Synthesis of (E)-1, 3-diphenylprop-2-en-1-ol (Table 3.3., Entry 1): It is same as in the case of hydrogenation of ketone. Reactions were carried out at 343 K and 27 atm H_2 using 10 mmol of the substrate (α, β-unsaturated ketone, (E)-1,3-diphenylprop-2-en-1-one). ^{1}H NMR ($CDCl_3$, 200MHz): δ= 7.15-7.33 (10H, m), 6.27 (1H, s), 6.06 (1H, s), 5.19 (1H, s), 4.59 (1H,s), ^{13} C NMR ($CDCl_3$): δ=141.4 (C), 135.1 (C), 129.5 (CH), 129.0 (CH), 128.9 (CH), 128.7 (CH), 128.5 (CH), 128.0 (CH), 127.5 (CH), 127.1 (CH), 127.0 (CH), 126.4 (CH), 126.3 (CH), 126.1 (CH), 77.0 (CH).

3.2.3.3. Hydrogenation of imines

Synthesis of N-(1-phenylethyl)benzenamine (Table 3.4., Entry 1): It is same as in the case of hydrogenation of ketones. Reactions were carried out at 348 K and 27 atm H_2 using 2.5 mmol of the substrate (imine, (E)-N-(1-phenylethylidene)benzenamine) Substrate / catalyst / base ratio of 6410/1/30 in 20 mL of 2-propanol. ^{1}H NMR ($CDCl_3$, 200MHz): δ=7.24-7.30 (m, 3H), 7.08-7.12 (m, 4H), 6.94(1H, m), 6.48 (m, 2H), 4.08 (1H, m), 1.5 (3H, d) ^{13}C NMR ($CDCl_3$): δ=147.6 (C), 143.5 (C), 129.6 (CH), 129.6 (CH), 128.6 (CH), 128.6 (CH), 126.9 (CH), 126.9 (CH), 126.8 (CH), 117.2 (CH), 113.5 (CH), 113.4 (CH), 56.5 (CH), 21.5 (CH_3).

3.3. Results and Discussions

As shown in scheme 3.1, the reaction of 1, 2-diaminocyclohexane (**1**) with the chloropropyl functionalised SBA-15 (**2**) in presence of triethylamine as a base in CH_2Cl_2 smoothly gave the supported ligand (**3**). Subsequent elemental analysis of ligand based on the wt% of N demonstrated that the loading ratio of the chiral ligand was 0.003 mmol g^{-1}. Complexation of the functionalized ligand was carried out with $RuCl_2(PPh_3)_3$ to give the covalently anchored chiral Ruthenium complex (**4**). The presence of the complex in the mesoporous silica was confirmed by different catalyst characterization techniques and was assessed in the enantioselective and chemoselective hydrogenation of prochiral ketones, α, β-unsaturated ketones and imines.

3.3.1. Catalyst Characterization

3.3.1.1. Low angle XRD

The powder low angle XRD patterns of the siliceous SBA-15 showed hexagonal structure characteristic of this material and a well-resolved pattern with a prominent peak at 0.8º and two peaks at 1.4º and 1.6º 2θ, which matches well with the pattern reported for SBA-15. In low angle XRD of the material, the intensities of the reflections essentially did not change after the ligand functionalization and complexation over SBA-15 (Fig. 3.1). Low angle XRD peaks can be indexed to a hexagonal lattice with a d (100) spacing of 110 Å, corresponding to a large unit cell parameter, a_0=127 Å (a_0=2d (100)/√3). These results indicate an ordered mesoporosity of the support is maintained even after the incorporation of organic functional groups and ruthenium complex.

3.3.1.2. N_2 sorption study

N_2 sorption isotherms were measured for the pure support and for the immobilized complex. Table 3.1. represents a comparison of sorption isotherms and textural characteristics of pure and immobilized catalyst samples. The sample displayed a type IV isotherm with H_1 hysteresis and a sharp increase in pore volume adsorbed above P/P_0 ~ 0.7 cm^3/g, which is a characteristic of highly ordered mesoporous materials. It is seen that N_2 adsorbed or desorbed volumes were higher in the case of pure support than complex immobilized catalysts. BET surface area was found to decrease from 780 m^2/g for the pure support to 418 m^2/g for [Ru(dach)$(PPh_3)_2(Cl_2)$]-SBA-15, with corresponding decrease in mesopore volume from 1.34 to 0.92 cm^3/g. These results indicate that the complex is most likely anchored inside the mesopore channels of SBA-15.

3.3.1.3. Thermal Analysis

Thermal analysis of the immobilized catalyst (Fig. 3.2.) shows a first weight loss at 200 °C which may be because of the loss of the linker group and the ligand. After that continuous weight loss was observed upto 420 °C (total 10%), which can be ascribed to the loss of ruthenium in the form of oxide. DTA shows an endothermic peak. This shows that the immobilized catalyst is stable under the applied reaction condition.

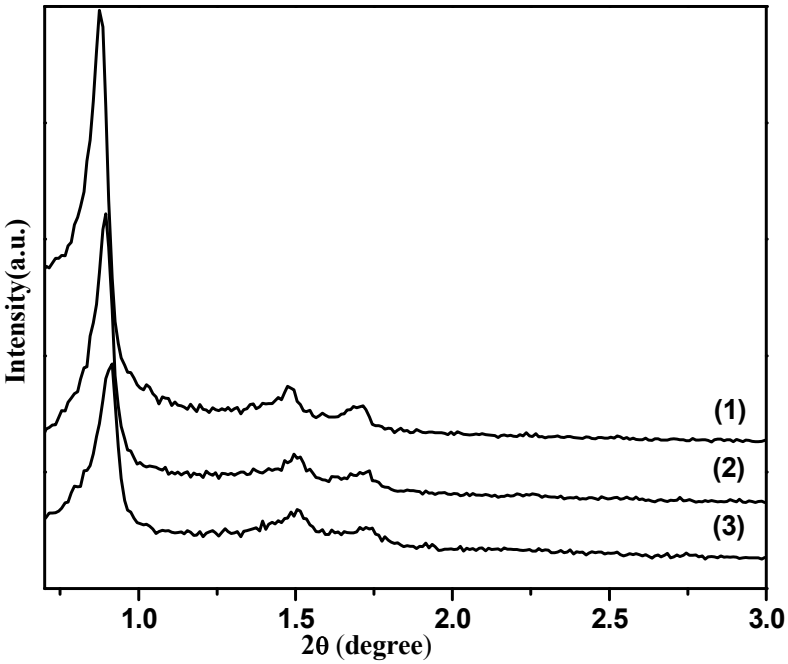

Fig. 3.1. Low angle XRD patterns of (1) SBA-15 (2) dach-SBA-15 (3) [Ru(dach)(PPh_3)$_2$(Cl_2)]-SBA-15

Table 3.1.

Physicochemical properties of the materials

Materials	Surface area (m^2/g)	Pore volume (cm^3/g)	Average pore diameter (nm)
SBA-15	780	1.34	9.1
Dach-SBA-15	576	1.14	8.8
[Ru(dach)(PPh_3)$_2$(Cl_2)]-SBA-15	418	0.92	7.9

Note. Dach-SBA-15 = Ligand functionalized SBA-15, [Ru(dach)(PPh_3)$_2$(Cl_2)]-SBA-15 = Anchored Ru complex inside the ligand functionalized mesoporous material

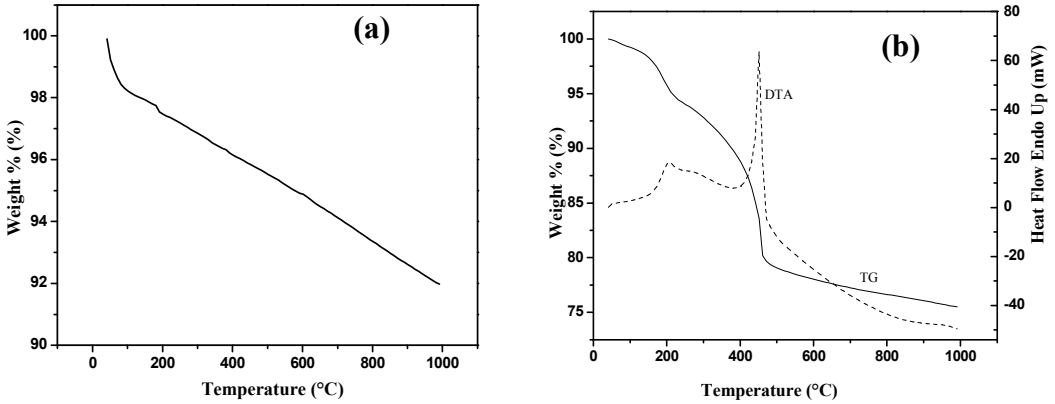

Fig. 3.2. TGA DTA curves of (a) SBA-15 and (b) [Ru(dach)(PPh_3)$_2$(Cl_2)]-SBA-15

3.3.1.4. FTIR

FTIR spectra of the dach-SBA-15 (Fig. 3.3.) showed two low intense bands at 3325, 3245 cm^{-1} which are the characteristic bands of $–NH_2$ moiety of the diaminocyclohexane ligand. The sharp bands at 2902, 2828 cm^{-1}, are the corresponding bands for asymmetric and symmetric $–CH_2$ group vibrations respectively, which belong to the propyl chain of the silylating agent. The vibrational bands at the same frequency were observed in the case of the complex anchored SBA-15 ([Ru(dach)(PPh_3)$_2$(Cl_2)]-SBA-15) also. This gave evidence of the presence of the complex inside the channels of SBA-15.

3.3.1.5. CP-MAS NMR

The successful immobilization of the chiral ruthenium complex and the structural integrity of the support were further evidenced from CP-MAS NMR spectra of [Ru(dach)(PPh_3)$_2$(Cl_2)]-SBA-15. CP-MAS ^{29}Si NMR showed several peaks that indicate different forms of silicon species (Fig. 3.4.). Peaks at −101 (*Q*3) and −110 ppm (*Q*4) are characteristic of *Q*-type (*Si*–(O–)4) silicates, which are in the bulk material. Both *Q*3 (Si–(O–Si)$_3$(OH)) and *Q*4-type (*Si*–(O–Si)$_4$) silicates are observed in relatively equal intensities suggesting that silanol groups are present in the bulk material. Peak at −67 ppm (*T*3) and the shoulder peak at -57 ppm (*T2*) are typical of *T*-type (R1–*Si*–(O–)3) silicates. This is the clearest indication that the ligand is covalently bound to the support.

The shoulder peak at −57 ppm is as a result of remnant ethoxide groups of chloropropyl triethoxysilane (*T*2 = R–Si–$(OSi)_2(OEt)$) that have not reacted with surface silanol groups. While the peak at −67 ppm is *T*3-type silcon species (*T*3 = R–$Si(OSi)_3$). No peak appeared at −45 ppm, corresponding to the chemical shift of silicon in liquid (3-aminopropyl) triethoxysilane, indicating the absence of free silane molecules physically adsorbed on the SBA-15 surface.

The integrity of organic group in [Ru(dach)$(PPh_3)_2(Cl_2)$]-SBA-15 was further identified by ^{13}C solid state NMR (Fig. 3.5). The ^{13}C CP-MAS NMR spectrum displays signals corresponding to the linker alkyl CH_2 and cyclic CH_2 in the range of 20.0-30.0 ppm [46, 47]. The signal at 35.70 may be due to the presence of residual OC_2H_5 of the cgloroproyltriethoxy silane linker. The signal at 50 ppm can be assigned to NCH_2. The existence of phenyl group (of PPh_3 ligand) was confirmed by the signals at 128.6, 134.9, and 141.4.

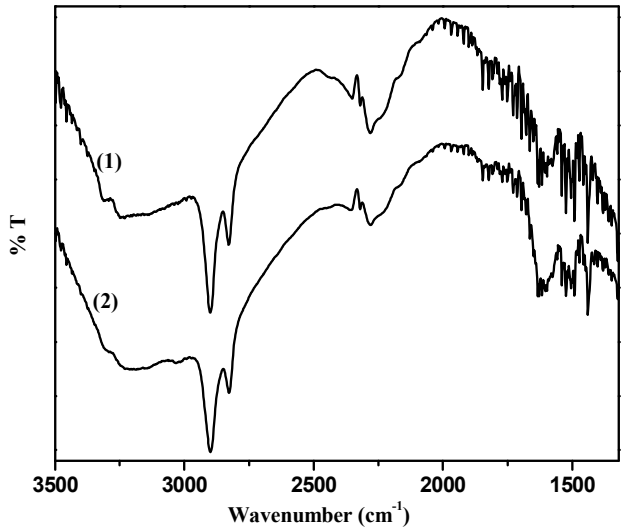

Fig. 3.3. FTIR spectra of (a) dach-SBA-15 (b) [Ru(dach)$(PPh_3)_2(Cl_2)$]-SBA-15

The ^1H - ^{31}P coupled CP-MAS NMR spectra of the [Ru(dach)$(PPh_3)_2(Cl_2)$]-SBA-15 (Fig. 3.6.) revealed two peaks at 37.9 and 47.6 which is a slight shift compared to the corresponding ^{31}P spectra of neat metal complex [48]. No peaks were observed in the region around 0 ppm where free phosphine would be expected to resonate.

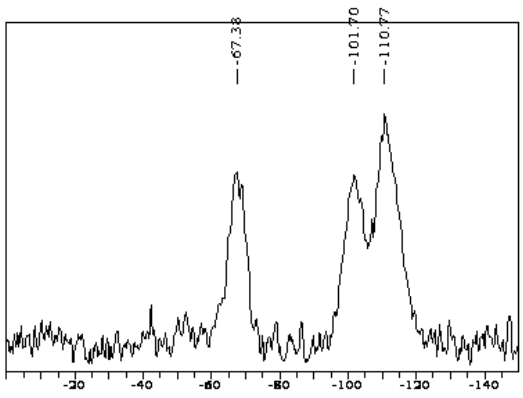

δ ppm

Fig. 3.4. ^{29}Si MAS NMR of [Ru(dach)(PPh_3)$_2$(Cl_2)]-SBA-15

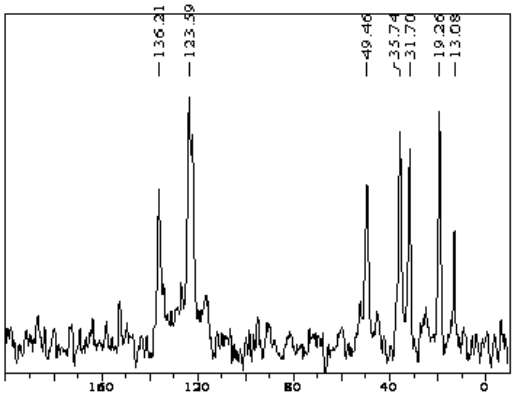

δ ppm

Fig. 3.5. ^{13}C MAS NMR of [Ru(dach)(PPh_3)$_2$(Cl_2)]-SBA-15

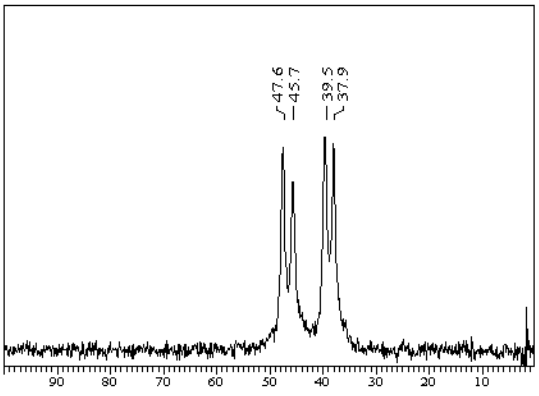

δ ppm

Fig. 3.6. ^{31}P MAS NMR of [Ru(dach)(PPh_3)$_2$(Cl_2)]-SBA-15

3.3.1.6. TEM

Fig. 3.7. represents the TEM images of (a) SBA-15, (b) [Ru(dach)(PPh_3)$_2$(Cl_2)]-SBA-15. TEM images of the parent SBA-15 and of the grafted samples provided strong evidence of the retainment of mesoporous structure of the supports. The characteristic hexagonal silicate structures shown on TEM, supports the observation made by low angle XRD.

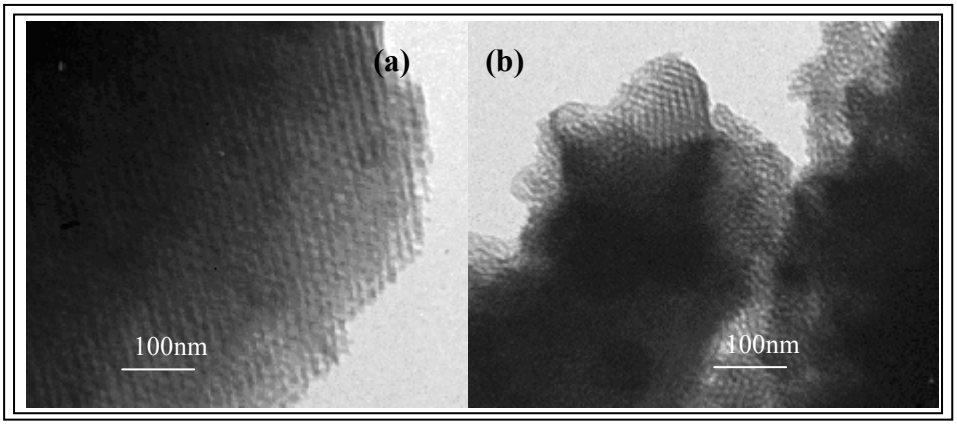

Fig. 3.7. TEM images of (a) SBA-15 (b) [Ru(dach)(PPh_3)$_2$(Cl_2)]-SBA-15

3.3.1.7. SEM

SEM images of (a) SBA-15, (b) [Ru(dach)(PPh_3)$_2$(Cl_2)]-SBA-15 samples are depicted in Fig. 3.8. SEM image of the RuPN–SBA-15 sample revealed well distributed hexagonal particles organized into rope-like structures. This observation suggests that the mesoporous matrices retained their morphological integrity (shape and size) after functionalization by organic groups, but small agglomeration occurred in immobilized catalyst.

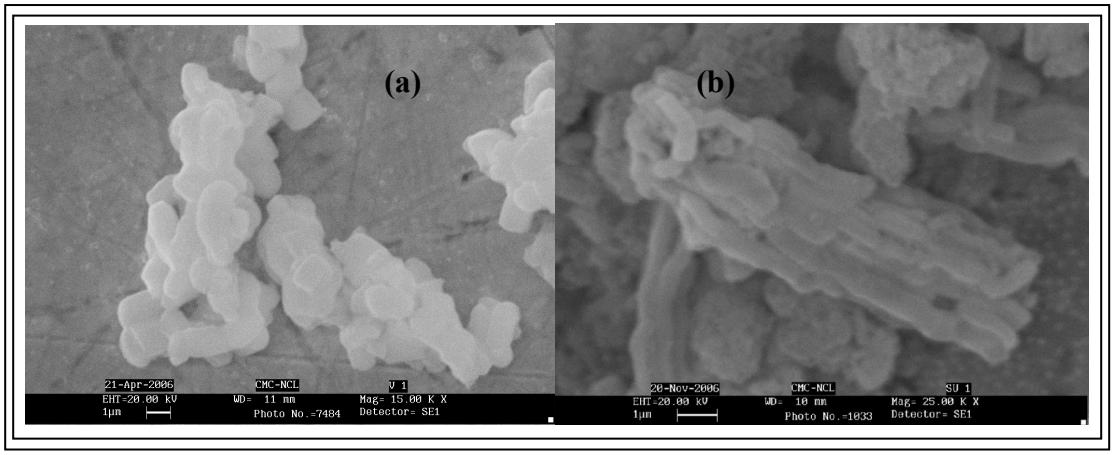

Fig. 3.8. SEM images of (a) SBA-15 (b) [Ru(dach)(PPh_3)$_2$(Cl_2)]-SBA-15

3.3.2. Catalytic activity

3.3.2.1. Enantioselective hydrogenation of ketones

The efficacy of the [Ru(dach)(PPh_3)$_2$(Cl_2)]-SBA-15 catalyst was assessed in the hydrogenation of prochiral ketones using a protocol similar to that developed for the homogeneous complex and is expressed in turnover frequencies (TOFs). 2-methylnaphthyl ketone was chosen as the substrate and potassium *tert*-butoxide as base for initial testing, and the reaction was carried out with a substrate/catalyst/base (S/C/B) ratio of 25640/1/30 at 343 K and 27 atm H_2. 1-(naphthalen-2-yl)ethanol was obtained in 90% yield (TOF 961) and 76% ee in 20 h. In comparison, the homogeneous catalyst, [$RuCl_2$ (PPh_3) $_2$((S, S)-CYDN)] gave 92% yield (TOF 982) and an ee of 75% under the same reaction conditions. The hydrogenation of 2-methylnaphthylketone with [Ru(dach)(PPh_3)$_2$(Cl_2)-MCM-41 (RuII-diphosphine/1, 2-diamine complex grafted over mesoporous silica MCM-41 by a similar procedure) resulted in the same enantioselectivity but the turnover frequency (TOF) was low as compared to the SBA-15 supported one (961versus 569) (Entry 9, Table 3.2.). This could be because of the less diffusional resistance faced by the substrate molecules to interact with the active sites of the complex in mesoporous channels, having large pore diameter in case of SBA-15 compared to MCM-41 [49, 50].

With the above results in hand, the asymmetric hydrogenation was then extended to other ketone substrates under the conditions of S/C/B =25640:1:30, 343 K and 27 atm H_2. As seen in Table 3.2, the immobilized [Ru(dach)(PPh_3)$_2$(Cl_2)]-SBA-15 exhibited high activity in terms of TOF and good enantioselectvities for various aromatic ketones, like actophenone, propiophenone, *p*-methoxyactophenone, *p*-chloroacetophenone, *p*-bromoacetophenone, and *o*-hydroxyacetophenone. The higher activity (TOF=1310) (Table 3.2, entry 5) and good enantioselectivity (75 %) was obtained in the hydrogenation of *p*-chloroacetophenone. In case of *o*-hydroxy acetophenone it afforded low conversion (TOF-641) and low ee (15%) (Table 3.2, entry 8). Acetophenone got hydrogenated to α-methylbenzyl alcohol with an ee of 52% (entry 3, Table 3.2). The *p*-methoxy acetophenone gave low ee of 34% (, Table 3.2, entry 4) with 1051 TOF value. Results with the substituted acetophenones suggested that electron-withdrawing groups showed higher substrate conversions and *o*-substitution with electron-donating groups tends to afford both low conversion and low ee. But *p* –bromoacetophenone was an exception. Low ee (30%) (Table 3.2, entry 6) was observed. These observations are reminiscent of those made with the parent homogeneous analogue.

Table 3.2.

Hydrogenation of prochiral ketones[a]

Entry	Substrate	Time (h)	Conv (%)	ee (%)	TOF
1	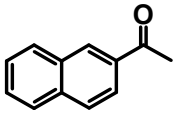	24	90	76	961
2[b]	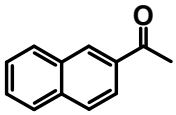	24	92	75	982
3	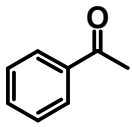	20	90	52	1153
4	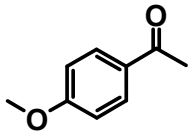	20	82	34	1051
5	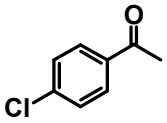	18	92	75	1310
6	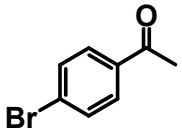	20	91.5	30	1173
7	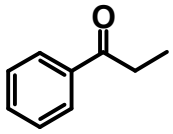	24	90	35	961
8	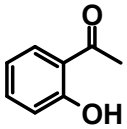	24	60	14	641
9[c]	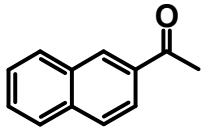	36	80	74	569

[a] Reactions were carried out at 343 K and 27 atm H_2 using 10mmol of the prochiral ketones and a substrate/catalyst/base ratio of 25640/1/30 in 40 mL of 2-propanol, [b] In the homogeneous condition [c] Reaction was carried out using MCM-41 as a support. Turnover frequency (TOF = mole of substrate converted per mole of Ru complex per hour).

3.2.2.2. Chemoselective hydrogenation of α, β-unsaturated ketones

The chemoselective hydrogenation of α, β-unsaturated ketones were carried out with a substrate/catalyst/base (S/C/B) ratio of 25640/1/30 at 343 K and 27 atmH_2, (E)-1,3-diphenyl-2-en-1-one was converted to the corresponding allyl alcohol in high conversion (TOF 2519) and high selectivity (>99%) (Table 3.3, entry 1). The reduction of 1-phenylbut-2-ene-1-one occurred with a TOF of 2435 and >99% selectivity for the corresponding allyl alcohol (Table 3.3, entry 2). In case of the chemoselective hydrogenation of cyclohex-2-enone, the major product was cyclohexanone and the selectivity of the corresponding allyl alcohol was only 10%, but when one methyl group is present in the 3rd position, the major product was the corresponding allyl alcohol (Table 3.3, entries 3 and 4).

Table 3.3.

Chemoselective Hydrogenation of α, β- unsaturated ketones[a]

Entry	Substrate	Time (h)	Convn. (%)	Selectivity (%)	TOF
1.	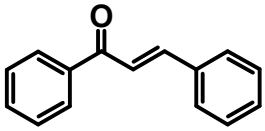	14	98	>99	1794
2.	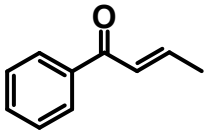	10	95	>99	2435
3.	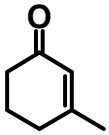	20	70	>90	897
4.	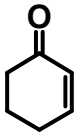	22	100	10	1165

[a] Reactions were carried out at 343 K and 27 atm H_2 using 10 mmol of the prochiral ketones and a substrate/catalyst/base ratio of 25640/1/30 in 40 mL of 2-propanol

3.3.2.3. Hydrogenation of imines

[Ru(dach)(PPh_3)$_2$(Cl_2)]-SBA-15 was also active in the hydrogenation of imines to the corresponding secondary amines. Here, no enantiomeric excess of the product was obtained as in the case of its homogeneous analogue [51] but it showed good activity as compared to its homogeneous analogue.

Table 3.4.

Hydrogenation of imines[a]

Entry	Substrate	Time(h)	Convn.(%)	TOF
1.	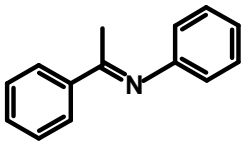	18	98	349
2.	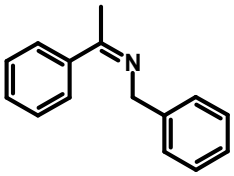	20	97	311
3.	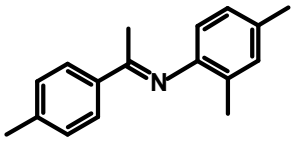	24	60	160
4.	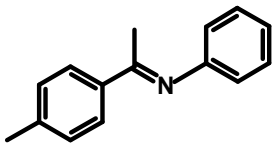	20	90	288

[a]Reactions were carried out at 348 K and 27 atm H_2 using 2.5 mmol of the substrate (imine); Substrate / catalyst / base ratio of 6410 /1 /30 in 20 mL of 2-propanol

The hydrogenation of imines was carried out with a substrate/ catalyst/base (S/C/B) ratio of 6410/1/30 at 348 K and 27 atm H_2. Hydrogenation of N-(1-phenylethylidine) benzenamine to corresponding secondary amine has a TOF of 349 h^{-1} (Table 3.4, entry 1). Phenyl-N-(1-phenylethylidine)methanamine was converted to the corresponding secondary amine with 97% conversion (Table 3.4, entry 2). The 2,5-

dimethyl-N-(1-phenylethylidine)benzenamine showed less reactivity (Table 3.4, entry 3) in its hydrogenation, which may be due to the steric effect caused by the adjacent methyl groups in the aniline ring. Hydrogenation of N-(1-*p*-tolylethylidine)benzenamine showed activity of 90% conversion (with a TOF of 288 h^{-1}) to give the corresponding secondary amine. Since imines are generally derived from the corresponding aldehydes or ketones, the overall reaction in one-pot constitutes a method for direct reductive amination, which would be an attractive synthetic route to secondary and tertiary amines.

3.3.2.4. Catalyst recycling

An attractive feature of the reported catalytic system lies in the fact that the catalyst from the product can be easily removed by filtration and reused in the next cycle. Thus, when the hydrogenation was completed, the reaction mixture was filtered over a G-4 crucible; the used catalyst was thoroughly washed with 2-propanol and dried in vacuo. After this treatment, the catalyst was ready for the next cycle. For example, in each following runs, the amounts of Methylnaphthylketone, 2-propanol, and base were the same as in the first run. In three consecutive runs, the following conversions (ee's in parenthesis) were observed: 90 %(75%), 89 %(75%), and 74 %(69%) (Table 3.5). These data suggest that it is possible to recycle the [Ru(dach)(PPh_3)$_2$(Cl_2)]-SBA-15 catalyst atleast for 4 cycles.

Table 3.5.

Recyclability of the catalyst in the hydrogenation of Methylnaphthalene ketone

Entry	Cycle	Time(h)	Convn. (%)	ee (%)	TOF
1	Fresh	24	90	76	961
2	1st	24	90	75	961
3	2nd	24	89	75	950
4	3rd	24	74	69	801

Reactions were carried out at 343 K and 27 atm H_2 using 10 mmol of the prochiral ketones and a substrate/catalyst/base ratio of 25640/1/30 in 40 mL of 2-propanol

3.4. Conclusions

In summary, we have synthesized easily accessible chiral 1, 2-diaminocyclohexane-derived organic-inorganic hybrid ligands by attaching the homogeneous chiral ligand covalently onto mesoporous SBA-15. The catalyst was evaluated by different techniques including NMR and FTIR, revealing the intact of structural integrity of the immobilized catalysts after functionalization. Ruthenium amine complex immobilized on to SBA-15 was found to be the most active immobilized multifunctional catalyst system for the enantioselective hydrogenation of prochiral ketones and in the chemoselective hydrogenation of carbonyl group over olefin group in α, β- unsaturated ketones. This catalyst showed good activity in the heterogeneous hydrogenation of imines also. The activities were comparable with that of homogeneous analogues in all the reactions studied. Most importantly this catalyst could be recyclable. The simplicity of the process (mild reaction condition, easy catalyst recover), the high yields and good enantioselectivity render this heterogeneous process an attractive alternative to the few existing heterogeneous methods available for metal-catalyzed asymmetric hydrogenation of prochiral ketones.

3.5. References

1. R. Noyori, Asymmetric catalysis in Organic Synthesis, Chapter 2, Willey, New York, 1994.
2. H. Bauer, C. Malan, B. Pugin, F. Spindler, H. Steiner, M. Studer, Adv. Synth. Catal. 345 (2003) 103 and the references cited therein.
3. R.M. Machado, K.R. Heier, R.R. Broekhuis, Curr. Opinion Drug Discov. Devel. 4 (2001) 745.
4. R. Noyori, M. Koizumi, D. Ishii, T. Ohkuma, Pure Appl. Chem. 73 (2001) 227.
5. M. Yamakawa, H. Ito, R. Noyori, J. Am. Chem. Soc. 122 (2000) 1466.
6. D.A. Alonso, P. Brandt, S.J.M. Nordin, P.G. Andersson, J. Am. Chem. Soc. 121 (1999) 9580.
7. J.A. Kenny, K. Versluis, A.J.R. Heck, T. Walsgrove, M. Wills, Chem. Commun. (2000) 99.
8. R. Hartmann, P. Chen, Angew. Chem., Int. Ed. 40 (2001) 3581.
9. K. Abdur-Rashid, M. Faatz, A. J. Lough, R. H. Morris J. Am. Chem. Soc. 123 (2001) 7473.
10. A.K. Ghose, V.N. Viswanadhan, J.J. Wendoloski, J. Comb. Chem. 1 (1999) 55.
11. T. Henkel, R.M. Brunne, H. Mueller, F. Reichel, Angew. Chem., Int. Ed. 38 (1999) 643.
12. B.R. James, Catal. Today 37 (1997) 209.
13. M.D. Fryzuk, W.E. Piers, Organometallics 9 (1990) 986.
14. E.W. Baxter, A.B. Reitz, Organic Reactions, Wiley: New York, 2002 Vol. 59, p 1.
15. V.I. Tararov, R. Kadyrov, T.H. Riermeier, C. Fischer, A. Börner, Adv. Synth. Catal. 346 (2004) 561.
16. R. Apodaca, W. Xiao, Org. Lett. 3 (2001) 1745.
17. B. Miriyala, S. Bhattacharyya, J.S. Williamson, Tetrahedron 60 (2004) 1463.

18. R. Noyori, T. Ohkuma, Angew. Chem., Int. Ed. 40 (2001) 40.
19. R. Noyori, T. Ohkuma, Pure Appl. Chem. 71 (1999) 1493.
20. H. Doucet, T. Ohkuma, K. Murata, T. Yokozawa, M. Kozawa, E. Katayama, A.F. England, T. Ikariya, R. Noyori, Angew. Chem., Int. Ed. 37 (1998) 1703.
21. T. Ohkuma, M. Koizumi, H. Doucet, T. Pham, M. Kozawa, K. Murata, E. Katayama, T. Yokozawa, T. Ikariya, R. Noyori, J. Am. Chem. Soc. 120 (1998) 13529.
22. T. Ohkuma, M. Koizumi, K. Munfiz, G. Hilt, C. Kabuto, R. Noyori, J. Am. Chem. Soc. 124 (2002) 6508.
23. M.J. Burk, W. Hems, D. Herzberg, C. Malan, A. Zanotti-Gerosa, Org. Lett. 2 (2000) 4173.
24. K. Mikami, T. Korenaga, T. Ohkuma, R. Noyori, Angew. Chem. Int. Ed. 39 (2000) 3707.
25. C.J. Cobley, J.P. Henschke, Adv. Synth. Catal. 345 (2003) 195.
26. N.B. Johnson, I.C. Lennon, P.H. Moran, J.A. Ramsden, Acc. Chem. Res. 40 (2007) 1291.
27. D.E. Bergbreiter, Chem. Rev. 102 (2002) 3345.
28. N.E. Leadbeater, M. Marco, Chem. Rev. 102 (2002) 3217.
29. C.A. McNamara, M.J. Dixon, M. Bradley, Chem. Rev.102 (2002) 3275.
30. T.J. Dickerson, N.N. Reed, K.D. Janda, Chem. Rev. 102 (2002) 3325.
31. G.E. Oosterom, J.N.H. Reek, P.C.J. Kamer, P.W.N.M. Van Leeuwen, Angew. Chem., Int. Ed. 40 (2001) 1828.
32. D. Astruc, F. Chardac, Chem. Rev. 101 (2001) 2991.
33. R. Van Heerbeek, P.C.J. Kamer, P.W.N.M. Van Leeuwen, J.N.H. Reek, Chem. Rev. 102 (2002) 3717.
34. C.E. Song, S. Lee, Chem. Rev. 102 (2002) 3495.
35. Q.H. Fan, Y.M. Li, A.S.C. Chan, Chem. Rev. 102 (2002) 3385.
36. D.E.D. Vos, M. Dams, B.F. Sels, P.A. Jacobs, Chem. Rev. 102 (2002) 3615.
37. D. Zhao, J. Feng, Q. Huo, N. Melosh, G.H. Frederickson, B.F. Chmelka, G.D. Stucky, Science 279 (1998) 548.
38. D. Zhao, Q. Huo, J. Feng, B.F. Chmelka, G.D. Stucky, J. Am. Chem. Soc. 120

(1998) 6024.

39. J. Fan, C.Yu, L. Wang, B. Tu, D. Zhao, Y. Sakamoto, O. Terasaki, J. Am. Chem. Soc. 123 (2001) 12113.
40. A. Hu, H. L. Ngo, W. Lin, J. Am. Chem. Soc. 125 (2003) 11490.
41. D. Wu, E. Linder, H.A. Mayer, Z. Jiang, V. Krishnan, H. Bertagnolli, Chem. Mater. 17 (2005) 3951.
42. Y. Liang, Q. Jing, X. Li, L. Shi, K. Ding, J. Am. Chem. Soc. 127 (2005) 7694.
43. A. Ghosh, R. Kumar, J. Catal. 228 (2004) 386.
44. P. Schnider, G. Koch, R. Preto, G. Z.Wang, F.M. Bohnen, C. Kruger, A. Pfaltz, Chem. Eur. J. 3 (1997) 887.
45. T.A. Stephenson, G. Wilkinson, J. Inorg. Nucl. Chem. 28 (1996) 945.
46. S. Handoudi, Y. Yang, I.L. Moudrakovski, S. Lang, A. Sayari, J. Phys. Chem. B 105 (2001) 9118.
47. A. Adima, J.J.E. Moreau, M. Wong Chi Man, J. Mater. Chem. 7 (1997) 2331.
48. Y.Q. Xia, Y.Y. Tang, Z.M. Liang, C. Yu, X. Zhou, R. Li, X. Li, J. Mol. Catal. A: Chemical 240 (2005) 132.
49. T. Joseph, S.S. Deshpande, S.B. Halligudi, A. Vinu, S. Ernst, M. Hartman, J. Mol. Catal. A: Chemical 206 (2003) 13.
50 R.I. Kureshy, I. Ahmed, N.H. Khan, S.H.R. Abdi, K. Pathak, R.V. Jasra, J. Catal. 238 (2006) 134.
51. K.A. Rashid, A.J. Lough, R H. Morris, Organometallics 19 (2000) 2655.

CHAPTER IV

Hydrogenation of Olefins

4. Enantioselective hydrogenation of olefins by chiral iridium phosphorothioite complex covalently anchored on mesoporous silica

4.1. Introduction

The pioneering work [1-4] at the beginning of this century brought about a renaissance on the use of monodentate phosphorus ligands in the asymmetric hydrogenation reactions. The development of binol derived monodentate phosphorus ligands has been a research topic of increasing interest because of their easy preparation methods, higher stabilities, and excellent activities and enantioselectivities in asymmetric catalysis [5]. Because of high cost of chiral ligands and noble metals employed in catalyst preparation, the recovery of the catalyst becomes an important issue for the application of enantioselective catalyst in large-scale processes. In recent years, an enormous progress has been made in interdisciplinary research on the development of stereoselective solid phase catalysis for asymmetric synthesis [6]. The heterogenization of a homogeneous catalyst would provide many advantages such as easy separation, efficient recycling, minimization of metal traces in the product, and process control, which would finally reduce the overall process cost. It is reported that heterogeneous catalysts are even more selective than their homogeneous analogues in some reactions [7, 8] and also the potentials of heterogeneous chiral catalysts have been reported in recent reviews [9-14]. Simons et al. have reported the successful immobilization of rhodium complex of the monodentate ligand on silica support [15, 16] and its use in the asymmetric hydrogenation reactions. The covalent anchoring of ligands suffers from lengthy steps involved in functionalization of ligand and effective covalent anchoring onto the support [17, 18]. Inorganic material-immobilized catalysts possess some advantages, though they attracted little attention [19-21] compared to immobilized catalysts prepared from organic polymeric supports. The immobilized chiral transition metal catalysts prepared from inorganic materials would prevent intermolecular aggregations of the active species because of their rigid structures. These catalysts often exhibit superior thermal and mechanical stabilities, and they do not swell or dissolve in organic solvents.

Recently iridium complex of monodentate phosphoramidite ligand has been reported for the asymmetric hydrogenation reactions in homogeneous conditions by Giacomina et al [22]. Hydrogenation products like chiral 2-substituted succinic acids have attracted a great interest for their utility as chiral building blocks in recent years [23, 24]. In this chapter, we will describe the synthesis of a binol derived monodentate triethoxysilyl phosphorothioite PS ligand (hereafter PS) and its iridium complex covalently anchored onto high surface area mesoporous silica supports as well as their applications in the asymmetric hydrogenation of itaconic acid and its derivatives. The effects of reaction parameters such as substrate to catalyst mole ratio, temperature, hydrogen pressure, catalyst concentration and solvents on the optimum substrate conversions and product enantioselectivities in the hydrogenation of olefinic substrates has been discussed.

4.2. Experimental

4.2.1. Chemicals

$[Ir(COD)Cl]_2$, *S*-binol, 3-thiopropyltriethoxysilane, TEOS, pluronic-123, dimethylitaconate, itaconic acid, triethyl amine were purchased from Aldrich. Diethylitaconate was prepared from itaconic acid by esterification with ethanol. Phosphorous trichloride and CTAB (cetyltrimethylammonium bromide) were procured from Loba Chemie, India and they were used as received without further purification. Dichloromethane, ethyl acetate, toluene, methanol, tetrahydrofuran and diethyl ether were purchased from Ranbaxy, India and distilled prior to their use following the standard procedure. For the quantitative estimation of enantiomers, the racemic products were obtained by Pd-charcoal catalyzed reduction.

4.2.2. Catalyst preparation

4.2.2.1. Synthesis of triethoxysilyl phosphorothioite ligand (PS)

Scheme 4.1. depicts the synthesis of the monodentate PS ligand. S-binol (0.5 g) in 3 mL of phosphorous chloride (PCl_3) was heated under reflux for 8 h. Then excess PCl_3 was removed by evaporation under vacuum. The resultant solid was subjected to azeotropic distillation with toluene and dried under vacuum. The resulting residue was dissolved in toluene (10 mL) and added to a solution of 0.38 g (1.8 mmol) of

thiopropyltriethoxysilane and 0.6 mL triethylamine in 5 ml of dry tetrahydrofuran at 0 °C.

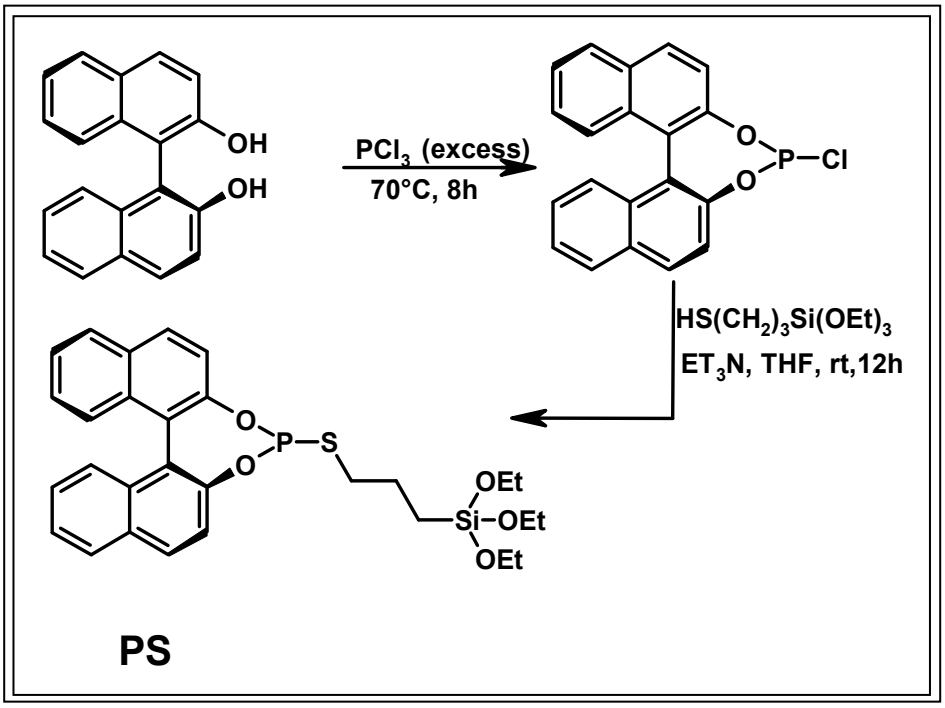

Scheme 4.1. Synthesis of the monodentate triethoxysilylphosphorothioite ligand

The resulting mixture was diluted with diethyl ether (12 mL), filtered over a plug of silica and washed with 50 mL of diethyl ether. The solvent was then removed under vacuum. Column chromatography on silica gave pure PS ligand. $[\alpha]_D$= + 57.53 (C=2.01, $CHCl_3$) ^{1}H NMR ($CDCl_3$): δ 0.64 (m, 2H), 1.25-1.33 (t, 12H), 1.65 (m, 2H), 1.93-1.97 (m, 2H), 3.40-3.52(m, 6H), 7.08 (1H), 7.27-7.40 (m, 7H), 7.84-7.95(m, 4H) ^{31}P NMR ($CDCl_3$): δ 115. It was immediately used in the synthesis of phosphorothioite functionalized SBA-15. FTIR (cm^{-1}): 3059, 2942, 2839, 1460, 740, 809, 459.

4.2.2.2. Synthesis of homogeneous iridium complex of PS ligand (IrPS)

The homogeneous iridium phosphorothioite complex was synthesized as reported in the literatue [22]. [{Ir(cod)Cl}$_2$] (65 mg, 0.096 mmol) was placed in a 10-mL Schlenk flask and the entire apparatus was evacuated and back-filled with N_2 three times to establish an inert atmosphere. Dry, degassed dichloromethane (1 mL) and PS ligand (100 mg, 0.192 mmol) were added and the reaction mixture was stirred at room temperature

for 10 min. The solvent was removed under vacuum to give homogeneous IrPS complex. ^{1}H NMR(300 MHz, CDCl3): ^{1}H NMR ($CDCl_3$): δ 0.65 (m, 2H), 1.26-1.35 (t, 12H), 1.63 (m, 2H), 1.95-1.99 (m, 2H), 2.74-2.83(m, 4H), 3.14-3.24 (m, 4H), 3.41-3.53(m, 6H), 5.13-5.24 (m, 2H), 5.29-5.40 (m, 2H), 7.08 (1H), 7.27-7.40 (m, 7H), 7.84-7.95(m, 4H) ^{31}P NMR ($CDCl_3$): δ 83.1. FTIR (cm^{-1}): 3059, 2942, 2839, 1460, 740, 809, 459.

4.2.2.3. Synthesis of siliceous support

The pure siliceous supports like MCM-41, MCM-48 and SBA-15 were prepared according to the earlier reports [25-27].

4.2.2.4. Synthesis of ligand functionalized SBA-15

3 g of SBA-15 and 0.5 g of the PS ligand were mixed in 50 mL chloroform and refluxed for 18 h (Scheme 4.2). The resulting material was filtered and washed with chloroform for several times and dried under vacuum at 50 °C to give ligand functionalized SBA-15 (PSSBA-15). Ligand functionalization of MCM-41 and MCM-48 were carried out similarly to obtain PSMCM-41 and PSMCM-48, respectively.

4.2.2.5. Covalent anchoring of iridium complex onto ligand modified SBA-15

$[Ir(COD)Cl]_2$ (0.05 g) dissolved in 50 mL of dichloromethane was added slowly to 3 g of the PSSBA-15 and the mixture was stirred at room temperature overnight. The resulting solid was filtered, washed repeatedly with dichloromethane and then dried under vacuum at 40 °C to get iridium complex covalently anchored onto SBA-15 (hereafter IrPSSBA-15). Similarly, IrPSMCM-41 and IrPSMCM-48 were prepared by following the above procedure.

4.2.3. Catalyst testing

In a typical reaction, olefin (10 mmol) and IrPSSBA-15 (0.20 g, 0.006 mmol of iridium) in 50mL of dichloromethane were placed in a 300 mL Parr autoclave and the autoclave was purged with hydrogen for five times and then was pressurized with 20 bar H_2 and stirred at 40 °C. Samples were withdrawn at regular intervals of time and analyzed for its contents by Shimadzu 14B gas chromatograph, equipped with a flame ionization detector using HP-chiral capillary (30 m x 0.320 mm x 0.25 μm) column. The conversions of substrate and product enantioselectivities were estimated from gas chromatographic analysis by following a standard method.

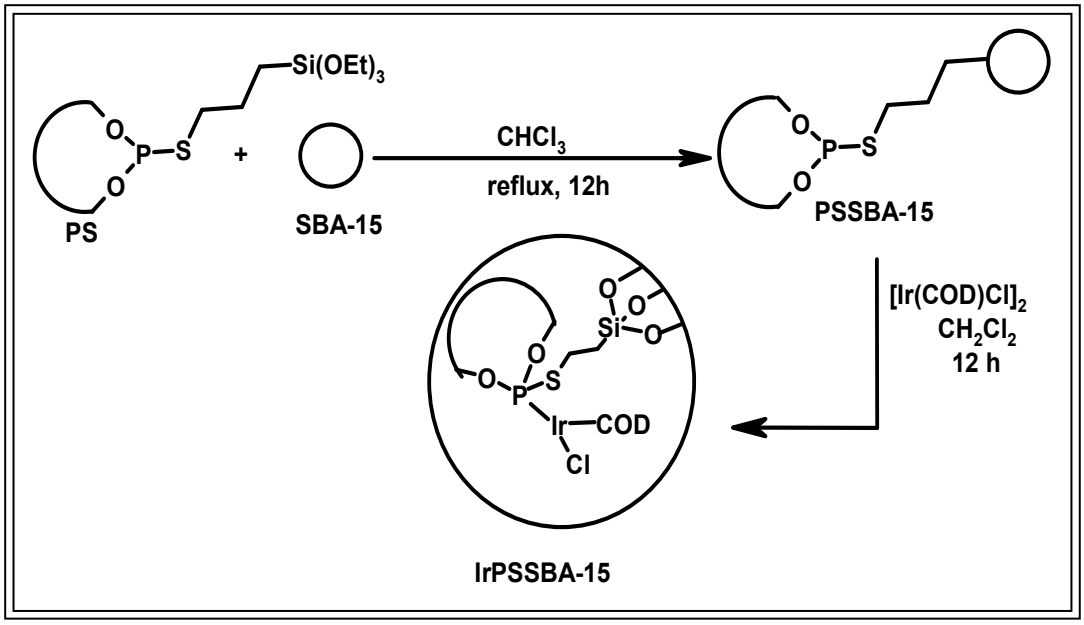

Scheme 4.2. Covalent anchoring of the ligand onto the mesoporous silica SBA-15

After completion of the reaction, the reaction mixture was filtered to remove the catalyst and the solvent was removed under reduced pressure. The resultant mixture was dried and purified by column chromatography on silica gel as the stationary phase (petroleum ether/ ethyl acetate, 90/10). The optical rotation of products was measured by Jasco P-1020 polarimeter. For example, dimethylmethylsuccinate: Colorless liquid, enantiomeric excess was found to be 94 % (GC condition: 90 °C isothermal, 60 min., minor isomer: 36.7, major isomer: 40.0) ^{1}H NMR ($CDCl_3$, 200MHz): δ = 3.61 (s,1H), 3.63 (s, 1H), 2.66-2.74 (2H, m), 2.36-2.39 (1H, m), 1.13-1.17 (3H, d), GCMS *m/z* (relative intensity): 161 (0.05) [M^+], 129 (20.30), 100 (10.93), 87 (8.68), 69 (10.50), 59 (100), 41 (31.91), Absolute configuration – *R*, Optical rotation, $[\alpha]_D$ = + 4.5, C = 3 in chloroform (literature value: $[\alpha]_D$ = + 4.9, C = 2.9 in chloroform).

4.3. Results and discussion

Our main objective in this study was the easy covalent anchoring of monodentate binol derived ligands to mesoporous silica support through the phosphorous heteroatom in minimum number of steps. For the covalent anchoring of the phosphoramidite ligand through nitrogen part of the ligand, the nitrogen precursor has to be monoalkylated as a

secondary amine is needed as reported in literature. The monoalkylation of aminopropyltriethoxysilane was difficult as it gave both mono- and dialkylated product, which made the procedure tedious. The precursor for the covalent anchoring of the monodentate phosphite ligand is not readily available and hence we tried with the readily available thiopropyltriethoxysilane as the precursor for the covalent anchoring of phosphorothioite ligand. This ligand is new and reported for the first time, for easy covalent anchoring to the mesoporous support. The monodentate triethoxysilyl phosphorothioite ligand (PS) was easily synthesized from commercially available starting materials in minimum number of steps. The ^{1}H and ^{31}P NMR of the PS ligand confirmed the presence of the phosphorous anchoring moiety in the ligand. The optical rotation data confirmed the retention of chirality of the ligand after functionalization with the thio propyltriethoxysilane group. The homogeneous complex (IrPS) was synthesized from the iridium precursor, $[Ir(COD)Cl]_2$, with iridium to ligand ratio one as reported in case of the iridium monodentate complex [22]. Mesoporous silica supports such as SBA-15, MCM-41 and MCM-48 were functionalized with monodentate triethoxysilyl phosphorothioite ligand and then complexation with iridium was carried out to get covalently anchored catalysts. These catalysts were characterized for their physicochemical properties by different techniques to establish their integrity and stabilities for use as heterogeneous catalysts in asymmetric hydrogenation reactions. The efficacies of these catalysts were assessed in the enantioselective hydrogenation of itaconic acid and its derivatives under different reaction conditions. The reaction conditions have been optimized to get higher substrate conversions and enantiomeric excess (ee) for products.

4.3.1. Catalyst characterization

4.3.1.1. Low angle XRD

The powder XRD patterns of ligand functionalized and complex immobilized supports and corresponding parent supports are shown in Fig. 4.1. Parent MCM-41 and SBA-15 supports exhibited three XRD peaks assigned to reflections at (100), (110), and (200), which are characteristic of 2D hexagonal lattice (Figs. 4.1(a) and 1(c)) and indicate a significant degree of long range ordering in the structure. The XRD patterns of MCM-

48 (Fig. 4.1(b)) showed an intense peak corresponding to (211) reflection along with a shoulder peak at (220) reflection, which are typical for cubic cells. Phosphorothioite ligand modified sample (PSSBA-15) showed decreased intensities of all the peaks, with a marginal shift towards lower 2θ values, indicating silylation inside the mesopores of SBA-15. The peak intensities at (100), (110) and (200) reflections of IrPSSBA-15 were further decreased, indicating the immobilization of iridium complex inside the mesoporous channels of SBA-15. However, the mesoporous structure of the support remained intact under the conditions used for immobilization. Similar results were observed for MCM-41 and MCM-48 supported catalysts (Fig. 4.1(a) and 1(b)). These results indicate an ordered mesoporosity of the supports even after the incorporation of organic functional groups and iridium complexes.

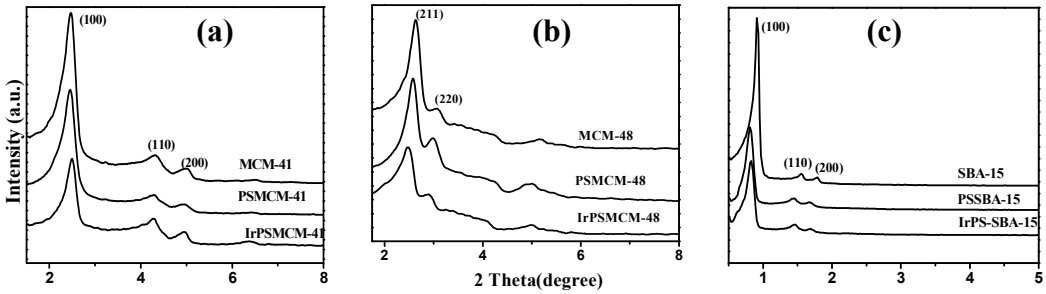

Fig. 4.1. Low angle powder XRD patterns of the materials.

4.3.1.2. N_2 sorption study

The specific surface area, pore volume, and pore diameters estimated from N2 sorption studies of ligand-functionalized and iridium complex immobilized materials are presented in Table 4.1. BET surface areas and BJH pore size distributions were calculated using N2 adsorption at -196 °C. Ligand functionalization and iridium complex immobilization affected the surface area and pore distribution of the modified samples. The samples displayed a type IV isotherm (as defined by IUPAC) with H1 hysteresis and a sharp increase in pore volume adsorbed above *P/P*0 0.7 cm^3/g (Fig. 4.2), which is a characteristic of highly ordered mesoporous materials. The textural properties of SBA-15 were substantially maintained over ligand functionalization and on subsequent complexation of $[Ir(COD)Cl]_2$. The parent SBA-15 sample exhibited a maximum pore

diameter (79 Å) and surface area (730 m^2/g) as seen in Table 4.1. Ligand functionalization of mesoporous silica resulted in a shift of the pore maximum to smaller diameters and a decrease in surface area (617 m^2/g). The complexation led to a further decrease in surface area and pore volume. Same trend was observed in case of the other two supports.

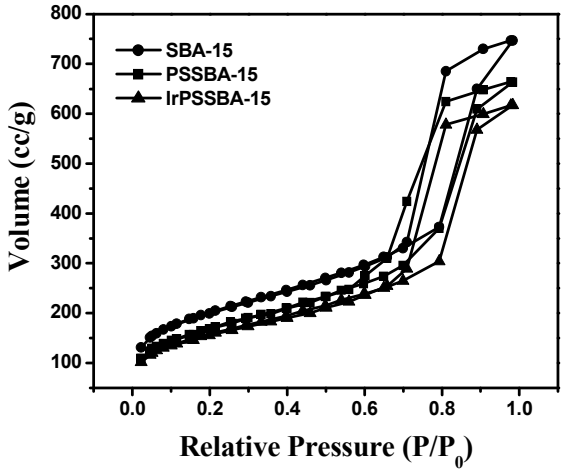

Fig. 4.2. Nitrogen sorption isotherms

Table 4.1.

Physicochemical properties of the materials

No.	Catalyst	Surface area BET ($m^2\ g^{-1}$)	Pore volume (cm^3/g)	Average pore diameter(Å)
1.	MCM-41	1093	0.88	32.6
2.	MCM-48	983	0.75	27
1	SBA-15	730	1.15	79
2	PSMCM-41	685	0.57	24
3	PSMCM-48	556	0.51	20
4	PSSBA-15	617	0.54	68
5	IrPSMCM-41	441	0.28	19
6	IrPSMCM-48	430	0.23	17
7	IrPSSBA-15	572	0.30	20

4.3.1.3. Microscopic analysis

SEM images of IrPSSBA-15 (Fig. 4.3) shows the rope-like micro morphology of SBA-15 remained intact, even after functionalization with ligand and iridium complex. TEM measurements were carried out to study the morphology of SBA-15 and IrPSSBA-15 catalysts (Fig. 4.4). TEM images of these catalysts showed retention of the periodic structure of parent SBA-15 precursor, which confirms that the hexagonally arranged mesopores of SBA-15 are retained after modification with ligand and iridium complex.

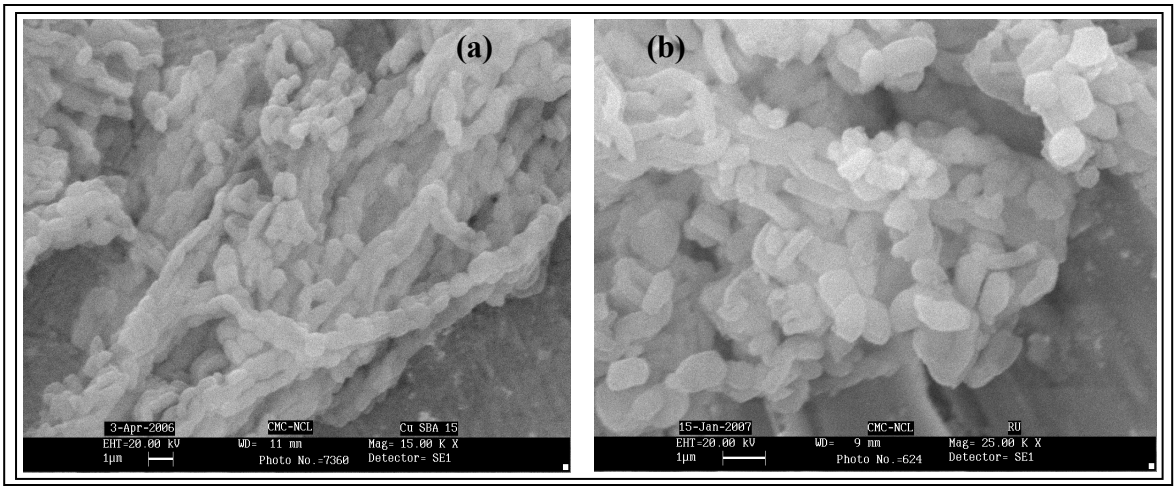

Fig. 4.3. SEM photographs of (a) SBA-15 and (b) IrPSSBA-15

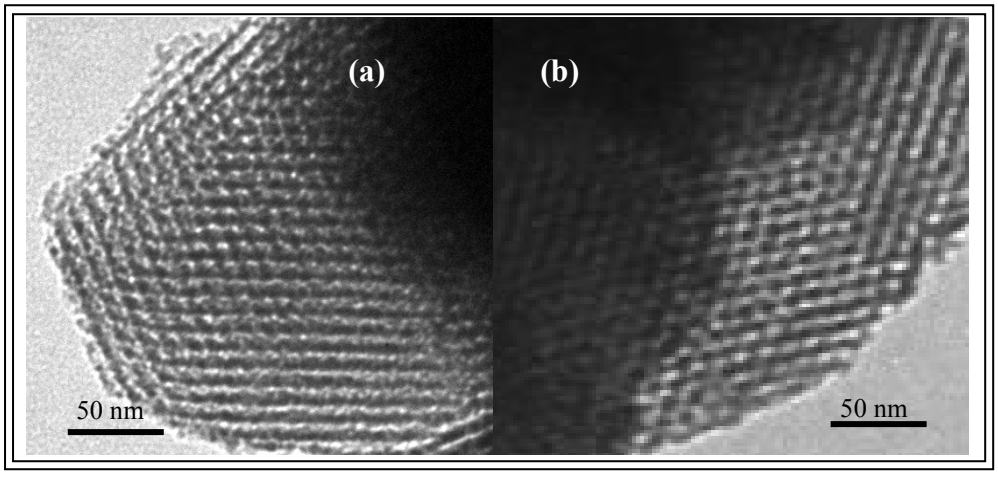

Fig. 4.4. TEM photographs of (a) SBA-15 and (b) IrPSSBA-15

4.3.1.4. Nuclear Magnetic Resonance

MAS NMR is a good technique for investigating ligand functionalization and complex anchored onto the mesoporous support. PSSBA-15 and IrPSSBA-15 samples contain small amount of phosphorus, so we used cross polarization (^{1}H-^{31}P) MAS NMR to enhance the sensitivity of ^{31}P signal. ^{1}H - ^{31}P coupled CP-MAS NMR spectra of the ligand functionalized SBA-15 (PSSBA-15) and iridium complex anchored SBA-15 (IrPSSBA-15) are depicted in Fig. 4.5 (a) and 4.5 (b), respectively. ^{31}P peak corresponding to PSSBA-15 has a marginal shift at 113.6 ppm, compared to neat ligand (115 ppm), which could be due to the difference in the ligand environment. IrPSSBA-15 exhibits ^{31}P peak at δ 81.6 ppm, which clearly indicates that the iridium complex has covalently anchored to the modified SBA-15 support and the shift is a clear confirmation of the presence of the iridium complex in a new environment [22].

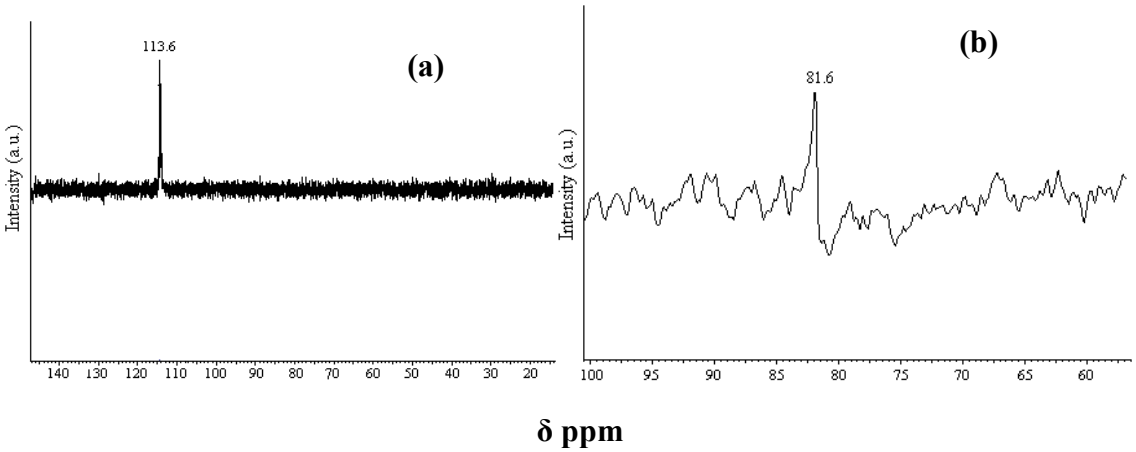

Fig. 4.5. ^{31}P MAS NMR spectra of (a) PSSBA-15 and (b) IrPSSBA-15

4.3.1.5. FTIR

FTIR spectra of PSSBA-15 and IrPSSBA-15 are shown in Fig. 4.6 (a) and 4.6 (b). SBA-15 showed characteristic FTIR peaks in the range 2900-3800, 1080, and 450 cm^{-1} due to O–H of the silanols, adsorbed water molecules and Si–O–Si stretching vibrations, respectively. PSSBA-15 showed an additional peak at 1460 cm^{-1} due to the C=C stretching of the aromatic ring and 2975 and 2845 cm^{-1} due to C-H and C-C stretching modes of the propyl spacer, respectively. The bands observed in the range 730-

800 cm^{-1} are due to the O-P-O stretching (Fig. 4.6 (a)) and P-S stretching band (460 cm^{-1}) [28] gets merged with Si–O–Si stretching vibrations. Similar results were observed for MCM-41 and MCM-48 supports. FTIR results support the successful incorporation of metal complex onto the surface of mesoporous silica.

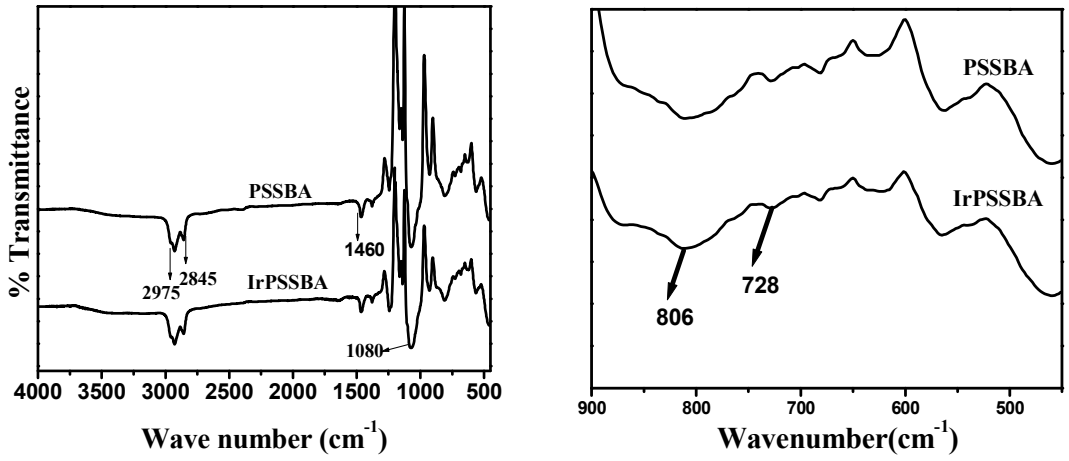

Fig. 4.6. FTIR spectra of PSSBA-15 and IrPSSBA-15, (a) Wave number range (500- 900 cm^{-1}), (b) wave number range (500-4000 cm^{-1})

4.3.2. Catalytic results

The efficiency of the three immobilized catalysts prepared was assessed in the enantioselective hydrogenation of itaconic acid and its derivatives. These results are summarized in Table 4.2. Dimethylitaconate was chosen as the test substrate and the heterogeneous enantioselective liquid phase hydrogenation was carried out with a substrate to catalyst molar ratio of 1660:1 in dichloromethane at 40 °C and 20 bar H_2. A homogeneous liquid phase reaction was also performed with neat iridium complex (IrPS) under similar conditions for comparative purpose. It was found that the activity (in terms of turn over number (TON), which is defined as mole of substrate converted per mole of iridium) of neat complex was two times higher than the heterogeneous system. This could be due to a slower interaction between the substrate and the catalyst in heterogeneous tri-phasic gas-solid–liquid system compared to homogeneous liquid system [29]. From the results presented in Table 4.2, it is evident that dimethylitaconate was hydrogenated with very high conversion (up to 99%) and high product enantioselectivity (up to 94% ee), which are comparable with the homogeneous analogue (Table 4.2, entry 2). It is reported

previously that higher catalyst loadings (substrate: catalyst molar ratio = 50:1) were usually required to get higher enantioselectivity [30-32]. But surprisingly in our studies, we have found excellent activity and enantioselectivity (ee) even with a substrate to catalyst molar ratio of 1660, which is nearly 30 fold higher than the reported iridium phosphoramidite complex [22] and the other rhodium monodentate phosphorous complexes. This could be attributed to an increase in electron density around the metal centre [33, 34]. Phosphorus-sulfur π-bond formation is less favored geometrically than phosphorus-oxygen π-bond formation [35]. So there might be an increase in electron density around the iridium metal centre compared to the reported phosphite and phosphoramidite ligands which favoured the oxidative addition of hydrogen in the catalytic hydrogenation reaction cycle and changes the reactivity pattern of the major and minor diastereomeric complexes [36]. Hence, our catalyst reported here provided high enantioselectivities in asymmetric hydrogenation reactions under milder reaction conditions.

By increasing the substrate to catalyst molar ratio from 1660 to 3000, there was no significant decrease in the conversion of dimethylitaconate, however there was a decrease in the enantioselectivity of dimethylmethylsuccinate (Table 4.2, entries 7 and 8). By increasing the iridium to ligand molar ratio from 1:1 to 1:2, no significant changes in catalyst activity and selectivity was observed in the hydrogenation of dimethylitaconate. So, iridium complex with a single monodentate phosphorothioite ligand covalently anchored to mesoporous silica supports are the most active catalysts for enantioselective hydrogenation reactions, which is a significant and important achievement of our studies.

All the three siliceous mesoporous supports resulted in the same product enantioselectivity in the hydrogenation of dimethylitaconate, but the TON were different. IrPSSBA-15 proved to be the most efficient catalyst (conversion 99% and TON = 1650) compared to IrPSMCM-41 (conversion 85%, TON-1416) and IrPSMCM-48 (conversion 82%, TON-1366) (Table 4.2, entries 1, 5 and 6) in the above reaction. IrPSSBA-15 was found to be an efficient catalyst because SBA-15 support afforded less diffusional resistance for the substrate molecules to interact with active sites of the complex in its mesoporous channels having bigger pore diameter compared to MCM-41 and MCM-48 supports [37, 38].

Enantioselective hydrogenation of itaconic acid and diethylitaconate were carried out under similar conditions. Diethylitaconate was hydrogenated to the corresponding succinic acid derivative with 90% conversion and 91% enantiomeric excess (Table 4.2, entry 4) and similarly itaconic acid was also hydrogenated to the corresponding chiral product with higher conversion (98%) and optimum enantiomeric excess 93% ee (Table 2, entry 3) indicating no significant influence of substitution over substrate molecules.

Table 4.2.

Asymmetric hydrogenation of Itaconic acid and its derivatives.[a]

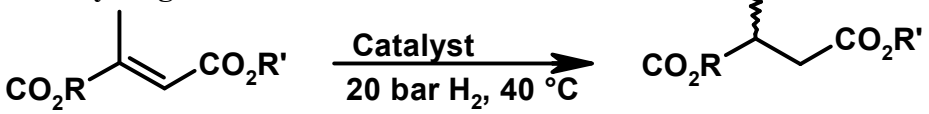

Entry	R	R'	Conv (mol %)	TON [b]	% ee [c]
1.	Me	Me	99	1650	94
2.[d]	Me	Me	99	1650	96
3.[e]	H	H	98	1633	93
4.	Et	Et	90	1500	91
5.[f]	Me	Me	85	1416	94
6.[g]	Me	Me	82	1366	94
7.[h]	Me	Me	98	3005	57
8.[i]	Me	Me	97	1981	73

[a] Reaction conditions: 10 mmol of the substrate, substrate to catalyst molar ratio = 1660: 1, dichloromethane 50 mL, Temperature 40 °C, 20 bar H_2, time 20 h;

[b] TON (turn over number) mole substrate converted per mole of Ir,

[c] % ee was calculated by GC analysis using HP-Chiral column;

[d] The reaction was carried out under homogeneous condition, which was completed within 12 h;

[e] The product was analyzed by converting the acid to the corresponding methyl ester;

[f] Using IrPSMCM-41 as catalyst;

[g] Using IrPSMCM-48 as catalyst;

[h] The substrate to catalyst molar ratio taken was 3000:1;

[i] The substrate to catalyst molar ratio taken was 2000:1.

4.3.2.1. Effect of solvent

To determine the effect of solvent on the substrate conversion and enantioselectivity, the hydrogenation of dimethylitaconate was carried out with IrPSSBA-15 catalyst using different solvents. The results along with reaction conditions are presented in Table 4.3. Among the solvents studied, dichloromethane, chloroform and ethyl acetate were found to be more effective solvent systems. The enantioselectivities varied within 1 to 2% and showed excellent enantioselectivities upto 94% in all the solvents studied. In protic polar solvent (methanol), a slight decrease in the product enantioselectivity was obtained which is in consistence with the previous reports [39]. The lack of activity in toluene might be due to the tendency of iridium to form stable η^6-arene complexes with aromatic compounds as reported in case of rhodium complexes [40, 41].

Table 4.3.

Effect of solvent in the enantioselective hydrogenation of dimethylitaconate with IrPSSBA-15 [a]

Entry	Solvent	Conversion (mol %)	TON[b]	%ee[c]
1.	Dichloromethane	99	1650	94
2.	Chloroform	99	1650	94
3.	Acetone	95	1583	93
4.	Ethyl acetate	99	1650	94
5.	Methanol	94	1533	89
6.	Toluene	25	416	-

[a] Reaction conditions: 10 mmol of the substrate, substrate to catalyst molar ratio = 1660: 1, solvent 50 mL, Temperature 40 °C, 20 bar H_2, time 20 h;

[b] TON (turn over number) mole substrate converted per mole of ir;

[c] % ee was calculated by GC analysis using HP-Chiral column.

4.3.2.2. Effect of reaction time

The results on the effect of reaction time over substrate conversion and enantioselectivity in the hydrogenation of dimethylitaconate are shown in Fig. 4.7. (a) and 4.7. (b), respectively. Fig. 4.7(a) shows that the substrate conversion increases as a function of time for all the catalysts and reaches optimum conversion in 20 h for IrPSSBA-15 (>99%) followed by others. The enantiomeric excess values, however, attained a maximum from the very beginning of the reactions shown in Fig. 4.7(b). There is no significant influence of reaction time on the enantiomeric excess of product and maximum ee around 90% is obtained with all the three catalysts after 1 h of reaction.

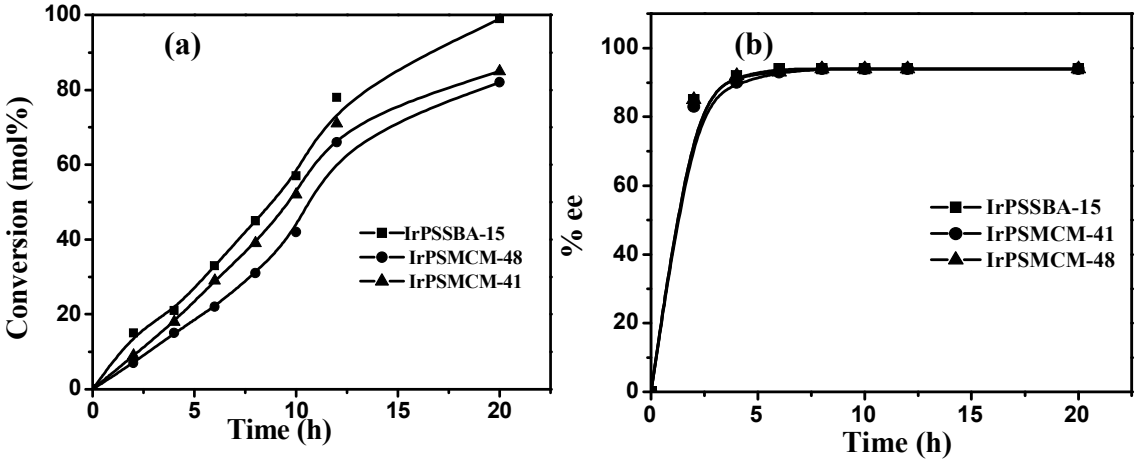

Fig. 4.7. Effect of reaction time (a) conversion of dimethylitaconate and (b) enantiomeric excess of dimethylmethylsuccinate

4.3.2.3. Effect of temperature

The catalysts were used to study the effect of temperature (30-50 °C ranges) in the hydrogenation of dimethylitaconate. The results indicate that a critical temperature of 40 °C is required to acquire the activation energy for hydrogenation for the three immobilized catalyst systems. At this temperature, the maximum conversion of dimethylitaconate (up to 94%) was obtained by all the catalyst systems under the reaction conditions studied. When the temperature was raised above 40 °C, there was no further change in the conversion of substrate for all the catalysts as seen from the Fig. 4.8. (a). Temperature did not affect the enantiomeric excess of the product. However, slight

decrease in enantioselectivity was observed with increase in temperature from 40-50 °C (Fig. 4.8. (b)) under the selected reaction conditions.

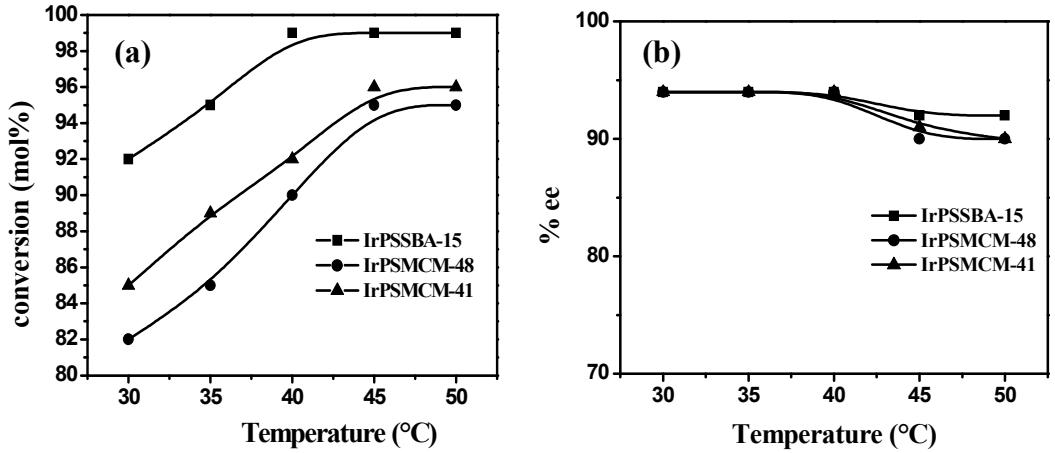

Fig. 4.8: Effect of reaction temperature (a) conversion of dimethylitaconate and (b) The enantiomeric excess of dimethylmethylsuccinate

4.3.2.4. Effect of hydrogen pressure

The hydrogen pressure inside the reaction vessel has a pronounced effect over the substrate conversion in the hydrogenation of dimethylitaconate as shown in Fig. 4.9 (a). But, the enantioselectivity of the heterogeneous catalyst does not significantly depend on the hydrogen pressure above 10 bar as shown in Fig, 4.9 (b). As represented in Fig. 4.9 (a), the conversion of dimethylitaconate markedly increases with increase in hydrogen pressure. The maximum conversion of the substrate and ee were achieved at 20 bar hydrogen pressure, beyond which no further enhancement in the conversion as well as in ee was achieved.

4.3.2.5. Catalyst stability

To understand whether any active species of the catalyst are leaching into the reaction medium, hydrogenation of dimethylitaconate to give dimethylmethylsuccinate was carried out at selected conditions with IrPSSBA-15 catalyst. The reaction was stopped after 2 h, and the autoclave was cooled to room temperature and conversion of dimethylitaconate was estimated. Then, the catalyst was separated by filtration and the filtrate was added to the vessel and the reaction was continued with fresh hydrogen

pressure (20 bar) and carried out for 20 h. It was found that no increase in the conversion of the substrate was observed and was the same as estimated in presence of the catalyst. This observation confirms the complete absence of leaching of any active species of the catalyst into the reaction mixture and the catalyst truly acted as heterogeneous.

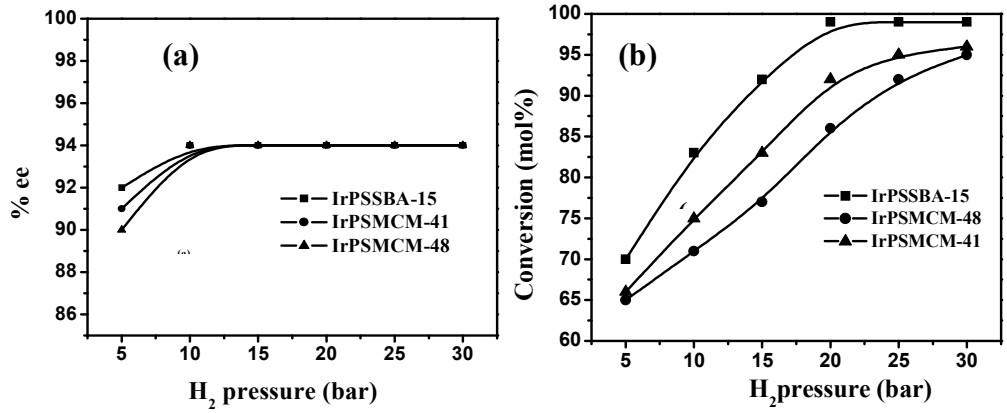

Fig. 4.9. Effect of H_2 pressure (a) conversion of dimethylitaconate and (b) enantiomeric excess of dimethylmethylsuccinate

The recyclability of IrPSSBA-15 catalyst was tested in the hydrogenation of dimethylitaconate by conducting five runs and the results are presented in Table 4.4. After each run, the catalyst (orange in color) was repeatedly washed with dichloromethane, dried under vacuum at 70 °C for 2 h and was then used in the hydrogenation reaction with a fresh reaction mixture. It was found that the conversion of dimethylitaconate was practically the same (99%) in all the five cycles with marginal decrease at 4^{th} and 5^{th} cycles without change in enantioselectivity of the product (94%). So, by recycling the immobilized catalyst 5 times, the substrate to catalyst ratio (s/c) of the whole reaction has been increased to 8300, wherein the activity remains the same with enantioselectivity >94%. For comparison, a homogeneous reaction at s/c 8300 carried out gave less enantioselectivity (49%). It indicates the successful immobilization of the iridium complex onto the support.

Table 4.4.

Recyclability of IrPSSBA-15 in the enantioselective hydrogenation of dimethylitaconate [a]

Entry	Cycle	Conversion (mol %)	% ee [b]
1	Fresh	99	94
2	1st	99	94
3	2nd	99	94
4	3rd	99	94
5	4th	97	94
6	5th	96	94

[a] Reaction conditions: 10 mmol of the substrate, substrate to catalyst molar ratio = 1660: 1, dichloromethane 50 mL, Temperature 40 °C, 20 bar H_2, time 20 h

4.4. Conclusions

In conclusion, we have demonstrated an effective and a new class of heterogeneous catalyst through synthesis of monodentate phosphorothioite iridium complex covalently anchored to mesoporous silica from inexpensive S-binol in lesser number of steps. Catalyst diagnosis demonstrated the successful incorporation of ligand and metal complex onto the mesoporous silica. Among the catalysts investigated, iridium complex immobilized over SBA-15 (IrPSSBA-15) was found to be the ideal heterogeneous catalyst system for the enantioselective hydrogenation of itaconic acid derivatives. High conversions (99%) and excellent enantioselectivities (up to 94% ee) were observed under milder reaction conditions with a substrate to catalyst ratio 30 times higher than the previously reported monodentate ligand based catalytic systems. The catalyst was reused at least five times maintaining the same activity and selectivity. Therefore, we consider this protocol as a readily accessible pathway to highly enantioselective immobilized hydrogenation catalysts.

4.5. References

1. M.T. Reetz, G. Mehler, Angew. Chem., Int. Ed. 39 (2000) 3889.
2. M. Berg, A.J. Minnaard, E.P. Schudde, J. Esch, A.H.M. de Vries, J.G. de Vries, B. L. Feringa, J. Am. Chem. Soc. 122 (2000) 11539.
3. C. Claver, E. Fernandez, A. Gillon, K. Heslop, D.J. Hyett, A. Martorell, A.G. Orpen, P.G. Pringle, Chem. Commun. (2000) 961.
4. I.V. Komaro, A. Börner, Angew. Chem. Int. Ed. 40 (2001) 1197.
5. M.T. Reetz, A. Meiswinkel, G. Mehler, K. Angermund, M. Graf, W. Thiel, R. Mynott, D.G. Blackmond, J. Am. Chem. Soc. 127 (2005) 10305.
6. J.M. Thomas, W.J. Thomas (Eds.), Principles and practice of heterogeneous catalysis, Wiley-VCH, Weinheim, 1997, p. 13.
7. M.D. Jones, R. Raja, J.M. Thomas, B.F.G. Johnson, D.W. Lewis, J. Rouzard, K.D.M. Harris, Angew. Chem. Int. ed. 42 (2003) 4326.
8. C.E. Song, D.H. Kim, D.S. Choi, Eur. J. Inorg. Chem. (2006) 2927.
9. D.E. Bergbreiter, Chem. Rev. 102 (2002) 3345.
10. N.E. Leadbeater, M. Marco, Chem. Rev. 102 (2002) 3217.
11. G.E. Oosterom, J.N.H. Reek, P.C.J. Kamer, P.W.N.M. Van Leeuwen, Angew. Chem., Int. Ed. 40 (2001) 1828.
12. M. Heitbaum, F. Glorius, I. Escher, Angew. Chem. Int. Ed. 45 (2006) 4732.
13. C. Jakel, R. Paciello, Chem. Rev. 106 (2006) 2912.
14. P. Barbaro, Chem. Eur. J. 12 (2006) 5666.
15. C. Simons, U. Hanefeld, I.W.C.E. Arends, J.M. Adriaan, T. Maschmeyer, R.A. Sheldon, Chem. Commun. (2004) 2830.
16. C. Simons, U. Hanefeld, I.W.C.E. Arends, T. Maschmeyer, R.A. Sheldon J. Catal. 239 (2006) 212.
17. X.P. Hu, J.D. Huang, Q.H. Zengab Z. Zheng, Chem. Commun. (2006) 293.

18. S. Doherty, E.G. Robins, I. Pal, C.R. Newman, C. Hardacre, D. Rooney, D.A. Mooney, Tetrahedron Asymmetry. 14 (2003) 1517.

19. C.E. Song, S. Lee, Chem. Rev. 102 (2002) 3495.

20. Q.H. Fan, Y.M. Li, A.S.C. Chan, Chem. Rev. 102 (2002) 3385.

21. D.E.D. Vos, M. Dams, B.F. Sels, P.A. Jacobs, Chem. Rev. 102 (2002) 3615.

22. F. Giacomina, A. Meetsma, L. Panella, L. Lefort, A.H.M. Vries, J.G. Vries, Angew. Chem. Int. Ed. 46 (2007) 1497.

23. T. Morimoto, M. Chiba, K. Achiwa, Tetrahedron Lett. 31 (1990) 261.

24. H. Heitsch, R. Henning, H.W. Kleemann, W. Linz, W.U.Nickel, D. Ruppert, H. Urbach, A. Wagner, J. Med. Chem. 36 (1993) 2788.

25. T. Joseph, M. Hartmann, S. Ernst, S.B. Halligudi, J. Mol. Catal. (A) Chem. 207 (2004) 131.

26. J.S. Beck, J.C. Vartuli, W.J. Roth, M.E. Leonowicz, C.T. Kresge, K.D. Schmitt, C.T.W. Chu, D.H. Olson, E.W. Sheppard, S.B. McCullen, J.B. Higgins, J.L. Schlenker, J. Am. Chem. Soc. 114 (1992) 10834.

27. D.Y. Zhao, J.L. Feng, Q.S. Huo, N. Melosh, G.H. Fredrickson, B.F. Chmelka, G.D. Stucky, Science 279 (1998) 548.

28. K. Nakamoto (Ed.), Infrared and Raman Spectra of Inorganic and Coordination Compounds, part A: Theory and Applications in Inorganic Chemistry, John Wiley & Sons, Inc. 1997, p. 266.

29. A. Gosh, R. Kumar, J. Catal. 228 (2004) 386.

30. T. Jerphagon, J.L. Renaud, C. Bruneau, Tetrahedron Asymmetry 15(2004) 2101.

31. T. Jerphagnon, J.L. Renaud, P.Demochaux, A.Ferreira, C. Bruneau, Adv. Synth. Catal. 346 (2004) 33.

32. M.T. Reetz, X. Li, Tetrahedron 60 (2004) 9709.

33. T.V. Rajanbabu, B. Radetich, K.K. You, T.A. Ayers, A.L. Casalnuovo, J.C. Calabrese, J. Org. Chem. 64 (1999) 3429.

34. T.V. Rajanbabu, T.A. Ayers, A.L. Casalnuovo, J. Am. Chem. Soc. 116 (1994) 4101.

35. R.F. Hudson, Structure and Mechanism in Organo-Phosphorus Chemistry, Academic Press, New York, N.Y., 1965, Chapter 3.

36. O. Pa`mies, G. Net, A. Ruiz, C. Claver, Eur. J. Inorg. Chem. (2000) 1287.

37. T. Joseph, S.S. Deshpande, S.B. Halligudi, A. Vinu, S. Ernst, M. Hartman, J. Mol. Catal. A: Chemical 206 (2003) 13.

38. R.I. Kureshy, I. Ahmed, N.H. Khan, S.H.R. Abdi, K. Pathak, R.V. Jasra, J. Catal. 238 (2006) 134.

39. M.V. Berg, A.J. Minnaard, R.M. Haak, M. Leeman, E.P. Schudde, A. Meetsma, B.L. Feringa, A.H.M. Vries, C. Elizabeth, P. Maljaars, C.E. Willans, D. Hyett, J.A.F. Boogers, H.J.W. Henderickx, J.G. de Vries, Adv. Synth. Catal. 345 (2002) 308.

40. D. Heller, H.J. Drexler, A. Spannenberg, B. Heller, J. You, W. Baumann, Angew. Chem., Int. ed. 41 (2002) 777.

41. C. Simons, U. Hanefeld, I.W.C.E. Arends, R.A. Sheldon, T. Maschmeyer, Chem. Eur. J. 10 (2004) 5829.

CHAPTER V

Oxidative kinetic resolution of alcohols

5. Oxidative kinetic resolution of secondary alcohols using chiral Mn-salen complex immobilized onto ionic liquid modified mesoporous silica

5.1. Introduction

Optically active alcohols are extremely useful starting materials and intermediates in synthetic organic chemistry and the pharmaceutical industry [1]. Over the last 10 years, highly efficient asymmetric hydrogenation, involving asymmetric transfer hydrogenation of prochiral ketones catalyzed by metal complexes to attain chiral alcohols, has made great progress [2-6]. Besides that, oxidative kinetic resolution of racemic alcohols is also another feasible approach giving optically active alcohols [7-10]. Enzymatic and catalytic kinetic resolution of racemic alcohols through acylation or deacylation has been extensively studied [11-15]. Effective oxidative kinetic resolution of racemic alcohols has been reported by Sigman's group and Stoltz's group which involves the aerobic oxidative kinetic resolution of secondary alcohols catalyzed by (-)-sparteine/ Pd(II) to conveniently access enantiomerically enriched secondary alcohols [16-19]. Several ruthenium and iridium complexes have also been reported for the oxidative kinetic resolution of secondary alcohol [1, 20]. Recently, Sun et al. reported chiral Mn(III) salen complex catalyzed kinetic resolution of secondary alcohols with excellent enantioselectivity (up to 98% ee) in water in the presence of a phase transfer catalyst with hypervalent iodine as the co-oxidant [21, 22].

The demands for economical, eco-friendly and recyclable supported catalysts led some groups to attach chiral complexes on solid supports [23-27]. However, these systems suffer from various disadvantages such as decrease in activity, leaching of active species in reaction media, and low accessibility of substrate either due to hydrophobicity or low surface area. Ionic liquids have become commonplace in recent years and are a significant alternative medium for the traditional organic synthesis and catalytic reactions [28-30]. Moreover, since ionic liquids are expensive it is desirable to minimize the amount of ionic liquid used in usual biphasic reaction systems. In addition, the high viscosity of ionic liquid can induce mass transfer limitations if the chemical reaction is fast, in which case the reaction takes place only within the narrow diffusion layer not in the bulk of the ionic liquid catalyst solution. Dissolving

organometallic complexes in supported films of ionic liquids has recently been introduced as a strategy to immobilize molecular catalysts (Fig. 5.1). This allows fixing molecular catalysts in a widely tailorable environment without the drawbacks of complex grafting chemistry [31-34].

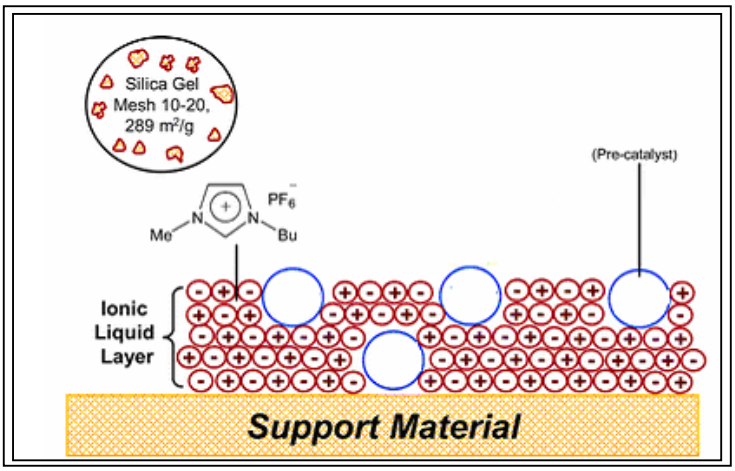

Fig. 5.1.

Few reports regarding the heterogeneous oxidative kinetic resolution of secondary alcohols are there in literature [35-38]. A recently discovered pure silica phase, designated SBA-15, has long-range order, large monodispersed mesopores (up to 50 nm), and thicker walls (typically between 3 and 9 nm), which make it thermally and hydrothermally stable [39]. Herein we are reporting for the first time, supported ionic liquid phase chiral Mn-salen catalysis in the heterogeneous oxidative kinetic resolution of secondary alcohol. This involves the simple anchoring of ionic liquid supported metal complex onto mesoporous silica SBA-15 support, which provides good activity with k_{rel} [40, 41] value compared to the homogeneous one. Furthermore this catalyst is recyclable up to five cycles with retention of activity and enantioselectivity.

5.2. Experimental

5.2.1. General

All the solvents procured from Merck (AR grade), India were distilled and dried prior to their use. Tetraethyl orthosilicate (TEOS), Diacetoxyiodobenzene ($PhI(OAc)_2$), KBr, BMIMBr, MIMBr, $N(CH_3)_4Br$ were procured from Aldrich chemicals and used as received. All the racemic alcohols were synthesized from ketones by sodium borohydride reduction. The ionic liquid $BMIMPF_6$ [42] and the

chiral Mn (III) salen [43] complex were synthesized as reported in the literature. Mn contents in the resulting solids were estimated by ICP-AES.

5.2.2. Catalyst preparation

5.2.2.1. 1-(3-Triethoxysilylpropyl)-3-methylimidazoliumchloride ***(1)***

A mixture of 1-methylimidazole (3.36 g, 40 mmol) 3-chloropropyltriethoxysilane (9.63 g, 40 mmol) was heated under an argon atmosphere at 95 °C for 24 h. After cooling a viscous oil was obtained. This viscous oil was used immediately in the next step. ^{1}H NMR ($CDCl_3$): δ= 0.71-0.78 (m, 2H), 1.25-1.33 (t, 9H), 1.85-1.91 (m, 2H), 3.40-3.52 (m, 6H), 4.11 (s, 3H), 8.26 (d,1H), 8.34 (d,1H), 8.53 (s,1H); ^{13}C NMR ($CDCl_3$): δ=7.0 ($SiCH_2$), 11.2 (CH_3), 25.1 (CH_2), 36.4 (NCH_3), 51.4 (CH_3O), 52.2 (CH_2N), 122.8, 124.3, 136.1.

5.2.2.2. 1-(3-Triethoxysilylpropyl)-3-methylimidazoliumhexafluorophosphate ***(2)***

To a solution of the above salt (3.2 g, 10 mmol), in acetone (15 mL), potassium hexafluorophosphate (1.9, 10.5 mmol) was added in one portion. The mixture was stirred at room temperature for 3 days. After this time the mixture was filtered and the solvent evaporated under reduced pressure to give 2. The residue was taken up with chloroform.

^{1}H NMR ($CDCl_3$), δ= 0.61-0.70 (m, 2H), 1.27-1.35 (t, 9H), 1.88-1.94 (m, 2H), 3.89 (s, 3H), 4.23 (t, 2H), 7.55 (d, 1H), 7.58 (d, 1H), 8.90 (s,1H), ^{13}C NMR ($CDCl_3$), δ=6.9 ($SiCH_2$), 10.2 (CH_3), 24.9 (CH_2), 36.0 (NCH_3), 51.3 (CH_2O), 51.5 (CH_2N), 122.4, 124.0, 136.3. ^{31}P NMR ($CDCl_3$), δ=143.6.

5.2.2.3. Preparation of mesoporous silica

Mesoporous silica SBA-15 was prepared as described previously. The confirmation of the formation of material was confirmed by powder small angle X-ray diffraction technique.

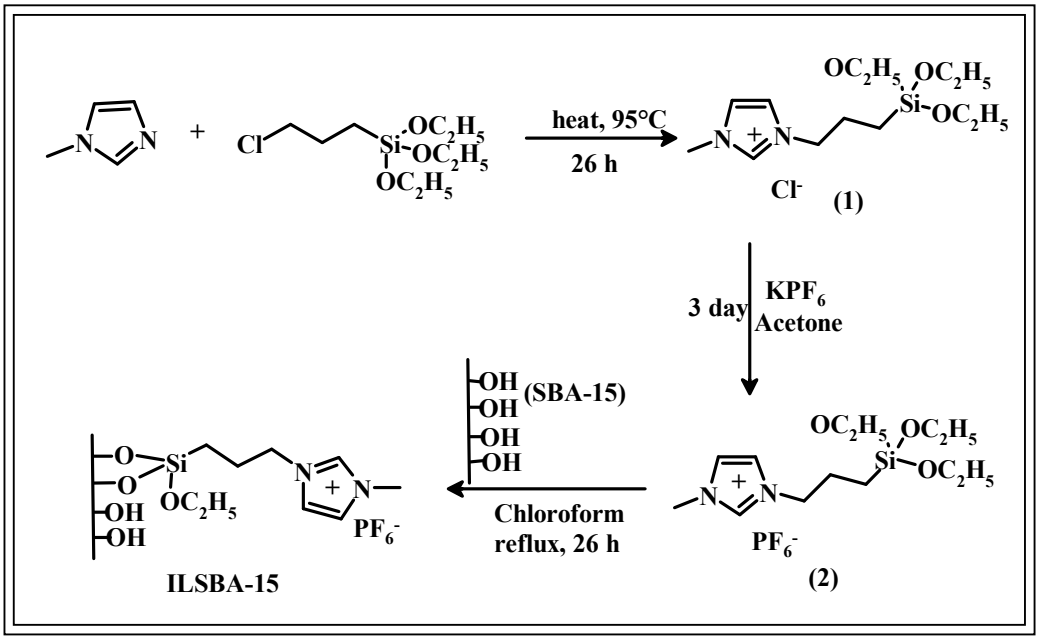

Scheme 5.1. Synthesis of ionic liquid modified SBA-15

5.2.2.4. Synthesis of ionic liquid modified SBA-15 (ILSBA-15)

The ionic liquid **2** (2.81 g, 6.5 mmol) was dissolved in chloroform (50 mL) and treated with mesoporous silica (dried under vaccum and heated at 180 °C overnight, 4.00 g). The mixture was heated under reflux (65 °C) for 26 h. After cooling to room temperature, the solid was isolated by filtration and washed with chloroform (50 mL) and diethyl ether (50 mL). The solid was dried under reduced pressure to give a powder.

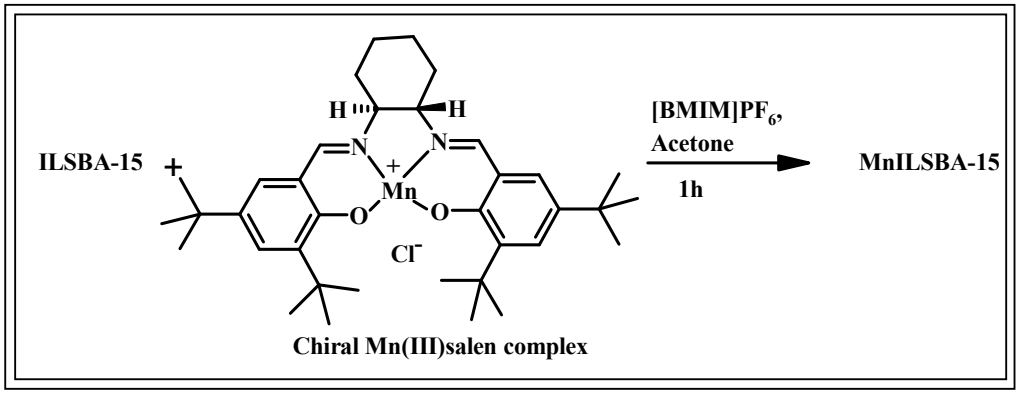

Scheme 5.2. Immobilization of (*S,S*)-(+)-*N,N'*-Bis(3,5-di-tert-butylsalicylidene)-1,2-cyclohexanediaminomanganese(III) chloride complex onto the ionic liquid modified SBA-15

5.2.2.5. Supported chiral Mn-salen materials (MnILSBA-15)

In a round-bottom flask chiral Mn(III) salen complex (0.19 g, 0.30 mmol), ionic liquid ([BMIM]PF_6, 300 mg) were dissolved in acetone (10 mL). To this solution the ionic liquid modified mesoporous silica (1.00 g) was added. The mixture was stirred for 1h, and then evaporated under reduced pressure for 25 h to give a free flowing powder.

5.2.3. Catalytic experiments

Typical Procedure for oxidative kinetic resolution

To a solution of racemic secondary alcohol (2.5 mmol) in hexane water mixture (5 and 10 mL respectively), additive (0.1 mmol), catalyst (0.030 g, 0.003 mmol) was added and stirred for 5 mins. After this time oxidant, diacetoxyiodobenzene (1.75 mmol), was added. The reaction was monitored in gas chromatograph equipped with chiral column. After completion of the reaction, the catalyst was filtered, washed with 10 mL of hexane dried and recharged with fresh substrate, additive and oxidant for the next catalytic cycle. The solvent was removed under reduced pressure and the resultant mixture was dried and purified by column chromatography on silica gel as the stationary phase (petroleum ether/ ethyl acetate, 90/10). The optical rotation of the products was measured by Jasco P-1020 polarimeter. For example: α-methyl benzyl alcohol: Gas chromatograph (CP-Chirasil-Dex CB capillary column, 90 °C isothermal) t_S (major) = 29.79 min, t_R (minor) = 28.52 min. Absolute configuration – S, Optical rotation, $[\alpha]_D$ = -43.5, C = 0.8 in chloroform (literature value: $[\alpha]_D$ = -44, C =0.8 in chloroform).

5.3. Results and Discussion

The supported ionic liquid catalyst over mesoporous silica, SBA-15, was synthesized following the literature procedure (Sheme 5.1) [44, 45]. Ionic liquid 1-(3-triethoxysilylpropyl)-3-methylimidazoliumhexafluorophosphate **(2)** was synthesized by the ion exchange of 1-(3-triethoxysilylpropyl)-3-methylimidazoliumchloride **(1)** with potassium hexaflourophosphate. SBA-15 was modified with the ionic liquid **(2)** to provide covalently anchored ionic liquid (Scheme 5.1.), ILSBA-15. To a solution of BMIMPF_6^- and (*S,S*)-(+)-*N,N'*-Bis(3,5-di-tert-butylsalicylidene)-1,2-cyclohexanediaminomanganese(III) chloride (chiral Mn(III) salen) complex in acetone, ILSBA-15 was added. After evaporation of the solvent the catalyst

(MnILSBA-15) was obtained as a free-flowing powder (Scheme 5.2.). DR UV–Vis, FTIR and NMR. spectroscopy confirmed the successful immobilization of chiral Mn(III)salen complex onto the mesoporous silica. N_2 sorption, XRD showed that the long-range mesoporous ordering of parent SBA-15 support was maintained after the immobilization.

5.3.1. Catalyst Characterization

5.3.1.1. Low angle XRD

The powder XRD patterns of ligand functionalized and complex immobilized supports and corresponding parent supports are shown in Figure 5.2. Parent SBA-15 supports exhibited three XRD peaks assigned to reflections at (100), (110), and (200), which are characteristic of 2D hexagonal lattice and indicate a significant degree of long range ordering in the structure. The peak intensities at (100), (110) and (200) reflections of ILMnSBA-15 were decreased, indicating the immobilization of Mn(III) salen complex inside the mesoporous channels of ionic liquid modified SBA-15. However, the mesoporous structure of the support remained intact under the conditions used for immobilization. These results indicate an ordered mesoporosity of the supports even after the incorporation of ionic liquid and the chiral Mn-salen complex.

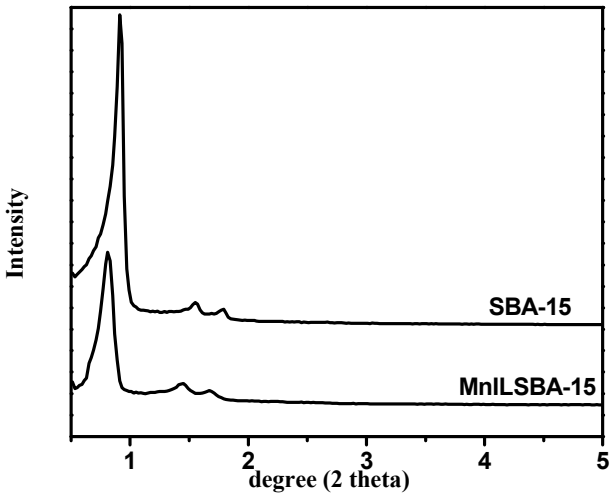

Fig. 5.2. Low angle powder XRD patterns of SBA-15 and MnILSBA-15

5.3.1.2. N_2 sorption study

N_2 adsorption measurements, which have been a powerful tool for nano- or mesoporous material characterization, were performed on to attain more insight of the porous silica gels by using ionic liquids as templates. The samples displayed a type IV isotherm (as defined by IUPAC) with H_1 hysteresis and a sharp increase in pore volume adsorbed above P/P_0 0.7 cm^3/g which is a characteristic of highly ordered mesoporous materials (Fig. 5.3.). The textural properties of SBA-15 were substantially maintained over ionic liquid functionalization and subsequent complexation with chiral Mn-salen complex. A sharp decrease in surface area was observed for ILSBA-15 and MnILSBA-15 from 730 to 321 and 106 m^2g^{-1} respectively and the average pore volume decreased from 1.10 to 0.69 and 0.26 (Table 5.1.). The average pore diameters also decreased from 63 Å to 21 Å.

Table 5.1.

Physicochemical properties of the materials

No.	Catalyst	Surface area BET ($m^2 g^{-1}$)	Pore volume (cm^3/g)	Average pore diameter(Å)
1	SBA-15	730	1.10	63
2	ILSBA-15	321	0.69	43
3	MnILSBA-15	106	0.26	21

This suggests that ionic liquids and the chiral Mn-salen complex may be well confined in the pores of mesoporous silica, SBA-15.

5.3.1.3. Thermal analysis

The decomposition behaviour of the ionic liquid modified support and complex immobilized onto ionic liquid modified support been compared to get an indication whether the complex is embedded into the mesopores or located outside. The ionic liquid modified support ILSBA-15 was found to be stable upto 300 °C (Fig. 5.4. (a)). After that gradual loss in weight was observed. The free complex decomposed during heating to 500 °C in several well defined steps [46].

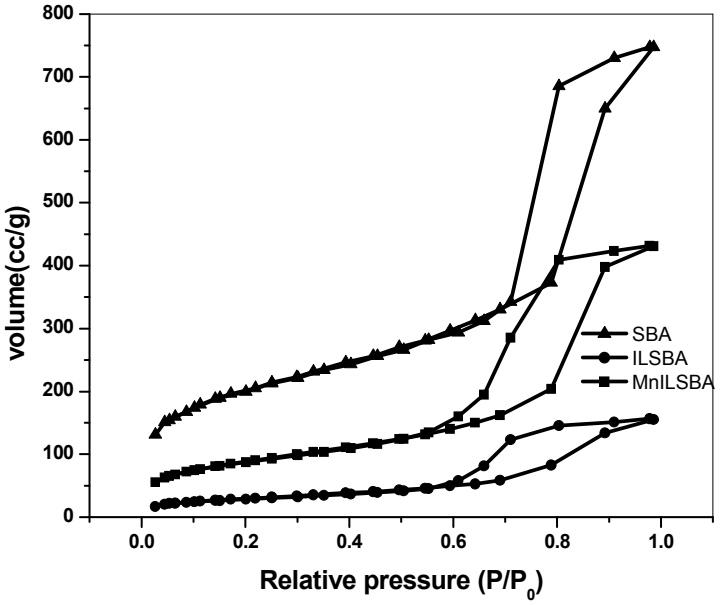

Fig. 5.3. Nitrogen adsorption desorption isotherms of SBA-15, ILSBA-15 and MnILSBA-15

In case of MnILSBA-15, the first loss in weight of 3.5% occured at 130 °C and was slightly endothermic. A comparison of the weight losses in the single steps with possible cleavage of bonds and formation of fragments implies that the first weight loss should be due to release of chlorine as hydrogen chloride (see Fig. 5.4. (b)). This was in accordance to the neat Mn(III) salen complex. This showed that the positive charge of the complex was balanced by chloride and not by the anionic host framework. This finding indicates that the Jacobsen complex is not held by ionic interaction between guest and the host framework.

A second, exothermic loss in weight of 10% appears at 230 °C and is followed by an additional large weight loss of 28% at 320 °C. The two steps overlap in the TG curve but are well distinguished in the corresponding DTA curve. This process extends up to ca. 400 °C. Above this temperature the remaining organic oxidizes up to 500 °C. The non-removable residue of ca. 14% belongs to the formation of manganese oxide. The sample remains dark. The proposed first cleavage of the *tert*-butyl groups by homolytic bond cleavage can be explained by the known stabilization of radicals intermediately formed via hyperconjugation. In addition, the bulky methyl groups cause a weakening of the C-C bond which links the *tert*-butyl group to the aromatic ring. Decomposition was completed at 600 °C.

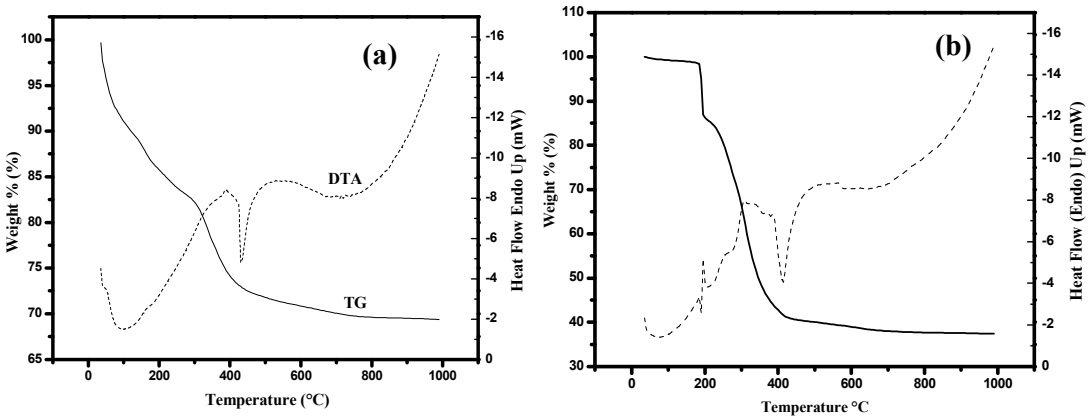

Fig. 5.4. TGA DTA curves of (a) ILSBA-15 and (b) MnILSBA-15

5.3.1.4. Microscopic analysis

SEM images of MnILSBA-15 (Fig. 5.5. (a)) shows the rope-like micro morphology of SBA-15 remained intact, even after functionalization with ionic liquid and chiral Mn(III) salen complex. TEM measurements were carried out to study the morphology of SBA-15 and MnILSBA-15 catalysts (Fig. 5.5. (b)). TEM images of these catalysts showed retention of the periodic structure of parent SBA-15 precursor, which confirms that the hexagonally arranged mesopores of SBA-15 are retained after modification with ionic liquid and Mn(III) salen complex.

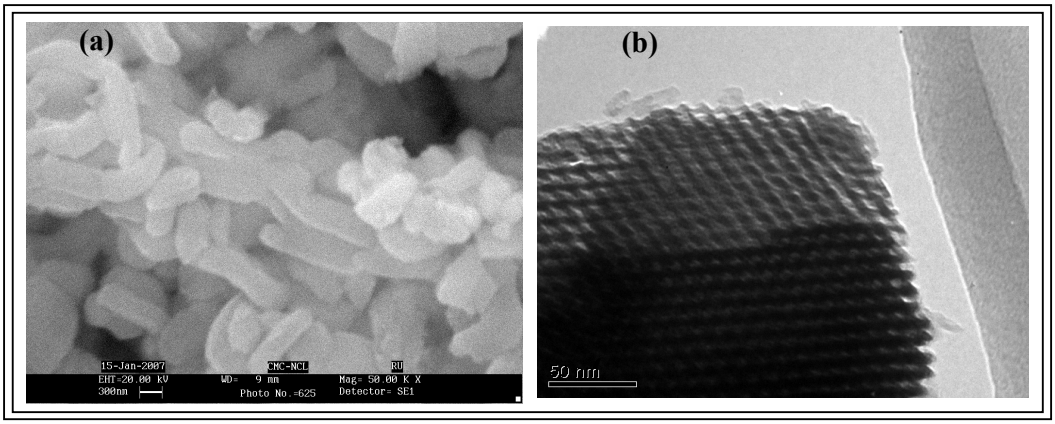

Fig. 5.5. (a) SEM and (b) TEM photographs of MnILSBA-15

5.3.1.5. DR UV–vis spectroscopy

The diffuse reflectance UV–vis spectra of neat complex and the supported ionic liquid catalysts are given in Figure 5.6. The spectra of the supported ionic liquid catalysts show features similar to those of neat complex. The bands at 244 and 324 nm can be attributed to the charge transfer transition of salen ligand. The band at 437 nm is due to ligand to-metal charge transfer transition, and the bands at 507 nm may be assigned to the *d–d* transition of Mn(III) salen complex. On immobilization of Mn(III) salen complex, all of the characteristic bands appeared in their spectra. The DR UV–vis spectra confirmed the immobilization of chiral Mn (III) salen complex on the supports.

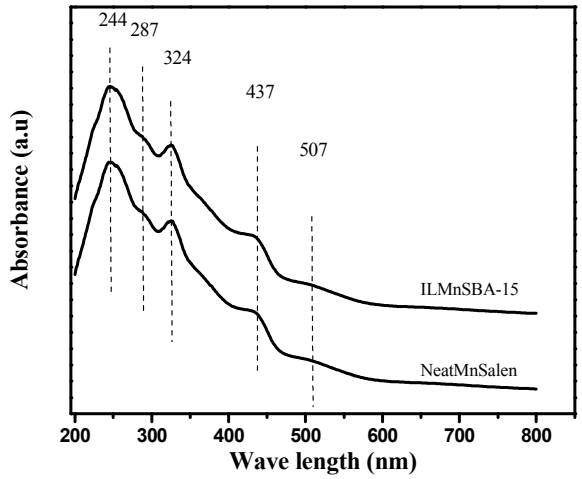

Fig. 5.6. DR UV–vis spectroscopy of Neat Mn(III) salen and ILMnSBA-15

5.3.1.6. FTIR spectroscopy

The FTIR spectra of parent supports showed specific bands at around 1080, 780, and 470 cm^{-1} assigned to characteristic vibrations of the mesoporous framework (Si–O–Si) and a broad band around 3450 cm^{-1} for the adsorbed H_2O molecules. These absorption peaks were maintained after organic modification and chiral Mn(III) salen complex immobilization. Fig. 5.7. depicts the representative FTIR spectra in the scan range 1300–3300 cm^{-1} for immobilized chiral Mn(III) salen catalyst MnILSBA-15. In the spectrum the IR bands at 3159 and 3112 cm^{-1} were assigned to C–H stretching vibrations of aromatic imidazole rings, and the bands near 3000 cm^{-1} were due to C–H stretching vibrations of alkyl groups belonging to the silylating agent. The

IR bands at 1566 and 1454 cm^{-1} can be attributed to C=C stretching vibrations of imidazole rings and C–H deformation vibrations of alkyl groups, respectively. Besides these, the IR band assigned to C=N stretching vibrations was seen at around 1620 cm^{-1}, compared to 1632 cm^{-1} attributed to the presence of C=N in salen ligand, which participated in coordination with manganese ions. Furthermore, a new characteristic band of Mn(III) salen at 1541 cm^{-1} appeared in the spectrum, indicating that the chiral Mn(III) salen complex was immobilized on the support.

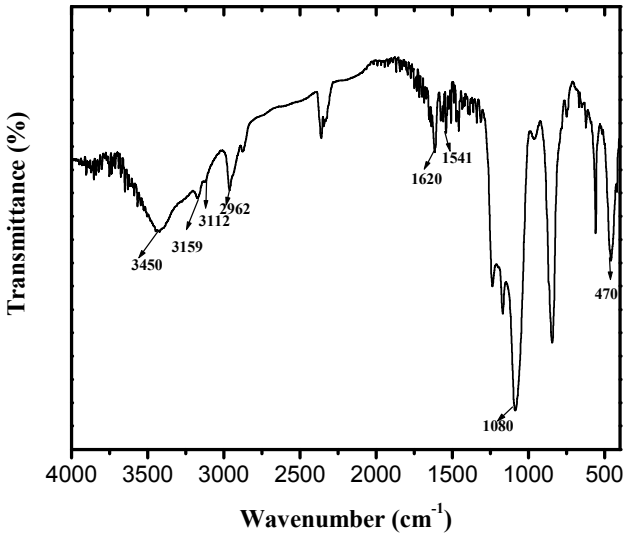

Fig. 5.7. FTIR spectra of MnILSBA-15

5.3.1.7. Nuclear Magnetic Resonance

When looking at the proton spectra (Figure 5.8.), it shows very sharp lines due to species with a high mobility, probably the $BMIM^+$ species. The peaks at 7.2 -8.3 ppm corresponds to the aromatic protons present and the peaks at 0.74 – 3.8 ppm correspond to the aliphatic side chain of the imidazolium moiety as well as the cyclohexyl and *tert.* butyl group of the Mn(III) salen complex. The ^{13}C MAS NMR spectra (Figure 5.9.) provide useful information on the nature of the incorporated ionic liquid on the internal surface of the SBA-15. The well resolved peaks at 136, 124 and 122 ppm are due to the aromatic ring carbons and the peaks 8-63 ppm confirm the presence of linker propyl group, ethoxy ($SiOCH_2CH_3$) and the cyclohexyl group of the Mn(III) salen complex. The ^{29}Si MAS NMR spectra of the parent SBA-15 exhibited a broad peak and was dominated by an intense peak at −112 ppm assigned to $Si(OSi)_4$ and one shoulder peaks at −102 ppm due to $Si(OSi)_3OH$ (Q3)

structural units present in SBA-15. On incorporation of the imidazolium moiety, in addition to the aforementioned three peaks, two more peaks at −58 and −68 ppm appeared (Figure 5.10.). No peak appeared at −45 ppm, corresponding to the chemical shift of silicon in liquid (3-(1- methylimidazolium)propyl) trialkoxysilane, indicating the absence of free silane molecules physically adsorbed on the SBA-15 surface.

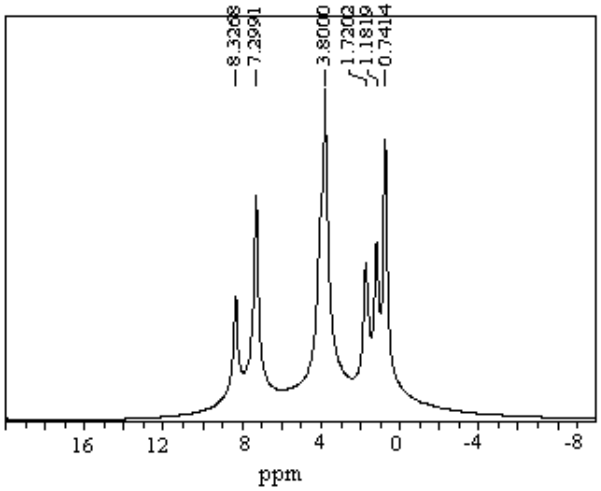

Fig. 5.8. ^{1}H NMR spectra of MnILSBA-15

A peak at −67 ppm indicates the formation of new siloxane linkages (Si—O—Si) of imidazoliumpropylsilane to the surface silicon atoms of the SBA-15 via three siloxane bonds, $(—O—)_3Si—CH_2CH_2CH_2NH_2$ (T_3), and a peak at −56 ppm via two siloxane bonds, $(—O—)_2Si—CH_2CH_2CH_2NH_2$ (T_2). This is in accordance to the literature value [47]. The phosphorus spectrum (Figure 5.11) shows only the resonance of PF_6^-. This confirms the presence of covalently anchored ionic liquid and Mn(III) salen complex onto the mesoporous silica SBA-15.

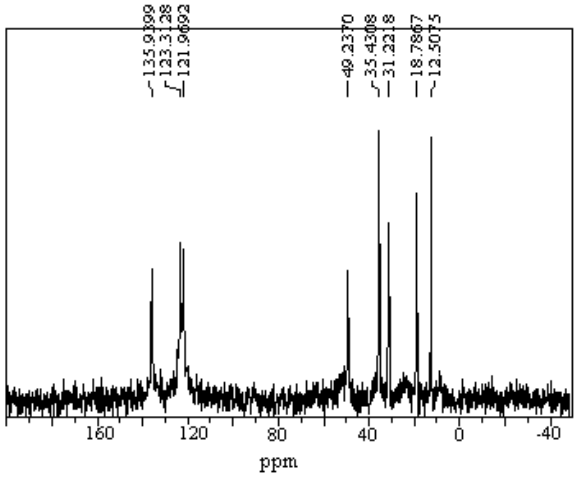

Fig. 5.9. ^{13}C NMR spectra of MnILSBA-15

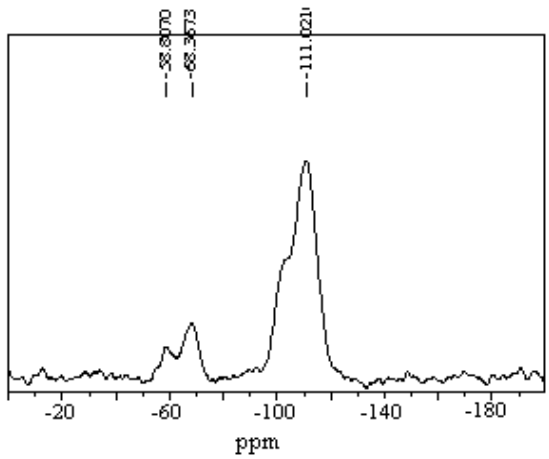

Fig. 5.10. ^{29}Si NMR spectra of MnILSBA-15

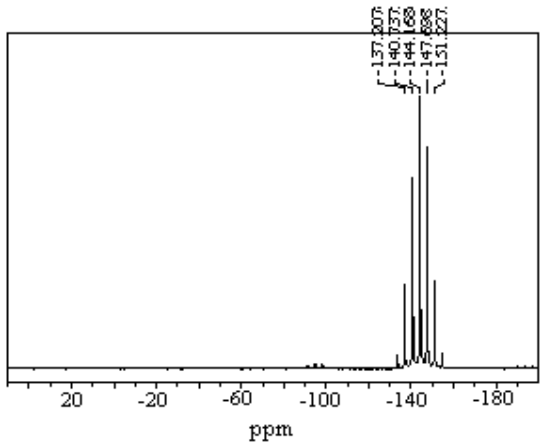

Fig. 5.11. ^{31}P NMR spectra of MnILSBA-15

5.3.2. Catalytic activity

In order to assess the efficiency of these immobilized catalysts in oxidative kinetic resolution of secondary alcohols, the experimental conditions were first optimized for the oxidative kinetic resolution of α-methyl benzyl alcohol as a model substrate using diacetoxy iodobenzene ($PhI(OAc)_2$) as the oxidant. The reaction was carried out by using different additives (Table 5.2). Among them $N(CH_3)_4Br$ and KBr gave good results in terms of %ee and k_{rel} which was in accordance to the literature (Table 5.2, entries 2 and 6) [21] . Additives having bromide as the anion gave excellent enantioselectivity compared to other additives. There was almost low conversion and less enantioselectivity when additive was not used. We tried to use bromide ion containing ionic liquid which can act as both a support and the additive

(Table 5.2, entries 9 and 10). We got excellent results. But these bromide ion containing ionic liquids are soluble in water and in this ionic liquid the Mn(III)salen complex was less soluble. So $BMIMPF_6$ was chosen as the ionic liquid in the supported ionic liquid catalysis.

Different silica supports, MCM-41, MCM-48, SBA-15 and amorphous silica were studied. Supports hardly make any difference in this oxidative kinetic resolution of secondary alcohol. Slight low activity (k_{rel} 14.7) was observed while taking amorphous silica as the support compared to the SBA-15 support. In all the supports the %ee of α-methylbenzyl alcohol were almost the same (~99%) (Table 5.3). It showed that there was hardly any effect of support structure in the oxidative kinetic resolution of secondary alcohols by the Mn(III) salen complex immobilized onto ionic liquid modified support.

Screening of different solvents was studied in the supported ionic liquid phase catalyzed oxidative kinetic resolution of secondary alcohols. In case of dichloromethane and water all the metal complex got leached into the reaction organic phase. So the reaction occurred in the homogeneous biphasic system. After completion of the reaction the solvent was removed under vacuum and the organic phase was extracted by repeated washings with hexane or diethylether. Now the residue can be used for the next cycle of oxidative kinetic resolution. So, instead of carrying out the reaction in DCM, removing the solvent after reaction and again washing it with hexane, it is better to carry out the reaction in hexane. Hexane and water as well as diethyl ether and water mixture were found to be the best solvent medium for this resolution because of less leaching of the complex into the organic phase and in these solvent systems good activity and selectivity were obtained in the oxidative kinetic resolution of secondary alcohol.

Among the different oxidants studied, diacetoxyiodobenzene was found to be the best oxidant in this oxidative kinetic resolution. No oxidation was observed while using H_2O_2 and *tert*-butylhydrogenperoxide as oxidants. While using IBX, the most frequently used hypervalent iodine oxidant in alcohol oxidation, no enantiomeric enrichment of the alcohol was observed.

Table 5.2.

Screen with various additives[a]

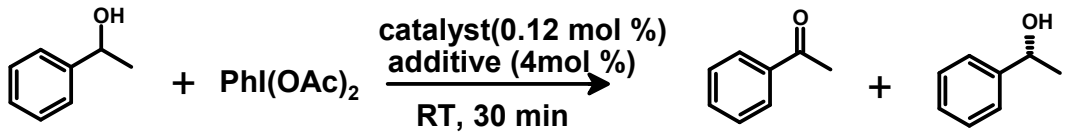

Entry	Additive	Conversion (%)[b]	% ee[c]	k_{rel}[d]
1.	-	35	18	2.3
2.	$N(CH_3)_4Br$	64	99	16.8
3.	$N(CH_3)_4Cl$	61	15	1.3
4.	$N(C_2H_5)_4Br$	62	97	15.5
5.	KCl	59	12	2.2
6.	KBr	63	99	18.3
7.	NaBr	59	94	18.1
8.	CTAB	45	53	7.9
9.	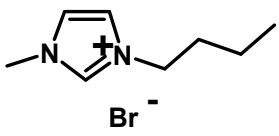	64	99	16.8
10.	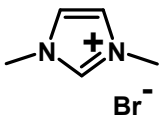	63	98	15.7

[a] Reactions performed at room temperature with MnILSBA-15 (0.03 g, 0.003 mmol), additive (0.1mmol), substrate (2.5 mmol), $PhI(OAc)_2$ (1.75 mmol), and H_2O/hexane (10 mL/5 mL).

[b] Determined by performing GC analysis.

[c] Determined by performing GC analysis using a CP-Chirasil-Dex CB capillary column.

[d] $k_{rel}=\ln[(1-C)(1-ee)]/\ln[(1-C)(1+ ee)]$.

Table 5.3.

Screen with various mesoporous silica supports in the oxidative kinetic resolution of α-methylbenzyl alcohol[a]

Entry	Supports	Time(min)	Convesion	ee(%)	k_{rel}
1.	SBA-15	30	63	99	18.3
2.	MCM-41	30	64	99	16.9
3.	MCM-48	30	63	98	15.7
4.	Amorphous silica	40	67	99	14.7

[a]Reactions performed at room temperature with MnILSBA-15 (0.03, 0.003 mmol), additive (0.1mmol), substrate (2.5 mmol), $PhI(OAc)_2$ (1.75 mmol), and H_2O/hexane (10 mL/5 mL).

With all these results in hand, the effect of reaction time on conversion, enantiomeric excess and the selectivity factor, k_{rel}, was studied. It was observed that enantiomeric excess increased with increase in conversion and time. Figure 5.12. reveals that, although the highest conversion and ee values were obtained after twenty minutes, k_{rel} remained at a value of around 15 during the course of oxidative kinetic resolution of α-methyl benzyl alcohol.

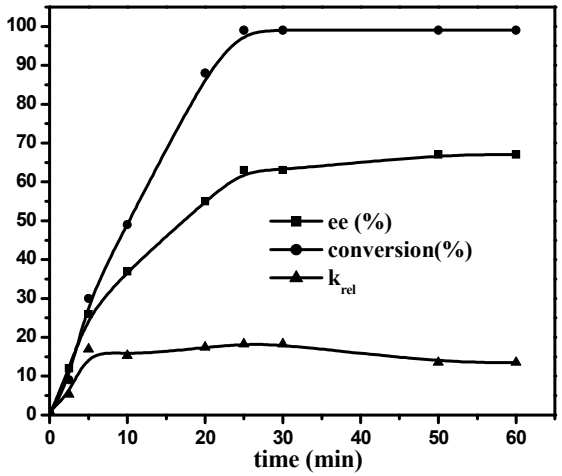

Fig. 5.12. Plot of conversion, ee, and k_{rel} versus reaction time for the oxidative kinetic resolution of α-methylbenzyl alcohol.

After determining the optimized oxidative kinetic resolution conditions, the scope of the method was investigated in different racemic systems. As shown in Table 5.4, the chosen catalytic system was suitable for a wide range of secondary alcohols. The enantiomeric excess of the secondary alcohols obtained from this resolution was comparable to that of the homogeneous one. Both aliphatic and aromatic secondary alcohols resulted in the high conversion, enantioselectivity and k_{rel}.. Due to solubility reasons, the oxidative kinetic resolution of 1-naphtylethanol was carried out in a mixture of diethyl ether and water 1:2). Oxidative kinetic resolutions of other substrates were carried out in hexane. Among all the substrates studied α-methyl-*p*-methoxy benzylalcohol and 1-naphtylethanol resulted in the low enantioselectivity (30% and 69% respectively) and k_{rel} values (4.9, 7.9) (Table 5.4, entries 5 and 6). 1-phenyl-1-propanol also gave, in low enantiomeric purity, a krel value of 5.84 (Table 5.4, entry 4). α-methyl-*p*-bromobenzylalcohol and α-methyl-*p*-chlorobenzylalcohol got resoluted with excellent enantioselectivity of 99% and 99% with k_{rel} values of 18.3 and 15.6 respectively (Table 5.4, entries 2 and 3). Oxidative kinetic resolution of 2-decanol resulted in the enantioenriched 2-decanol with a k_{rel} value of 16.2 (Table 5.4, entry 7). Heteroatoms containing aromatic secondary alcohols were also subjected to the oxidative kinetic resolution using this catalyst system. Furyl and pyridyl substituted alcohols did not undergo any oxidation even after 2 h of reaction time (Table 5.4, entries 8 and 9). Even no oxidation of the nitrogen heteroatom was observed under this condition. So, this catalyst is highly chemoselective also.

Some different alcohols' oxidative kinetic resolution was also carried out with this catalyst system under the optimized reaction conditions. A primary alcohol, 2-phenyl-1-[ropanol, was oxidized to the corresponding aldehyde without any enantiomeric enrichment. In case β-hydroxy ester, ethyl-3-hydroxybutyrate, no oxidation of the hydroxyl group was observed, hence no enantioenrichment also. Meso-diols also got oxidized to the corresponding hydroxyl ketones, but with no enantiopurity. So, this catalyst was active for the oxidative kinetic resolution of secondary alcohols only.

Table 5.4.

Oxidative kinetic resolution of various secondary alcohols using MnILSBA-15[a]

Entry	substrate	Time(min)	Conversion[b] (%)	ee (%)[c]	k_{rel}[d]
1.	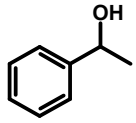	30	63	99	18.3
2.	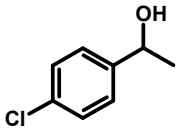	30	65	99	15.6
3.	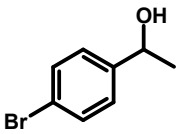	30	63	99	18.3
4.	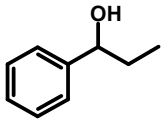	40	44	43	5.84
5.	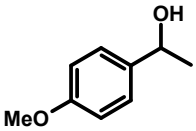	60	40	30	4.9
6.	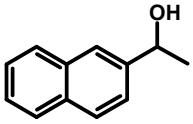	80	55	69	7.2
7.	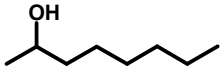	30	59	94	16.2
8.	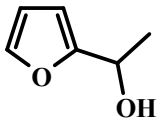	120	-	-	-
9.	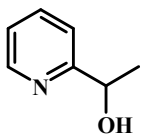	120	-	-	-

[a] Reactions performed at room temperature with MnILSBA-15 (0.03g, 0.003 mmol), additive (0.1mmol), substrate (2.5 mmol), $PhI(OAc)_2$ (1.75 mmol), and H_2O/hexane (10 mL/5 mL).

[b] Determined by performing GC analysis.

[c] Determined by performing GC analysis using a CP-Chirasil-Dex CB capillary column.

[d] $k_{rel} = \ln[(1-C)(1-ee)]/\ln[(1-C)(1+ ee)]$, where C is the conversion and ee is the enantiomeric excess

The regenerability and recyclability of the catalyst system are most important for any catalytic reaction. To understand whether any active species of the catalyst were leaching into the reaction medium, oxidative kinetic resolution of α-methyl benzyl alcohol to give enantiomerically pure α-methyl benzyl alcohol was carried out at optimized conditions with MnILSBA-15 catalyst. The reaction was stopped after 5 min; conversion of α-methyl benzyl alcohol was estimated. Then, the catalyst was separated by filtration and the filtrate was added to the vessel and the reaction was continued carried out for 1 h. It was found that no increase in the conversion and enantiomeric excess of the alcohol were observed and were the same as estimated in presence of the catalyst. This observation confirmed the complete absence of leaching of any active species of the catalyst into the reaction mixture and the catalyst truly acted as heterogeneous.

Table 5.5.

Recyclability of MnILSBA-15 in the oxidative kinetic resolution of α-methylbenzyl alcohol [a]

Entry	Cycle	Conversion (mol %)	% ee [b]	k_{rel}
1.	Fresh	63	99	18.3
2.	1st	63	99	18.3
3.	2nd	63	99	18.3
4.	5th	61	97	16.8

[a] Reactions performed at room temperature with MnILSBA-15 (0.03g, 0.003 mmol), additive (0.1mmol), substrate (2.5 mmol), $PhI(OAc)_2$ (1.75 mmol), and H_2O/hexane (10 mL/5 mL), time-30 min

The recyclability of MnILSBA-15 catalyst was tested in the oxidative kinetic resolution of α-methyl benzyl alcohol by conducting five runs and the results are presented in Table 5.5. After each run, the catalyst (orange in color) was repeatedly washed with hexane, dried under vacuum at 70 °C for 2 h and recharged with fresh

substrate, additive and oxidant for the next cycle of oxidative kinetic resolution. It was found that the conversion of α-methyl benzyl alcohol was practically the same (63%) in all the five cycles with marginal decrease at 4^{th} and 5^{th} cycles without change in enantioselectivity of the product (99%) and k_{rel} value (18) (Table 5.5).

5.4. Conclusions

In conclusion, we have developed a heterogeneous chiral catalyst based on the concept of supported ionic liquid phase catalysis. The amounts of both ionic liquids as well as the transition metal species involved in the preparation of catalysts were very low and the preparation procedure was very easy, thus displaying very good performance from an economic point of view. The catalyst was well characterized by different physicochemical techniques to confirm its structural integrity. The supported ionic liquid catalyst performed well in the heterogeneous oxidative kinetic resolution of secondary alcohols in hexane and could be recovered by simple filtration and reused at least in four consecutive runs with no significant erosion of the conversion and enantioselectivity without adding further metal complex**.** This confirms this protocol, supported ionic liquid phase catalysis, as a readily accessible pathway to highly enantioselective heterogeneous oxidative kinetic resolution catalyst in selected reaction conditions.

5.5. References

1. L.X. Zhang, Z.R. Dong, W.Y. Shen, G. Chen, J.X. Gao, Org. Lett. 8 (2006) 5655.
2. S. Gladiali, E. Alberico, Chem. Soc. Rev. 35 (2006) 226.
3. J.S.M. Samec, J.E. Bäckvall, P.G. Andersson, P. Brandt, Chem. Soc. Rev. 35 (2006) 237.
4. S.E. Clapham, A. Hadzovic, R.H. Morris, Coordin. Chem. Rev. 248 (2004) 2201.
5. H.U. Blaser, C. Malan, B. Pugin, F. Spindler, H. Steiner, M. Studen, Adv. Synth. Catal**.** 345 (2003) 103.
6. R. Noyori, S. Hashiguchi, Acc. Chem. Res. 30 (1997) 97.
7. B. Morgan, A.C. Oehlschlager, T.M. Stokes, Tetrahedron 47 (1991) 1611.
8. T.M. Stokes, A.C. Oehlschlager, Tetahedron Lett. 28 (1987) 2091.
9. J.M. Keith, J.F. Larrow, E.N. Jacobsen, Adv. Synth. Catal. 343 (2001) 5.
10. D.E.J.E. Robinson, S.D. Bull, Tetrahedron: Asymmetry 14 (2003) 1407.
11. J.H. Choi, Y.H. Kim, S.H. Nam, S.T. Shin, M.J. Kim, J. Park, Angew. Chem., Int. Ed. 41 (2002) 2373.
12. A.L.E. Larsson, B.A. Persson, J.E. Backvall, Angew. Chem., Int. Ed. Engl. 36 (1997) 1211.
13. B.A. Persson, A.L.E. Larsson, M.L. Ray, J.E. Backvall, J. Am. Chem. Soc. 121 (1999) 1645.
14. E. Vedejs, O. Daugulius, J. Am. Chem. Soc. 121 (1999) 5813.
15. S.J. Miller, G.T. Copeland, N. Papaionnou, T.E. Horstmann, E.M. Ruel, J. Am. Chem. Soc. 120 (1998) 1629.
16. M.S. Sigman, D.R. Jensen, Acc. Chem. Res. 39 (2006) 221.
17. D.R. Jansen, J.S. Pugsley, M.S. Sigman, J. Am. Chem. Soc. 103 (2001) 7475.
18. B.M. Stoltz, Chem. Lett. 33 (2004) 362.
19. J.A. Mueller, D.R. Jensen, M.S. Sigman, J. Am. Chem. Soc. 124 (2002) 8202.
20. Y. Nishibayashi, A. Yamauchi, G. Onodera, S. Uemura, J. Org. Chem. 68 (2003) 5875.

21. W. Sun, H. Wang, C. Xia, J. Li, P. Zhao, Angew. Chem., Int. Ed. 42 (2003) 1042.
22. Z. Li, Z.H. Tang, X.X. Hu, C.G. Xia, Chem. Eur. J. 11 (2005) 1210.
23. X.P. Hu, J.D. Huang, Q.H. Zengab, Z. Zheng, Chem. Comm. (2006) 293.
24. S. Doherty, E.G. robins, I. Pal, C.R. Newman, C. Hardacre, D. Rooney, D.A. Mooney, Tetrahedron: Asymmetry 14 (2003) 1517.
25. C.E. Song, S. Lee, Chem. Rev. 102 (2002) 3495.
26. Q.H. Fan, A.S.C. Chan, Chem. Rev. 102 (2002) 3385.
27. D.E. De Vos, I.F.J. Vankelecom, P.A. Jacobs, Chiral Catalyst Immobilization and Recycling, Wiley-VCH, Weinheim, 2000.
28. T. Welton, Chem. Rev. 99 (1999) 2071.
29. D. Zhao, M. Wu, Y. Kou, E. Min, Catal. Today 74 (2002) 157.
30. P. Wasserchеid, T. Welton, Ionic Liquids In Synthesis, Wiley-VCH, Weinheim 2003.
31. A. Riisager, R. Fehrmann, S. Flicker, R. Van Hal, M. Haumann, P. Wasserchеid, Angew. Chem. Int. Ed. 44 (2005) 815.
32. M. Gruttadauria, S. Riela, C. Aprile, P.L. Meo, F. D'Anna, R. Noto, Adv. Synth. Catal. 348 (2006) 82.
33. C.P. Mehnert, Chem. Eur. J. 1 (2004) 50.
34. A. Riisager, R. Fehrmann, M. Haumann, P. Waserchеid, Topics in catalysis, 40 (2006) 91-102.
35. K. Pathak, I. Ahmad, S.H.R. Abdi , R.I. Kureshy, N.H. Khan, R.V. Jasra, J. Mol. Catal. A: chemical 274 (2007) 120.
36. W. Sun, X. Wu, C. Xia, Helv. Chim. Act. 90 (2007) 623.
37. M. Lakshmi Kantama, T. Ramania, L. Chakrapani, B.M. Choudary, J. Mol. Catal. A: Chemical 274 (2007) 11.
38. F.J. Hern´andez-Fern´andez, A.P. de los R´ıos, F. Tom´as-Alonso, D. G´omez, M. Rubio, G. V´ıllora, Chemical Engineering and Processing 46 (2007) 818.
39. D.Y. Zhao, J.L. Feng, Q.S. Huo, N. Melosh, G.H. Fredrickson, B.F. Chmelka, G.D. Stucky, Science 279 (1998) 548.
40. k_{rel} = ln[(1 - *C*)(1 - ee)]/ ln[(1 - *C*)(1 + ee)] where *C* is the conversion and ee is the enantiomeric excess. H.B. Kagan, J.C. Fiaud, Top. Stereochem. John Willey & Sons, Inc. 18, 1988, pp. 249.

41. C.S. Chen, Y. Fujimoto, G. Girdaukas, C.J. Sih, J. Am. Chem. Soc. 104 (1982) 1294.
42. T. Joseph, S. Sahoo, S.B. Halligudi, J. Mol. Catal. A: Chemical 234 (2005) 107-110.
43. W. Zhang, J.L. Loebach, S.R. Wilson, E.N. Jacobsen, J. Am. Chem Soc. 112 (1990) 2801.
44. L. Lou, K. Yu, F. Ding, W. Zhou, X. Peng, S. Liu, Tetrahedron Lett. 47 (2006) 6513.
45. C.P. Mehnert, R.A. Cook, N.C. Dispenziere, M. Afeworki, J. Am. Chem. Soc. 124 (2002) 12932.
46. T.C.O. Mac Leod, D.F.C. Guedes, M.R. Lelo, R. A. Rocha, B.L. Caetano, K. J. Ciuffi, M.D. Assis, J. Mol. Catal. A: Chemical 259 (2006) 319.
47. K. Yamaguchi, C. Yoshida, S. Uchida, N. Mizuno, J. Am. Chem. Soc**.** 127 (2005) 531.

CHAPTER VI

Asymmetric oxidation of sulfides

6. An immobilized chiral Ti-binol complex for the asymmetric oxidation of sulfides

6.1. Introduction

Many chiral sulfoxides exhibit interesting biological activities and show promise as therapeutic agents [1-4]. For example, omeprazole and some of its derivatives are used as proton-pump inhibitors to treat acid-related diseases [2], OPC-29030 is used as a platelet adhesion inhibitor [3], and compound 1 (scheme 6.1) derived in vivo from the corresponding phosphorothiolate is believed to be responsible for the inhibitory action of acetylcholine esterase [4]. In addition, optically active sulfoxides are valuable chiral auxiliaries and intermediates in contemporary organic synthesis [5, 6]. So, the development of methodologies to synthesize enantio pure sulfoxides has become an important pursuit in chemical research.

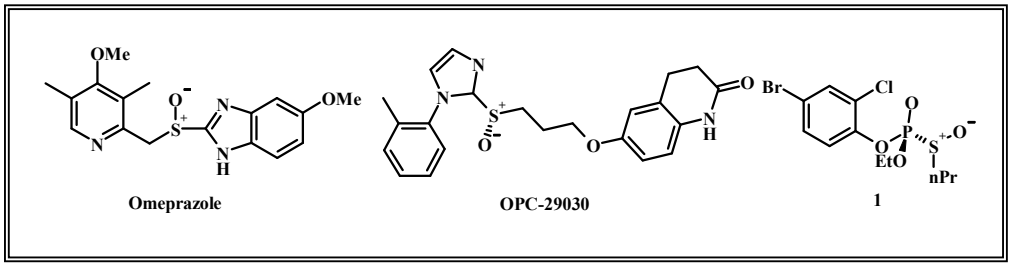

Scheme 6.1. Some biologically important sulfoxides

One of the major approaches towards enantiomeric pure sulfoxides is the stereospecific substitution of optically active sulfinates with Grignard reagents (Andersen's method) [7]. However, it suffers from important drawbacks such as the tedious procedure and, the limited substrate scope [8]. Other attempts involve stoichiometric chiral oxidants, such as oxaziridines [9], but this approach is less attractive due to high cost and restricted availability. The only practical synthetic route towards chiral sulfoxides that has already found acceptance by industry during the last two decades is the catalytic enantioselective oxidation of prochiral sulfides [10]. Based on transition metal-promoted sulfoxidation, Kagan et al. and Modena et al. reported independently a modified Sharpless procedure for the asymmetric oxidation of sulfides in the presence of stoichiometric diethyl tartrate (DET) and titanium attaining very high ee values [11-13]. Although the enantioselective

oxidation of sulfides catalyzed by chiral complexes of transition metals, such as titanium [14-16], vanadium [17, 18], iron [19], manganese [20], has been extensively studied, Kagan method and its improvements are mainly used in the large scale preparations of sulfoxides. The kinetic resolution of racemic sulfoxides and oxidation of sulfides accompanying kinetic resolution catalyzed by titanium-binol (Scheme 6.2.) often gave high ee values of sulfoxides, but low yields [11, 21]. Recently Chan developed a one-pot, titanium-catalyzed tandem sulfoxidation and kinetic resolution process, which proceeded at different temperatures and gave extremely high ee values and acceptable yields of chiral sulfoxides [22].

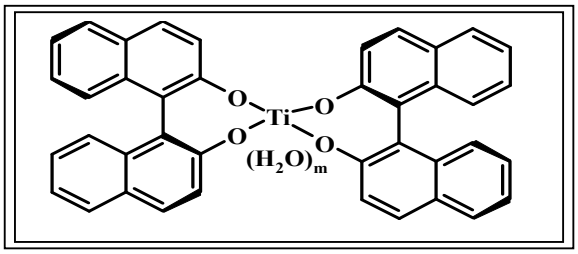

Scheme 6.2. Homogeneous Ti-(*S*)-binol complex

Many times the successes in organic transformations by soluble asymmetric catalysts affording high purity optical compounds are not reflected in the industrial front due to severe limitations including lower turn over numbers, difficulties in recovery, recycling and handling of the soluble catalysts. Therefore the enantioselective heterogeneous catalysts are preferable because of their ease of handling and separation properties from a technical and commercial point of view, provided the catalyst performance is satisfactory. Mesoporous silica had attracted much attention in many fields of science and engineering such as adsorption, separation, and catalysis due to their unique pore structures [23, 24]. In particular, their remarkable textural properties such as high surface area and large pore volume, good hydrothermal stability with varying pore size make them well suitable for application as catalyst supports especially in asymmetric catalysis [25–32]. A number of research papers have been published in the field of heterogeneous sulfide oxidation [33-37]. But a very few reports are there on the immobilization of chiral titanium complex on to mesoporous silica [38, 39]. All these heterogeneous catalysts (Ti-MCM-41) provided very low enantiomeric excess (13%) of the sulfoxides.

In this chapter, we have discussed the supported ionic liquid phase (SILP) strategy for the immobilization of chiral Ti-binol complex onto the ionic liquid

modified mesoporous silica (SBA-15) support. This catalyst system was applied in the tandem sulfide oxidation and kinetic resolution of sulfoxides and found to be comparable to the homogeneous system in activity and enantioselectivity. Also the non linear effect was addressed using this catalyst system.

6.2. Experimental

6.2.1. General

All the solvents procured from Merck (AR grade), India were distilled and dried prior to their use. Tetraethyl orthosilicate (TEOS), were procured from Aldrich chemicals and used as received. All the sulfides, $Ti(OiPr)_4$, (*S*)-binol, racemic binol, and *tert*-butylhydroperoxide were procured from sigma Aldrich. All the racemic sulfoxides were synthesized from sulfides by oxidation with *tert*-butylhydrogenperoxide. The ionic liquid $BMIMPF_6$ and the mesoporous silica were synthesized as described in chapter 2.

6.2.2. Catalyst preparation

6.2.2.1. 1-(3-Trimethoxysilylpropyl)-3-methylimidazoliumchloride (1)

A mixture of 1-methylimidazole (3.36 g, 40 mmol) 3-chloropropyltrimethoxysilane (9.63 g, 40mmol) was heated under argon atmosphere at 95 °C for 24h (Scheme 6.1.). After cooling viscous oil was obtained. ^{1}H NMR ($CDCl_3$): δ=0.71-0.78 (m, 2H), 1.25-1.33 (t, 9H),1.85-1.91 (m, 2H), 3.40-3.52 (m, 6H), 4.11 (s, 3H), 8.26 (d, 1H), 8.34 (d, 1H), 8.53 (s, 1H); ^{13}C NMR ($CDCl_3$): δ=7.0 ($SiCH_2$), 11.2 (CH_3), 25.1 (CH_2), 36.4 (NCH_3), 51.4 (CH_3O), 52.2 (CH_2N), 122.8, 124.3, 136.1.

6.2.2.2. 1-(3-Trimethoxysilylpropyl)-3-methylimidazoliumhexafluorophosphate (2)

To a solution of the above salt (3.2 g, 10 mmol), in acetone (15 mL), potassium hexafluorophosphate (1.9, 10.5 mmol) was added in one portion. The mixture was stirred at room temperature for 3 days. After this time the mixture was filtered and the solvent evaporated under reduced pressure to give **2**. The residue was taken up with chloroform.

^{1}H NMR ($CDCl_3$), δ= 0.61-0.70 (m, 2H), 1.27-1.35 (t, 9H), 1.88-1.94 (m, 2H), 3.89 (s, 3H), 4.23 (t, 2H), 7.55 (d, 1H), 7.58 (d, 1H), 8.90 (s, 1H), ^{13}C NMR ($CDCl_3$),

δ=6.9 ($SiCH_2$), 10.2 (CH_3), 24.9 (CH_2), 36.0 (NCH_3), 51.3 (CH_2O), 51.5 (CH_2N), 122.4, 124.0, 136.3. ^{31}P NMR ($CDCl_3$), δ=143.6

6.2.2.3. Synthesis of ionic liquid modified SBA-15 (ILSBA-15)

The ionic liquid **2** (2.81 g, 6.5 mmol) was dissolved in chloroform (50 mL) and treated with mesoporous silica (dried under vaccum and heated at 180 °C overnight, 4.00 g). The mixture was heated under reflux (65 °C) for 26 h. After cooling to room temperature, the solid was isolated by filtration and washed with chloroform (50 mL) and diethyl ether (50 mL). The solid was dried under reduced pressure to give a powder.

6.2.2.4. Synthesis of homogeneous Ti-Binol complex

In a round bottom flask (*S*)-binol (0.2 g, 2 mmol) in 20 mL of CCl_4 was taken. To this ligand solution, $Ti(OiPr)_4$ (0.1 g, 1 mmol) was added drop wise and stirred for 5 mins. Then water (0.18 g, 10 mmol) was added and stirred for another 1 h. Then the solvent was evaporated under reduced pressure to provide an orange colored Ti-binol complex (Scheme 6.2.). This complex was characterized by FTIR spectroscopy. FTIR (KBr pellet): 3522, 3056, 1587, 1463, 1338, 1240, 1079, 975, 819, 791 cm^{-1}.

6.2.2.5. Supported chiral Ti-binol materials (TiILSBA-15)

To a stirred solution of (*S*)-binol (0.2 g, 2 mmol) in 10 mL of CCl_4, $Ti(OiPr)_4$ (0.1 g, 1 mmol) and water (0.18 g, 10 mmol) were added one after the other dropwise. After that [BMIM] PF_6 (0.5 g) in 10 mL of CH_2Cl_2 was added (Scheme 6.4.). To this solution the ionic liquid modified mesoporous silica (1.5 g) was added. The mixture was stirred for 1h, and then evaporated under reduced pressure for 3 h to give a powder of TiILSBA-15.

6.2.3. Catalytic experiments

Typical experimental procedure for heterogeneous asymmetric sulfoxidation and catalyst recycling:

CCl_4 (10 mL) and thioanisole (0.5 mmol) were added to the solid-state catalyst TiILSBA-15 (0.4 g) obtained above. The mixture was stirred for 15 min before TBHP (70% in water, 1 g, 7.5mmol) was added dropwise at room temperature, and the heterogeneous mixture was stirred at room temperature for 20 h. After the isolation of

the solids by filtration, the insoluble catalyst was recharged with CCl_4 (10 mL), substrates (0.5 mmol), and oxidant (0.75 mmol) for the next run. The filtrate was concentrated and the residue was submitted to column chromatography on silica gel using pet ether/ethyl acetate (1:1) as eluent to give (*S*)-methylphenyl sulfoxde as colorless oil in 38% yield; The optical rotation of products was measured by Jasco P-1020 polarimeter. $[\alpha]_D$ = -134.5 (c=1.1, acetone); $[\alpha]_D$ = +135 (c=1, acetone), (*R*)-enantiomer, 99.2% ee); ^{1}H NMR (300 MHz, $CDCl_3$): δ=2.74 (s, 3 H), 7.52–7.55 (m, 3H), 7.64–7.68 ppm (m, 2H); EIMS: m/z (%): 140 (100) $[M]^+$, 125 (98), 97 (58), 77 (45), 51 (63). The ee value was determined by performing HPLC (CLASS-VP) using a Chiralcel OD-H column: UV detection at λ=254 nm; 20 °C; hexane/iPrOH, 9:1; flow rate, 0.5 mL/min (250 psi) ; t_{R1}= 24.5 min (minor isomer), t_{R2}=28.3 min (major isomer).

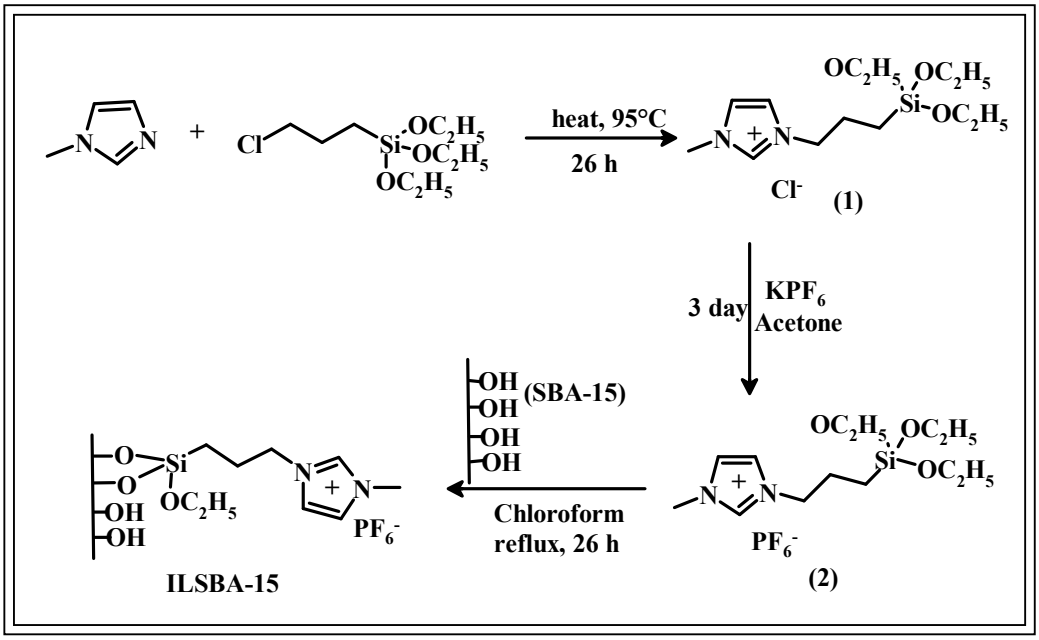

Scheme 6.3. Synthesis of ionic liquid modified SBA-15

Scheme 6.4. Immobilizaton of Ti-(S)-binol onto ionic liquid modified SBA-15

(*S*)-*p*-toluylmethylsulfoxide: $[\alpha]_D$ = -184.8 (c=1.08, acetone), >99.9% ee; ^{1}H NMR (300 MHz, CDCl3): d=2.42 (s, 3H), 2.71 (s, 3H), 7.32–7.35 (d, 2H, J=7.8 Hz), 7.53–7.56 ppm (d, J=7.8 Hz, 2H); EIMS: m/z (%): 154 (83) $[M]^+$, 139 (100).

(*S*)-*p*-bromophenylmethylsulfoxide: $[\alpha]_D$ = - 150.1 (c = 0.43, acetone), >99.9% ee; ^{1}H NMR (300 MHz, $CDCl_3$): δ=2.74 (s, 3 H), 7.53–7.55 (d, J=8.4 Hz, 2H), 7.67–7.70 ppm (d, J=8.4 Hz, 2H); EIMS: m/z (%): 220 (66) $[M+1]^+$, 218 (65) $[M-1]^+$, 205 (100), 203 (98).

(*S*)-*p*-fluorophenylmethylsulfoxide: $[\alpha]_D$ = -128.6 (c=1.5, acetone), 98.6% ee; ^{1}H NMR (300 MHz, $CDCl_3$): δ=2.72 (s, 3H), 7.20–7.26 (m, 2H), 7.63–7.68 ppm (m, 2H); EIMS: m/z (%): 158 (60) $[M]^+$, 143 (100), 115 (1), 95 (36), 75 (39).

(*S*)-*m*-bromophenylmethylsulfoxide: $[\alpha]_D$ = -110.4 (c=1.33, acetone), >99.9% ee; ^{1}H NMR (300 MHz, $CDCl_3$): δ=2.74 (s, 3H), 7.40–7.43 (m, 1H), 7.53–7.54 (m, 1H), 7.62 (m, 1H), 7.80–7.81 ppm (m, 1H); EIMS: m/z (%): 220 (81) $[M+1]^+$, 218 (81) $[M-1]^+$, 205 (93), 203 (96).

(*S*)-p-nitrophenylmethylsulfoxide: $[\alpha]_D$ = -126.5 (c=1.2, acetone), 89.1% ee; ^{1}H NMR (300 MHz, $CDCl_3$): d=2.79 (s, 3H), 7.82–7.85 (m, 2H), 8.38–8.40 ppm (m, 2H); EIMS: m/z (%): 185 (100) $[M]^+$, 170 (29), 140 (11).

(*S*)-phenylethylsulfoxide: $[\alpha]_D$ = -97.1 (c=1.3, acetone), 75.5% ee; ^{1}H NMR (300 MHz, $CDCl_3$): d=1.19–1.24 (t, J=7.5 Hz, 3 H), 2.75–2.96 (m, 2H), 7.51–7.65 ppm (m, 5H); EIMS: m/z (%): 154 (20) $[M]^+$, 126 (54), 97 (15), 78 (100), 51 (32).

6.3. Results and Discussion

The Ti-binol complex immobilized onto the ionic liquid modified SBA-15 support was characterized by different physicochemical techniques for the confirmation of its presence and the structural integrity of the mesoporous silica support after immobilization. The catalyst was assessed in the asymmetric oxidation of sulfides and subsequent kinetic resolution of the sulfoxides to get high enantiomeric excess.

6.3.1. Catalyst Characterization

6.3.1.1. Low angle XRD

The well-defined XRD patterns were obtained for all the samples which are similar to those recorded for SBA-15 materials as described by Zhao et al [40]. XRD

patterns of calcined SBA-15 and TiILSBA-15 materials (shown in Fig. 6.1. (a) and (b) respectively) consists of three well-resolved peaks in the 2θ range of 0.8 to 1.8 correspond to the (100), (110), (200) reflections which are associated with *p6mm* hexagonal symmetry in the materials. The peak intensities at (100), (110) and (200) reflections of TiILSBA-15 were decreased, indicating the immobilization of Ti-binol complex inside the mesoporous channels of ionic liquid modified SBA-15. However, the mesoporous structure of the support remained intact under the conditions used for immobilization.

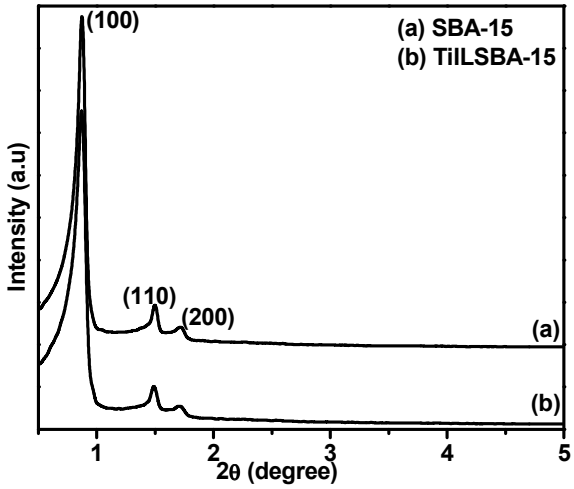

Fig. 6.1. Low angle XRD patterns of (a) SBA-15 and (b) TiILSBA-15

6.3.1.2. N_2 sorption study

The N_2 adsorption-desorption isotherms of SBA-15, ILSBA-15 and TiILSBA-15 are shown in Fig. 6.2. Isothermal N_2 adsorption measurements have allowed determining BET surface area, pore size distribution and total pore volume for the prepared materials. All these parameters decrease after the immobilization of ionic liquid and subsequent metal complex incorporation. The surface area observed for ILSBA-15 and TiILSBA-15, are 335 and 116 m^2g^{-1} respectively compared to 730 m^2g^{-1} for parent SBA-15. The average pore volume was decreased from 1.10 to 0.69 and 0.26. Also the average pore diameters decreased from 63 Å to 25 Å after immobilization. The pore size distribution was calculated from the Kelvin equation and is presented as a BJH plot (inset picture, Fig. 6.2.). Although the immobilized samples showed a decrease in surface area, pore diameter and pore volume, isotherms of all the materials were of type IV, as defined by IUPAC and exhibited a H1-type

broad hysteresis loop, which was typical of large-pore mesoporous solids. As the relative pressure increases (p/p_o > 0.6), all isotherms exhibit a sharp step characteristic of capillary condensation of nitrogen within uniform mesopores, where the p/p_o position of the inflection point is correlated to the diameter of the mesopore. This data confirmed the presence of chiral Ti-binol complex in the mesoporous SBA-15 support, and the intactness of the textural property of the support after functionalization.

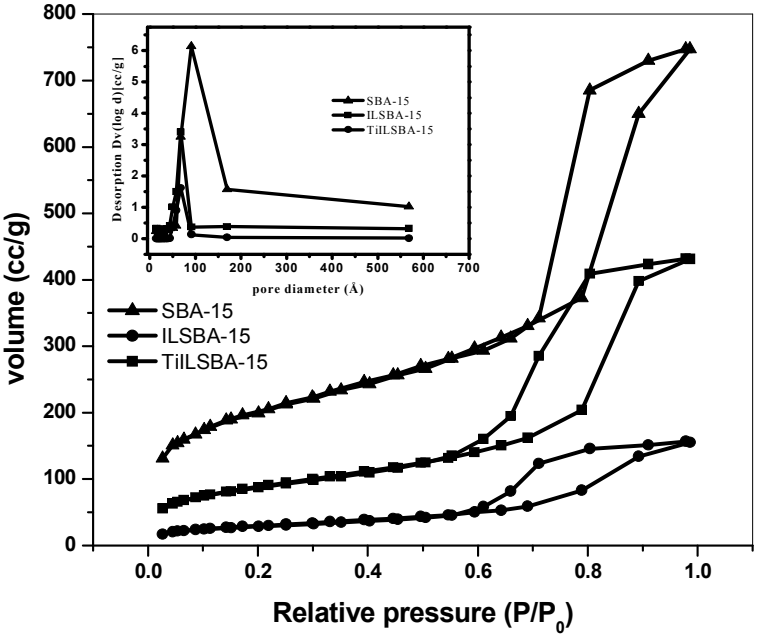

Fig. 6.2. N_2 adsorption-desorption isotherms of samples (a) SBA-15, (b) ILSBA-15 and (c)TiILSBA-15;); Inset picture: Pore size distribution of these materials

6.3.1.3. Microscopic analysis

As can be seen from the SEM images of TiILSBA-15 shown in Fig. 6.3. (a), the micro morphology i.e, rope like structure of mesoporous SBA-15 remained the same even after modification with ionic liquid and Ti-binol complex.

Fig. 6.3 (b) depicts TEM images obtained for the sample TiILSBA-15 catalyst as definitive evidence of the retention of structure ordering of SBA-15 after immobilization. The presence of equidistant parallel fringes demonstrates the nature of separation between layers and the unique well-packed arrangement of such monolayers. The well ordered hexagonal array of mesopores was also observed.

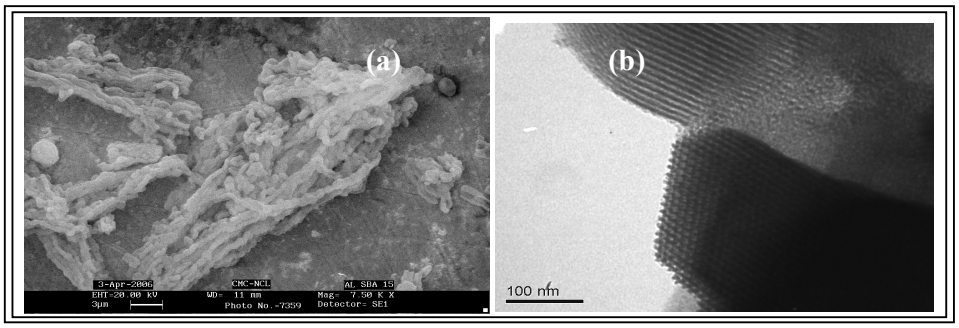

Fig. 6.3. (a) SEM and (b) TEM photographs of TiILSBA-15

6.3.1.4. Nuclear Magnetic Resonance

Regarding the successful immobilization of ionic liquid and the chiral metal complex, the NMR spectra were obtained for the accurate characterization. While looking at the proton spectra (Fig. 6.4), it showed very sharp lines due to species with a high mobility, probably the $BMIM^+$ species. The peaks at 6.8 -7.9 corresponds to the aromatic protons of the binol ligand and the imidazolium moiety of the ionic liquid present and the peaks at 0.27 – 3.29 correspond to the aliphatic side chain of the imidazolium moiety. The ^{13}C NMR spectra (Fig. 6.5) shows peaks at 136 and 121, which are due to the aromatic ring carbons and the peaks 13-49 confirm the presence of linker propyl group, ethoxy ($SiOCH_2CH_3$). ^{29}Si MAS NMR spectra of the parent SBA-15 exhibited a broad peak and was dominated by an intense peak at −110 ppm assigned to $Si(OSi)_4$ and one shoulder peaks at −102 ppm due to $Si(OSi)_3OH$ (Q3) structural units present in SBA-15. On incorporation of the imidazolium moiety, in addition to the aforementioned three peaks, one peak at 66 ppm appeared (Fig. 6.6.) which is the evidence of presence of T3 moiety only. No peak appeared at −45 and 58 ppm, indicates the absence of free silane moiety physically adsorbed on the SBA-15 surface and the T2 moiety respectively. The phosphorus spectrum (Figure 6.7) shows only the resonance of PF_6^- of the ionic liquid.

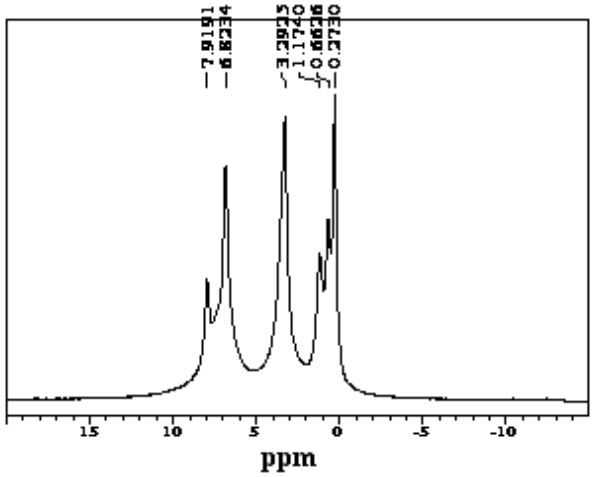

Fig. 6.4. ^{1}H NMR spectra of TiILSBA-15

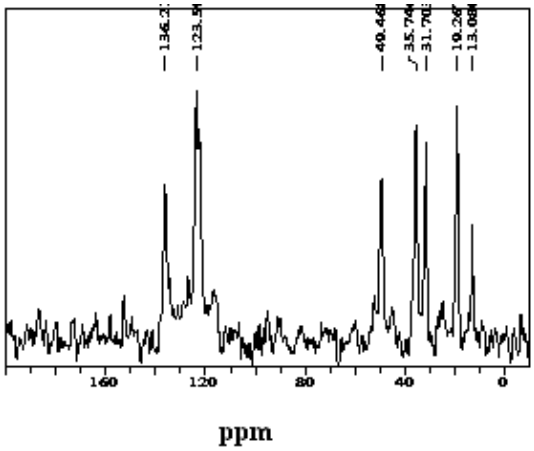

Fig. 6.5. ^{13}C CP-MAS NMR spectra of TiILSBA-15

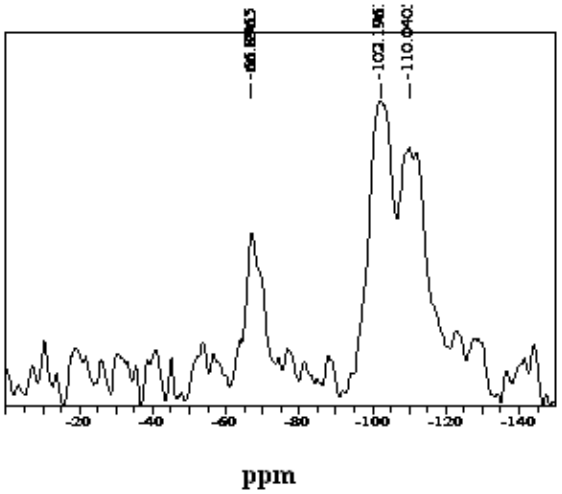

Fig. 6.6. ^{29}Si CP-MASNMR spectra of TiILSBA-15

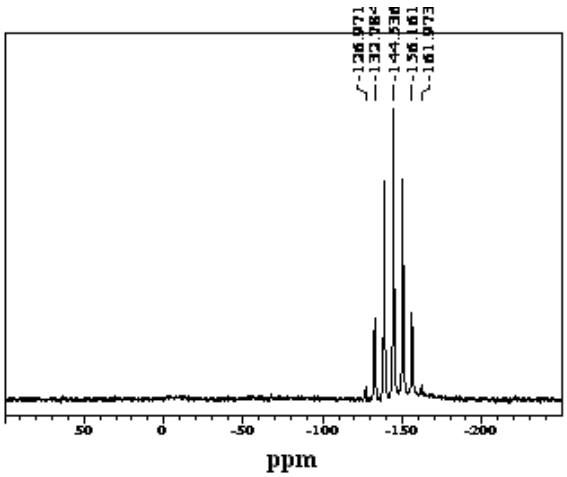

Fig. 6.7. ^{31}P MAS NMR spectra of TiILSBA-15

6.3.1.5. FTIR Spectroscopy

Another piece of evidence of the immobilized ionic liquid and the chiral Ti-binol complex was obtained by FTIR spectroscopy. Fig. 6.8. depicts the representative FTIR spectra in the range 400–4000 cm^{-1} for immobilized Ti-binol catalyst TiILSBA-15. In the spectrum in addition to the specific bands at 1080, 780 and 470 cm^{-1} of the parent mesoporous silica support, the IR bands observed at 3158 and 3110 cm^{-1} are assigned to C–H stretching vibrations of aromatic imidazole ring of the ionic liquid and binol. The bands near 3000 cm^{-1} are due to C–H stretching vibrations of alkyl groups belonging to the silylating agent. The IR bands at 1566 and 1454 cm^{-1} can be attributed to C=C stretching vibrations of imidazole rings and C–H deformation vibrations of alkyl groups, respectively. Besides these, the IR band assigned to C=N stretching vibrations was seen at around 1625 cm^{-1}. Furthermore, new characteristic bands of Ti-binol at 1464, 1334, 978 cm^{-1} appeared in the spectrum; indicate that the chiral Ti-binol complex was successfully immobilized on the support.

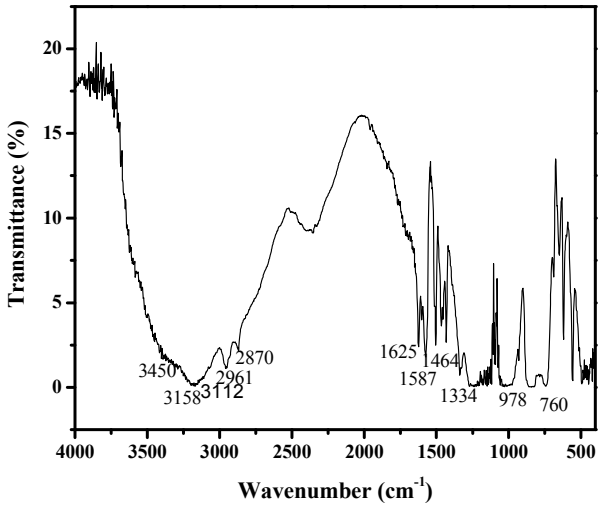

Fig. 6.8. FTIR spectra of TiILSBA-15

6.3.2. Catalytic Activity

The TiILSBA-15 catalyst was then tested in the enantioselective oxidation of sulfides taking thioanisole as a test substrate in CCl_4, and aqueous TBHP as the oxidant. First the reaction was carried out with a sulfide/Ti/ TBHP ratio of 1:0.05:1. After 10 h of reaction time maximum sulfoxide yield (85%) (Table 1, entry 1) was obtained with a low ee of 75%. Then Uemura's protocol was applied by subjecting it to oxidative kinetic resolution after adding another 0.5 equivalent of TBHP. It was observed that after 20 h of reaction time the enantiomeric excess of the sulfoxide was >99% with a sulfone yield of 30% (Table 2, entry 6). It can be well understood from Fig. 6.9. that with the increase in time, the sulfoxide yield first increases and then decreases, but the enantiomeric excess of the sulfoxide goes on increasing with the increase in time and sulfone yield. It can be concluded that the high enantiomeric excess of sulfoxide could be obtained by tandem oxidation and kinetic resoluti the similar conditions in the absence of the catalyst, but the resulted sulfoxide was found to be racemic.

Table 6.1.

TiILSBA-15-catalyzed oxidation of thioanisole: reaction time study[a]

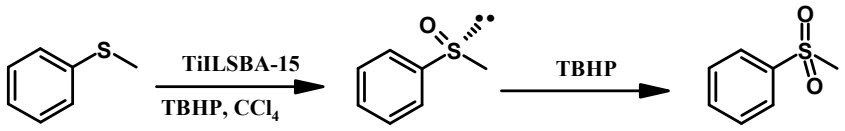

Entry.	Time	sulfoxide		sulfone
		Yield [%][b]	ee[%] [c, d]	Yield [%][b]
1.	10	85	75	0
2.	12	78	83	10
3.	14	75	88	16
4.	16	65	93	20
5.	18	62	99	25
6.	20	59	99	30
7.[e]	16	63	99	29

Reaction Condition: sulfide/Ti/TBHP (70% aqueous solution of TBHP was used) = 1.0: 0.0.5:1.5.
[b] Yields of isolated products.
[c] Determined by HPLC analysis on a Daicel Chiralcel OD column
[d] All in the *S* configuration.
[e] Under homogeneous condition.

Encouraged by our preliminary results described above we next investigated the heterogeneous catalysis of a variety of aryl alkyl sulfides with a sulfide/Ti/TBHP ratio of 1:0.05:1.5 in CCl_4 at room temperature. As shown in Table 6.2. all the sulfides get oxidized to the corresponding sulfoxides with good yield and enantiomeric excess. The oxidation of sulfides having both electron-donating as well as electron withdrawing substituents gave good enantiomeric excess with a sulfoxide yield of about 60% (Table 6.2, entries 2-5 and 8, 9). As shown in Table 6.2. both *para*-substituted (entry 3) and *meta*-substituted (entry 5) afforded very high enantioselectivity (99%) in about 55% yield. Notably in the oxidation of the *para*-nitro substituted sulfide (Table 6.2, entry 6), a lower enantiomeric excess of 88% was obtained as compared to the other substrates. The oxidation of ethylphenyl sulfide afforded the corresponding sulfoxide with an enantiomeric excess of 77% (Table 6.2, entry 7).

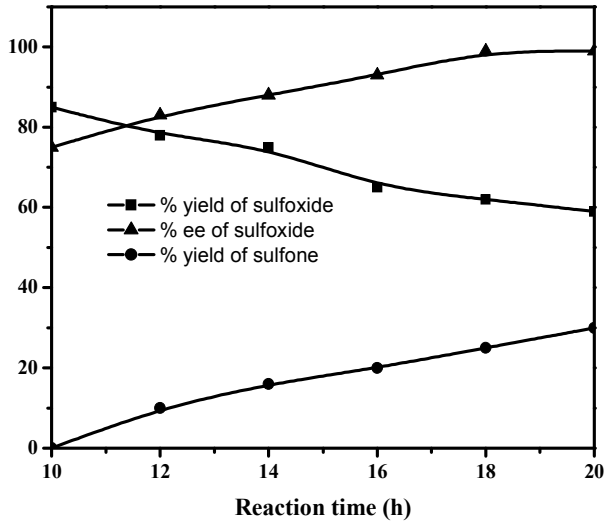

Fig. 6.9. Time course of the ee (%) of the sulfoxide, yield (%) of sulfoxide and relative concentration (%) of the sulfone

6.3.3. Non linear effect in asymmetric sulfoxidation

In recent years particular attention has been paid to the detection of NLE in a variety of asymmetric reactions [41-43], since they can be used to prepare compounds with high ees starting from only enantiomerically enriched ligands or auxiliaries and, furthermore, to obtain mechanistic information. In heterogeneous enantioselective catalysis only the latter "extended" nonlinear effect has been studied so far [44-46]. As regards the asymmetric sulfoxidation, Kagan pointed out a negative NLE, (−)-NLE, for the oxidation of methyl *p*-tolyl sulfide in the presence of the modified Sharpless reagent Ti(O-*i*-Pr)$_4$/*L*-DET/H_2O, that affected the level of enantioselectivity until the value of 70% ee was reached for diethyl tartrate; then, the linear relationship was observed until enantiomerically pure *L*-DET was used [47]. Recently Massa et al has reported a positive non linear effect in asymmetric sulfoxidation using Ti-(R)-binol as the catalyst [48]. No one has yet reported the non linear effect in the oxidation and tandem kinetic resolution using the immobilized Ti-binol complex. Herein we studied the non-linear effect by using the present immobilized Ti-binol complex onto ionic liquid modified support in the asymmetric oxidation tandem kinetic resolution of thioanisole.

Table 6.2.

Enantiselective oxidation of sulfides catalyzed by TiILSBA-15[a]

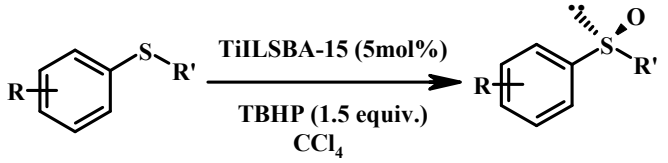

Entry	R	R'	sulfoxide	
			Yield (%)[b]	ee (%)[c,d]
1.	H	Me	59	99.9
2.	4-Me	Me	62	99.5
3.	4-Br	Me	58	99.2
4.	4-Cl	Me	61	96.7
5.	3-Br	Me	57	99.2
6.	4-NO_2	Me	54	88.3
7.	H	Et	63	77.2
8.	4-OMe	Me	55	99.9
9.	4-F	Me	59	98

[a]Reaction Condition : sulfide/Ti/ TBHP (70% aqueous solution of TBHP was used) = 1.0: 0.05:1.5
[b] Yields of isolated products.
[c] Determined by HPLC analysis on a Chiralcel OD-H column,
[d]All in the *S* configuration.

Partially resolved (S)-binol was used for this study under all other identical conditions. All the experiments were carried out for same reaction time (20 h). A positive non linear effect was observed in this study (Fig. 6.10). Almost ~99% ee of the methyl phenyl sulfoxide was obtained in case of 60% enantiomerically pure catalyst.

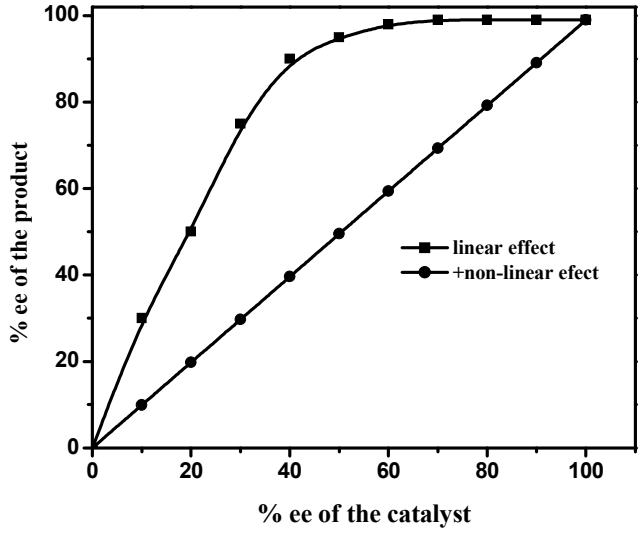

Fig. 6.10. Positive nonlinear effect in the asymmetric oxidation of thioanisole

6.3.4. Catalyst Stabilty

The heterogeneous nature of the above catalytic system was confirmed by using the supernatant of the catalyst in CCl_4 for the oxidation of thioanisole under the same conditions. The isolated product was racemic, similar to that obtained from the control experiment in the absence of catalyst under otherwise identical conditions. The inductively coupled plasma (ICP) spectroscopic analyses of the liquid phase after filtration of the insoluble catalysts indicated that no detectable titanium (< 0.1 ppm) was leached into the organic solution, which again supported the heterogeneous nature of the present system.

The facile recovery and remarkable stability are two other features exhibited by this type of heterogeneous catalyst. After completion of the reaction, simple filtration in open air enabled the separation of the solid-state catalyst from the product-containing solution. The separated solids were recharged with CCl_4, substrate, and oxidant, for the next run. As shown in Table 6.3, the catalyst TiILSBA-15 could be used for at least 8 cycles in the sulfoxidation of thioanisole without any loss of enantioselectivity. Moreover, no significant deterioration in activity of the recovered catalyst was observed after eight runs that covered a period of more than one month. Again, the titanium leaching during recycling of the catalysts was determined to be negligible (less than 0.1 ppm by ICP).

Table 6.3.

Recycling and reuse of the heterogeneous catalyst TiILSBA-15 in the enantioselective oxidation of thioanisole [a]

Run	Time (h)	Yield (%)[b]	ee(%)[c]
1	20	62	99.2
2	20	62	99.0
3	21	60	99.0
4	22	59	98.6
5	22	58	98.6
8	24	56	98.2

[a]All the reactions were performed at room temperature with 1.5 equivalents of TBHP(70% in water) in CCl_4;
[b]isolated yields; [c] determined by performing HPLC using a Chiralcel OD-H column

6.4. Conclusions

We have used the SILP strategy for the immobilization of chiral titanium-binol catalyst onto the ionic liquid modified mesoporous silica SBA-15 support. The catalyst was characterized by different physico-chemical techniques for the confirmation of the presence of the chiral complex as well as the retention of structural integrity after the immobilization procedure. The catalyst showed excellent enantioselectivity in the tandem oxidation kinetic resolution of sulfides. A positive non linear effect was observed in this system. The catalyst was highly stable and could be readily recycled and reused for over one month with no apparent loss of activity and enantioselectivity (up to > 99.9%). This represents a remarkable example of the heterogeneous catalysis of enantioselective reactions by using titanium catalysts. The features of SILP catalyst, such as facile preparation, robust chiral structure of solid state catalysts, and high density of the catalytically active units in the solids, as well as easy recovery and simple recycling are particularly important in developing methods for the synthesis of optically active compounds in industrial processes. The strategy described here indicates a possible new direction in the design of chiral catalysts for asymmetric synthesis.

6.5. References

1. P. Pitchen, Chem. Ind. 1994, 636.
2. S. von Unge, V. Langer, L. Sjlin, Tetrahedron Asymmetry 8 (1997) 1967.
3. M. Matsugi, N. Fukuda, Y. Muguruma, T. Yamaguchi, J. Minamikawa, S. Otsuka, Tetrahedron 57 (2001) 2739.
4. S. Tashiro, H. Miyagawa, N. Sugita, Y.J. Okada, Pestic. Sci. 18 (1993) 155.
5. M. Mikolaczyk, J. Drabowicz, Top. Stereochem. 13 (1982) 333.
6. D.H. Hua, S.N. Bharathi, F. Takusagawa, A. Tsujimoto, J.A.K. Panagan, M.H. Hung, A. Bravo, A.M. Erplelding, J. Org. Chem. 54 (1989) 5659.
7. K.K. Andersen, W. Gaffield, N.E. Papanikolau, J.W. Foley, R.I. Perkins, J. Am. Chem. Soc. 86 (1964) 5637.
8. Z. Han, D. Khrishnamurthy, P. Grover, H.S. Wilkinson, Q.K. Fang, X. Su, Z.-H. Lu, D. Magiera, C.H. Senanayake, Angew., Chem. 115 (2003) 2078; Angew. Chem., Int. Ed. 42 (2003) 2032.
9. F.A. Davis, A.C. Sheppard, Tetrahedron 45 (1989) 5703.
10. P. Pitchen, in: Chirality in Industry II, (Eds.: A.N. Collins, G.N. Sheldrake, J. Crosby), Willey, New York, 1997, p. 381.
11. J.-M. Brunel, P. Diter, M. Duetsch, H.B. Kagan, J. Org. Chem. 60 (1995) 8086.
12. F. Di Furia, G. Modena, R. Seraglia, Synthesis (1984) 325.
13. P. Pitchen, E. Dunach, M.N. Deshmukh, H.B. Kagan, J. Am. Chem. Soc. 106 (1984) 8188.
14. N. Komatsu, M. Hashizume, T. Sugita, S. Uemura, J. Org. Chem. 58 (1993) 4529.
15. M.I. Donnoli, S. Superchi, C. Rosini, J. Org. Chem. 63 (1998) 9392.
16. G. Pescitelli, L. Di Bari, P. Salvadori, J. Organomet. Chem. 691 (2006) 2311.
17. C. Bolm, F. Bienewald, Angew. Chem., Int. Ed. Engl. 34 (1995) 2640.
18. H. Vetter, A. Berkessel, Tetrahedron Lett. 39 (1998) 1741.
19. J. Legros, C. Bolm, Chem. Eur. J. 11 (2005) 1086.
20. H. Sasaki, R. Irie, Y. Ito, T. Katsuki, Synlett (1994) 356.
21. N. Komatsu, M. Hashizume, T. Sugita, S. Uemura, J. Org. Chem. 58 (1993) 7624.
22. X. Jia, X. Li, L. Xu, Y. Li, Q. Shi, T. T. L. Au-Yeung, C. W. Yip, X. Yao, A. S. C. Chan, Adv. Synth. Catal. 346 (2004) 723.

23. M.E. Davis, Nature 417 (2002) 813.
24. C. Li, Catal. Rev. Sci. Eng. 46 (2004) 419.
25. B.F.G. Johnson, S.A. Raynor, D.S. Shephard, T. Mashmeyer, J.M. Thomas, G. Sankar, S. Bromley, R. Oldroyd, L. Gladden, M.D. Mantle, Chem. Commun. (1999) 1167.
26. D. Reechavi, M. Lemaire, Org. Lett. 3 (2001) 2493.
27. C.G. Arellano, A. Corma, M. Lglesias, F. Sanchez, Adv. Synth. Catal. 346 (2004) 1758.
28. H. Zhang, Li. Can, Tetrahedron 62 (2006) 6640.
29. H. Zhang, Y. Zhang, Li. Can, J. Catal. 238 (2006) 369.
30. T.M. Lancaster, S.S. Lee, J.Y. Ying, Chem. Commun. (2005) 3577.
31. S.S. Lee, S. Hadinoto, J.Y. Ying, Adv. Synth. Catal. 348 (2006) 1248.
32. S.S. Lee, J.Y. Ying, J. Mol. Catal. A 256 (2006) 219.
33. B.H. Lipshutz, Y.J. Shin, Tetrahedron Lett. 41 (2000) 9515.
34. V.V. Thakur, A. Sudalai, Tetrahedron Asymmetry 14 (2003) 407.
35. X. Wang, X. Wang, H. Guo, Z. Wang, K. Ding, Chem. Eur. J. 11 (2005) 4078.
36. B.M. Choudary, S. Shobha Rani, N. Narender, Catal. Lett. 19 (1993) 299.
37. J. Gao, H. Guo, S. Liu, M. Wang, Tetrahedron Lett. 48 (2007) 8453.
38. J. Fraile, J. Garcia, B. Lazaro, J. Mayoral, Chem. Commun. (1998) 1807.
39. M. Iwamato, Y. Tanaka, J. Hirosumi, N. Kita, S. Triwahyono, Microporous Mesoporous Mater. 48 (2001) 271.
40. D. Zhao, J. Feng, Q. Huo, N. Melosh, G.H. Fredrickson, B.F. Chmelka, G.D. Stucky, Science 279 (1998) 548.
41. C. Girard, H.B. Kagan, Angew. Chem., Int. Ed. 37 (1998) 2922.
42. K. Mikami, M. Terada, T. Korenaga, Y. Matsumoto, M. Ueki, R. Angelaud, Angew .Chem., Int. Ed. 112 (2000) 3532.
43. H.B. Kagan, Synlett (2001) 888.
44. W.R. Huck, T. Mallat, A. Baiker, Adv. Synth. Catal. 345 (2003) 255.
45. A. Tungler, K. Fodor, T. Máthé, R.A. Sheldon, Stud. Surf. Sci. Catal. 108 (1997) 157.
46. L. Balazs, T. Mallat, A. Baiker, J. Catal. 233 (2005) 327.
47. C. Puchot, O. Samuel, E. Dunach, S. Zhao, C. Agami, H.B. Kagan, J. Am.

Chem. Soc. 108 (1986) 2353.

48. A. Massa, F.R. Siniscalchi, V. Bugatti, A. Lattanzi, A. Scettri, Tetrahedron Asymmetry 13 (2002) 1277.

CHAPTER VII

Summary and Conclusions

7. Summary and Conclusions

7.1. Summary

The present thesis gives an account of (i) immobilization of chiral metal complexes onto mesoporous silica support (ii) in-depth characterization of these materials, and (iii) application of these materials as catalysts in different asymmetric organic transformations.

Chapter 1 presents a brief introduction of asymmetric synthesis and their importance. It gives an introduction to homogeneous and heterogeneous asymmetric catalysis. It further describes the various physicochemical aspects of mesoporous materials with particular emphasis to different synthesis routes, mechanisms proposed for their formation. The different methods used for immobilization has also been reviewed. A review of the literature to date in these areas is included.

Chapter 2 deals with the experimental procedures for the synthesis of materials. It also presents a discussion of theory and experimental procedures of all characterization techniques such as N_2 sorption, AAS, XRD, TEM, SEM, FT-IR TG/DTA and MAS NMR for all materials used for catalyst screening whichever applicable to particular catalyst system. .

Chapter 3 describes the immobilization of chiral 1, 2-diaminocyclohexane (dach) based ruthenium triphenylphosphine complex onto the surface of mesoporous silica SBA-15, MCM-41 and MCM-48. All catalyst materials were characterized by elemental analysis, FT-IR, N_2 sorption measurements, SAXS, MAS-NMR, SEM and TEM for their structural integrity and physico-chemical properties. The potential of these heterogeneous catalysts in enantioselective hydrogenation of a number of prochiral ketones, chemoselective hydrogenation of α,β-unsaturated ketones and hydrogenation of imines under various reaction conditions have been demonstrated. The recycle studies of the catalysts have also been presented to emphasize the heterogeneous nature for the same.

Chapter 4 deals with the synthesis of binol derived monodentate phosphorothioite (PS) ligand from binol and thiopropyltriethoxysilane and immobilization of its iridium complex to mesoporous silica supports like SBA-15, MCM-41 and MCM-48 by covalent anchoring method. These catalysts were characterized by different physicochemical techniques and assessed for their catalytic performances in the heterogeneous asymmetric hydrogenation of itaconic acid and its derivatives. Effects of substrate to catalyst molar ratio, solvents and temperature on substrate conversions and enantioselectivities of the products were investigated in hydrogenation reactions.

Chapter 5 deals with the application of supported ionic liquid strategy for the immobilization of chiral Mn-salen complex onto ionic liquid modified mesoporous silica. These catalysts were characterized by N_2 sorption, XRD, FTIR, DRUV–Vis, and elemental analysis. The catalytic activity of this supported catalyst in oxidative kinetic resolution of secondary alcohols under different reaction conditions has been discussed in detail. Also different types of alcohols were subjected to oxidative kinetic resolution using this catalyst system.

Chapter 6 discusses the immobilization of chiral Ti-binol complex onto the ionic liquid modified mesoporous silica (SBA-15) support using the supported ionic liquid phase (SILP) strategy. This catalyst system was applied in the tandem sulfide oxidation and kinetic resolution of sulfoxides. Also the non linear effect was addressed in this heterogeneous catalyst system.

Chapter 7 summarizes the conclusions reached in this thesis.

7.2. Conclusions

- Structural integrity of the chiral metal complex and the support was well retained after immobilization onto mesoporous silica which was confirmed by different physicochemical characterizations.

- Heterogeneous enantioselctive hydrogenation of prochiral ketones using chiral diamino Ru complex immobilized onto mesoporous silica support gave the corresponding alcohols with an ee value of 76%. It also showed promising activity in the chemoselective hydrogenation of α,β-unsaturated ketones and hydrogenation of imines. The activities were comparable with that of homogeneous analogues in all the reactions studied.

- Iridium complex of monodentate phosphorothioite ligand was covalently anchored onto mesoporous silica supports in minimum number of steps. High conversions (99%) and excellent enantioselectivities (up to 94% ee) were observed under milder reaction conditions with a substrate to catalyst ratio 30 times higher than the previously reported monodentate ligand based catalytic systems in the hydrogenation of itaconic acid derivatives.

- Supported ionic liquid phase strategy was found to be an effective strategy for the immobilization of chiral Mn(III) salen and Ti-binol complexes. The immobilized Mn(III) salen catalyst gave good enantioselectivity and activity in the heterogeneously catalyzed oxidative kinetic resolution of secondary alcohol. Among different additives studied bromide containing additives were found to be effective in this transformation.

- Chiral Ti-binol complex immobilized onto ionic liquid modified SBA-15 showed excellent activity in the oxidation of sulfides. Tandem oxidation kinetic resolution was found to be necessary for the high ee (>99%) of the sulfoxides. A positive nonlinear effect was also observed which showed that upto >99% ee of the product can be obtained by applying a catalyst with ~60% enantiomeric purity.

- The features of SILP catalyst, such as facile preparation, high density of catalytically active units are particularly important in developing methods for the synthesis of optically active materials.

- All the catalyst systems studied were recovered by simple filtration and reused at least in five consecutive runs with no significant erosion of the conversion and enantioselectivity.

7.3. Future outlook

In this thesis, enantioselective hydrogenation of prochiral ketones and olefins has been studied. However, there is ample opportunity to study enantioselective hydrogenation of different types of functionalized ketones, *e.g.*, heteroaromatic ketones, amino ketones, β-ketoesters *etc*. employing the present heterogeneous catalyst system and asymmetric hydrogenation of a range of olefins other than the itaconic acid derivatives. These substrates are commercially applied as chiral synthons in the synthesis of vitamins, fragrances, pheromones, pharmaceuticals *etc*. Different monodentate ligands, such as phosphites, phosphoramidites and phosphonites, can be immobilized onto the mesoporous support and there complexes can be applied in asymmetric hydroamination, hydrosilylation, C-C bond forming reaction. Supported ionic liquid strategy can be applied for the successful immobilization of various metal complexes. Nonlinear effect can be studied in a number of heterogeneous asymmetric catalysis.

1. **Brönsted acidic ionic liquids: A green, efficient and reusable catalyst system and reaction medium for Fischer esterification**

Journal of Molecular Catalysis A: Chemical 234 (2005) 107–110

Trissa Joseph, **Suman Sahoo**, S.B. Halligudi*

2. **Mannich reaction in Brönsted acidic ionic liquid: A facile synthesis of β amino carbonyl compounds**

Journal of Molecular Catalysis A: Chemical 244 (2005) 179–182

Suman Sahoo, Trissa Joseph*, S.B. Halligudi

3. **Immobilized chiral diamino Ru complex as catalyst for chemo- and enantioselective hydrogenation**

Journal of Molecular Catalysis A: Chemical 273 (2007) 102–108

Suman Sahoo, Pradeep Kumar, F. Lefebvre, S.B. Halligudi*

4. **Enantioselective hydrogenation of olefins by chiral iridium phosphorothiotite complex covalently anchored on mesoporous silica**

Journal of Catalysis 254 (2008) 91–100

Suman Sahoo, Pradeep Kumar, F. Lefebvre, S.B. Halligudi*

5. **A Chiral Mn(III) salen complex immobilized onto ionic liquid modified mesoporous silica for oxidative kinetic resolution of secondary alcohols**

Tetrahedron Letters, Manuscript accepted

Suman Sahoo, Pradeep Kumar, F. Lefebvre, and S.B. Halligudi*

6. **Selective aerobic oxidation of alcohols to aldehydes and ketones catalysed by $H_5[PMo_{10}V_2O_{40}]\cdot 32.5H_2O$ immobilized on Ionic liquid-modified SBA-15**

Communicated

Ankur Bordoloi, **Suman Sahoo**, F. Lefebvre, S. B. Halligudi*

7. **Highly Selective Catalytic Hydrogenation of Arenes using Rhodium Nanoparticle Supported Multiwalled Carbon Nanotubes**

Communicated

Balchandra Kakde, **Suman Sahoo**, S.B. Halligudi, Vijayamohanan Pillai*

8. **An immobilized chiral Ti-binol complex for the asymmetric oxidation of sulfides**

Communicated

Suman Sahoo, Pradeep Kumar, F. Lefebvre, S.B. Halligudi*